On the relation between wave conditions and mathematical properties of some asymptotic water wave models

Martin Oen Paulsen

Department of Mathematics
University of Bergen

Master thesis in Applied and Computational Mathematics

May 2020

Acknowledgements

My deepest gratitude goes to my supervisor Henrik Kalisch for his guidance and help. I appreciate the many conversations and the opportunities he has given me, having introduced me to a wide range of interesting subjects.

I would also like to thank my friends and family for making this a year a nice experience. Especially thanks to my girlfriend Nadia for valuable input and support.

Table of contents

Abstract

This work is dedicated to the study of water wave models with applications in mind. Using fundamental equations as a basis we will analyze different systems and put forward applications that are useful in the field of oceanography. The main goal is to understand the development of waves from deep to shallow-water and its underlying theory.

First we will model unidirectional long gravity waves propagating up a gently sloping beach. This is based on formulating conservation laws in the context of the Korteweg-de Vries (KdV) equation. Within this framework, two models will be derived using an asymptotic expansion of the general water wave problem arising from the Euler equations for irrotational flow. Having derived the model we propose a scheme and run several numerical experiments for validation with existing theories. This work has been submitted to the Journal of Fluid Mechanics.

Secondly, as one gets closer to the shore one needs to change regimes due to nonlinear effects. In order to better understand some of the intricacies, consideration is given to the shallow-water equations. This is a hyperbolic system modeling the propagation of long waves at the surface of an incompressible inviscible fluid of constant depth. Here we will study admissibility conditions for the Riemann problem and discuss various scenarios in which the problem arises in a physically reasonable sense. This work has been excepted for publication in: Zeitschrift für Naturforschung A [50].

Introduction and general outline

The dynamics of water waves are typically understood through the concept of conservation laws. In particular conservation of mass, energy and momentum are often used within a certain framework. For instance, consider a continuum with a fixed volume V and density ρ. A basic principle of classical mechanics states that the change of mass within the volume must be equal the rate of inflow through the boundaries. Translated into mathematical terms,

$$\frac{d}{dt}\int_V \rho dV = -\int_{\partial V} \rho \mathbf{u} dA.$$

Applying the transport theorem on the left and divergence theorem on the right and collecting the terms, it can be argued that the volume V was arbitrary and therefore the following must hold

$$\frac{\partial \rho}{\partial t} + \nabla \cdot (\rho \mathbf{u}) = 0. \tag{1}$$

Since we are concerned with incompressible water flow and negligible changes in density one may simplify equation (1):

$$\nabla \cdot \mathbf{u} = 0, \tag{2}$$

which is the well-known continuity equation with the fluid velocity $\mathbf{u} = (u(x,z,t), v(x,z,t))$.

By similar means, the momentum equation can be expressed by the Euler equations when imposing the standard assumption of an ideal fluid being incompressible, inviscid in a domain with a flat bottom. It is given by

$$\frac{\partial \mathbf{u}}{\partial t} + (\mathbf{u} \cdot \nabla)\mathbf{u} = -\frac{1}{\rho}\nabla P - g\mathbf{j}. \tag{3}$$

Together with the continuity equation, the Euler equations will form the basis of this thesis. Keeping in mind that no theory can exceed its underlying assumptions, we must only consider scenarios within the specified framework. In this spirit, since we want to understand how

periodic waves vary when traveling up a gently sloping beach, we must first understand the framework we are working in and whether additional restrictions make sense.

In Chapter 1 we discuss basic theory of simplified models based on equation (2) and (3). These simplifications are needed since solving the Euler equations for large scale simulations is very computationally expensive. With this in mind, we try to justify the simplifications such that it achieves a satisfying level of precision at a lower cost. Adding assumptions to the problem can be useful when we are interested in particular phenomena and the simplest case is linear wave theory. This will be discussed in Section 1.2 when considering 'deep water waves'. Once we get closer to the shore we need to improve our model compared to our base (2) and (3). Building on the ideas from linear theory, higher-order theory will be discussed in the context of the KdV equation.

In light of the theory developed in Chapter 1, we present a new numerical model in Chapter 2. The goal is to model the variation of the waveheight up a gently sloping beach using conservation principles. This phenomena is known as shoaling, and will be based on conservation laws formulated in the context of the KdV equation. Applying the model correctly will allow for accurate and fast computations of a complex phenomenon. We first present the well-known linear shoaling equation in Section 2.1, before extending it in Section 2.2 using the KdV equation. Lastly, we discuss the validity of the new model in a rigorous framework in Chapter 3.

To conclude our studies, we consider some of the challenges that occur in the shallow-water region. In particular we would like to study admissibility conditions for the shallow-water equations. These equations have a hyperbolic structure, so we start the chapter by deriving the conditions a general system must satisfy. Then we apply these conditions to the shallow-water system in Section 4.2 for the Riemann problem. This is standard theory and we put forward the classical solution in Section 4.2.3. Though, having the desired framework we will argue in the proceeding sections that some of those solutions are nonphysical in this context, and we suggest a solution on how to overcome this issue.

Chapter 1

Modeling of surface water waves

We start this chapter with a brief description of the water wave problem. Consider a homogeneous liquid and gas at rest separated by a horizontal surface. We say that disturbances to the original state of equilibrium will take the form of surface gravity waves. The liquid domain is specified by $\{(x,z) \in \mathbb{R}^2 | -h < z < \eta(x,t)\}$ where h is the undisturbed water depth and η is the surface excursion. Imposing the standard assumptions of an ideal fluid being incompressible, inviscid and with a flat bottom leads to the Euler equations as previously discussed. Though, there are still several reasonable restrictions that can be made to further simplify the system for certain applications. We will mainly follow the standard derivation of 'potential theory' given in [37] with some additional notes.

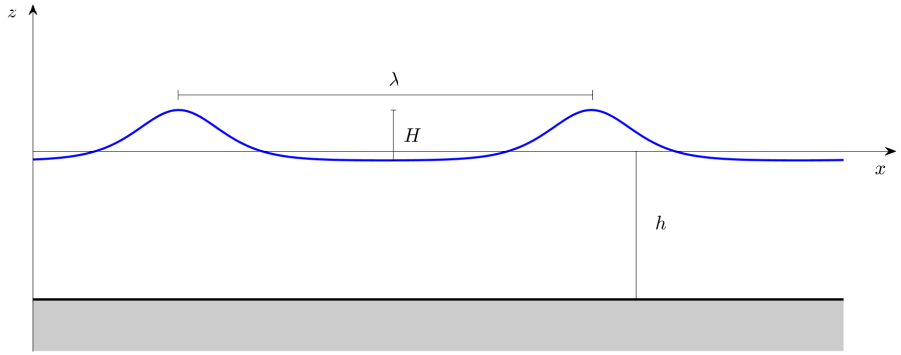

Fig. 1.1 Cnoidal wave propagating over a flat bottom.

First, we are interested in describing long waves allowing us to neglect small scale effects as surface tension. Moreover we assume that the fluid is irrotational (at least up to breaking), meaning the instantaneous rotation of the fluid or vorticity $\omega = \nabla \times \mathbf{u}$ is zero. An important consequence is the existence of a potential function ϕ such that $\mathbf{u} = \nabla\phi$. Applying the continuity equation (2) we obtain the Laplace equation:

$$\Delta\phi = 0,$$

describing the propagating part of the velocity field [45]. Another implication for an irrotational fluid can be found when looking at the advective term in the momentum equation (3). Observe,

$$\begin{aligned}\mathbf{u}\cdot\nabla\mathbf{u} &= u_j\frac{\partial u_i}{\partial x_j}\\ &= u_j(\frac{\partial u_i}{\partial x_j}-\frac{\partial u_j}{\partial x_i})+u_j\frac{\partial u_j}{\partial x_i}\\ &= -u_j\varepsilon_{ijk}\omega_k+\frac{\partial}{\partial x_i}(\frac{1}{2}u_ju_j).\end{aligned}$$

Writing (3) in terms of the velocity potential now gives

$$\nabla\{\rho\frac{\partial\phi}{\partial t}+\frac{\rho}{2}|\nabla\phi|^2+p+\rho gz\}=0,$$

or simply

$$\rho\frac{\partial\phi}{\partial t}+\frac{\rho}{2}|\nabla\phi|^2+p+\rho gz=0, \tag{1.1}$$

where the constant of integration is absorbed by redefining the velocity potential. Equation (1.1) is known as the Bernoulli equation and gives us information about the pressure acting below the surface. Though, we are interested in the development of the free surface where the pressure is atmospheric and therefore assumed constant. For simplicity, set $p = p_{atm} = 0$ at the interface $z = \eta$, which effectively neglects capillary effects.

Additional boundary conditions are needed for a well-defined system and next up is the kinematic boundary condition. This condition reflects that any fluid particle at the surface will always remain on the surface [37]. Let $z^* = \eta(x^*,t)$ denote the position of such a particle. A consequence of the previous statement is that its normal velocity must coincide with the normal velocity of the surface. Consider a small motion in space δz^* and time $t+\delta t$ then the equality must hold,

$$z^*+\delta z^* = \eta(x^*+\delta x^*, t+\delta t),$$

for it to remain on the surface. Now, Taylor expanding η around (x^*,t) gives

$$\eta(x^*+\delta x^*,t+\delta t) = \eta(x^*,t)+\frac{\partial\eta}{\partial x^*}\delta x^*+\frac{\partial\eta}{\partial t}\delta t+\mathcal{O}(\delta^2),$$

and in turn implies,

$$z^* + \delta z^* = \eta(x^*,t) + \frac{\partial \eta}{\partial x^*}\delta x^* + \frac{\partial \eta}{\partial t}\delta t.$$

On the surface we have that $z^* = \eta$, and therefore these terms cancel. Taking the limit we observe

$$\lim_{\delta t \to 0} \frac{\delta z^*}{\delta t} = \lim_{\delta t \to 0} \frac{\partial \eta}{\partial x}\frac{\delta x^*}{\delta t} + \frac{\partial \eta}{\partial t}.$$

Recognizing the vertical component v of the fluid velocity at the surface and the material derivative on the right, or in terms of the velocity potential yields

$$\frac{\partial \phi}{\partial z} = \frac{\partial \phi}{\partial x}\frac{\partial \eta}{\partial x} + \frac{\partial \eta}{\partial t}, \tag{1.2}$$

for $z = \eta$. This intuitive approach shows that a particle in the boundary surface will remain there and follow the normal velocity of the surface whenever equation (1.2) holds. Of course this holds in general, there is no flow through an impervious boundary or body and this brings us to the last condition, namely that there is no flow through the bottom surface. Meaning the velocity normal of the fluid normal to the ground must be zero and given by

$$\frac{\partial \phi}{\partial z} = 0, \tag{1.3}$$

for $z = -h$. The nonlinear problem is then fully described by the following equations

$$\phi_{xx} + \phi_{zz} = 0 \quad \text{for} \quad -h < z < \eta(x,t). \tag{1.4}$$

Subject to the conditions

$$\phi_z = 0 \quad \text{on} \ \ z = -h, \tag{1.5}$$

$$\eta_t + \phi_x \eta_x - \phi_z = 0 \quad \text{on} \ \ z = \eta(x,t), \tag{1.6}$$

$$\phi_t + \frac{1}{2}(\phi_x^2 + \phi_z^2) + g\eta = 0 \quad \text{on} \ \ z = \eta(x,t). \tag{1.7}$$

This system is still a very complicated and highly nonlinear model describing water waves in a fairly general setting. The plan for the remainder of the chapter will be devoted to making additional simplifications of the system defined above.

1.1 Linear wave theory

The simplest system is given by the linearized equations for 'deep water waves'. These waves are characterized by the assumption that the amplitude a, of oscillation of the free surface is small in the sense that both a/λ and a/h are much smaller than unity. Imposing these conditions one can show that the nonlinear terms may be excluded using a dimensional argument [37] where λ is the wavelength. Consider the non-dimensional quantities denoted with $(\tilde{\cdot})$,

$$x = \lambda\tilde{x}, \qquad z = h_0\tilde{z}, \qquad t = \frac{\lambda}{c_0}\tilde{t}, \qquad \phi = \frac{ga\lambda}{c_0}\tilde{\phi}, \qquad \eta = a\tilde{\eta}. \tag{1.8}$$

Here c_0 denotes the limiting long-wave speed $c_0 = \sqrt{gh_0}$. Substituting the non-dimensional variables into kinematic boundary equation (1.6) yields,

$$\tilde{\eta}_t + \frac{a}{\lambda}\tilde{\phi}_{\tilde{x}}\tilde{\eta}_{\tilde{x}} - \tilde{\phi}_{\tilde{z}} = 0,$$

allowing us to neglect the nonlinear term. Similarly for equation (1.7) we get

$$\tilde{\phi}_{\tilde{t}} + \frac{1}{2}(\frac{a}{\lambda}\tilde{\phi}_{\tilde{x}}^2 + \frac{a}{h_0}\tilde{\phi}_{\tilde{z}}^2) + \tilde{g}\tilde{\eta} = 0.$$

We may therefore neglect the nonlinear term given the assumption $a/\lambda << 1$ and $a/h_0 << 1$. Also, it is given that the wave elevation η is proportional with the amplitude a, which means we can evaluate the boundary condition at $z = 0$ rather than η. This is observed using a Taylor expansion around zero

$$\phi(x, z = \eta, t) = \phi(x, z = 0, t) + \frac{\partial\phi}{\partial z}\eta + ...$$

In non-dimensional terms gives

$$a\omega\lambda\tilde{\phi}(x, z = \eta, t) = a\omega\lambda\tilde{\phi}(x, z = 0, t) + \frac{a\omega\lambda}{h_0}\frac{\partial\tilde{\phi}}{\partial z}a\tilde{\eta} + ...$$

and may be simplified to recognize terms of higher-order

$$\tilde{\phi}(x, z = \eta, t) = \tilde{\phi}(x, z = 0, t) + \frac{a}{h_0}\frac{\partial\tilde{\phi}}{\partial\tilde{z}}\tilde{\eta} + \mathcal{O}(\frac{a^2}{h_0^2}).$$

Neglecting the terms containing a/h_0 allows us to evaluate the free surface conditions at $z = 0$ in this regime. Summing up the results we have the following theorem (see also [37]).

1.1.1 Periodic wave solution in linear theory

Theorem 1. *The linearized problem describing long gravity waves is fully described by the Laplace equation within the fluid domain,*

$$\phi_{xx} + \phi_{zz} = 0 \qquad \text{for} \quad -h < z < 0, \tag{1.9}$$

and is subject to the boundary conditions:

$$\frac{\partial \phi}{\partial z} = 0 \qquad \text{on} \quad z = -h, \tag{1.10}$$

$$\frac{\partial \phi}{\partial z} = \frac{\partial \eta}{\partial t} \qquad \text{on} \quad z = 0, \tag{1.11}$$

$$\frac{\partial \phi}{\partial t} = -g\eta \qquad \text{on} \quad z = 0, \tag{1.12}$$

with traveling-wave solution

$$\phi(x,z,t) = \frac{a\omega}{k} \frac{\cosh(k(z+h))}{\sinh(kh)} e^{ik(x-ct)}. \tag{1.13}$$

Additionally it follows that

$$\omega^2 = gk\tanh(kh), \tag{1.14}$$

and is known as the dispersion relationship, describing the relation between the angular frequency ω and the wavenumber k.

Proof. We will use the method 'separation of variables' assuming the solution takes the form

$$\phi(x,z,t) = f(z)\Lambda(x,t). \tag{1.15}$$

Continuing, we may use the Laplace equation (1.9) to retrieve additional information. Observe,

$$-\frac{f''(z)}{f(z)} = \frac{1}{\Lambda(x,t)} \frac{\partial^2 \Lambda(x,t)}{\partial x^2}. \tag{1.16}$$

Since the two expressions are equal and independent of their respective variables they must be equal to a constant $-k^2$. Moreover we seek a traveling-wave solution. Therefore, take $\Lambda(x,t) = g(\xi)$ with $\xi = x - ct$, describing a right moving wave with speed c and of constant form g. By (1.16) we have:

$$\frac{\partial^2 \Lambda}{\partial x^2} + k^2 \Lambda = 0,$$

and implies

$$\frac{dg(\xi)}{d\xi} + k^2 g(\xi) = 0,$$

and is a well-known ODE with solution

$$\Lambda(x,t) = g(x-ct) = ae^{ik(x-ct)}.$$

It is clear that the wave is moving sinusoidally with amplitude a. Returning to equation (1.16) we must also solve the differential equation

$$\frac{d^2 f(z)}{dz^2} - k^2 f(z) = 0.$$

Using the characteristic equation we find the solution

$$f(z) = Ae^{kz} + Be^{-kz}.$$

Now, impose the condition of no flow through the bottom given by equation (1.10):

$$B = Ae^{-2kh_0}.$$

Next, use the condition for the motion of the surface (1.11), resulting in

$$k(A-B) = a\omega.$$

with $c = \omega/k$. Combining the results yield

$$A = \frac{a\omega}{k(1-e^{-2kH})} \qquad \text{and} \qquad B = \frac{a\omega e^{-2kH}}{k(1-e^{-2kH})},$$

and from our original assumption, (1.15) we get the following velocity potential

$$\phi(x,z,t) = \frac{a\omega}{k}\left\{\frac{1}{1-e^{-2kH}}(e^{kz} + e^{-kz-2kH})\right\}\sin(kx-\omega t),$$

or simply

$$\phi(x,z,t) = \frac{a\omega}{k}\frac{\cosh(k(z+h_0))}{\sinh(kh_0)}e^{ik(x-ct)}.$$

Finally, we may use the linearized Bernoulli equation (1.12) to find the relationship between the wavenumber and frequency. We have that

$$\frac{\partial \phi}{\partial t}|_{z=0} = -g\eta,$$

and implies

$$-\frac{a\omega^2}{k}\frac{\cosh(k(z+h))}{\sinh(kh)}\Big|_{z=0} e^{i(kx-\omega t)} = -gae^{i(kx-\omega t)}.$$

We may therefore write,

$$\omega^2 = gk\tanh(kh).$$

The relation between frequency ω, and wavenumber k is known as the dispersion relationship which is what we wanted to find and completes the proof.

□

Remark 1. *The linear regime only holds for fairly long waves at a sufficient depth. A better model is typically found by the use of some kind of asymptotic approximation to the Euler equations. For instance, we turn to the Korteweg-de Vries (KdV) equation if there is a need to include nonlinear and dispersive effects. This is the subject of the next section.*

1.2 The KdV equation

The Korteweg-de Vries equation (KdV) models unidirectional waves that are weakly nonlinear and weakly dispersive. In addition, it is useful to define the relative amplitude $\alpha = a/h_0$ and the relative wavenumber as $\beta = h_0^2/\lambda^2$, where a denotes a representative amplitude and λ a representative wavelength. Using an asymptotic expansion and a dimensional argument we may neglect terms of order $\mathcal{O}(\alpha^2, \alpha\beta, \beta^2)$, covering a wide range of long waves that are interesting from the viewpoint of applications. Following the outline in [69], we first assume the velocity potential takes the form:

$$\phi(x,z,t) = \sum_{n=0}^{\infty} f_n(x,t)z^n.$$

We also assume for a moment that $z = 0$ at the horizontal bottom. To find the form of ϕ we apply the Laplace operator. Computing the derivatives gives

$$\sum_{n=0}^{\infty} \frac{\partial^2 f_n}{\partial x^2} z^n + \sum_{n=2}^{\infty} n(n-1) f_n z^{n-2} = 0.$$

Translate and factor the z^n term

$$\sum_{n=0}^{\infty} \{z^n [\frac{\partial^2 f_n}{\partial x^2} + (n+2)(n+1) f_{n+2}]\} = 0,$$

and should hold for all $z \in \mathbb{R}$, which in turn implies

$$f_{n+2} = \frac{-1}{(n+2)(n+1)} \frac{\partial^2 f_n}{\partial x^2}.$$

Note that we imposed that $f_1 = 0$ due to the condition $\phi_z|_{z=0} = 0$. Solving the recursive relation will reveal the form of ϕ. Noting that only even terms appear we may put $n = 2n$:

$$f_{2n} = \frac{-1}{2n(2n-1)} \frac{\partial^2 f_{2n-2}}{\partial x^2} = \frac{1}{2n(2n-1)(2n-2)(2n-3)} \frac{\partial^4 f_{2n-4}}{\partial x^4} = \ldots = \frac{(-1)^n}{(2n)!} \frac{\partial^{2n} f_0}{\partial x^{2n}}.$$

Therefore, the general form of the problem must be given by

$$\phi(x,z,t) = \sum_{n=0}^{\infty} (-1)^n \frac{z^{2n}}{(2n)!} \frac{\partial^{2n} f}{\partial x^{2n}}, \tag{1.17}$$

where $f = f_0$. Now, before we deliberate on the boundary conditions, it is useful to write the equations in non-dimensional terms using the previously defined scaling (1.8). For simplicity we drop the $(\tilde{\cdot})$ notation, then the Laplace equation becomes:

$$\nabla^2 \phi = \frac{g\lambda a}{c_0 \lambda^2} \frac{\partial^2 \phi}{\partial x^2} + \frac{g\lambda a}{c_0 h_0^2} \frac{\partial^2 \phi}{\partial z^2} = 0.$$

Next, factor the relative amplitude and wavenumber

$$\beta \frac{\partial^2 \phi}{\partial x^2} + \frac{\partial^2 \phi}{\partial z^2} = 0. \tag{1.18}$$

Having handled the Laplace operator we now turn to the the boundary conditions. With the current scaling we must evaluate z^* at $h_0 + \eta^*$ or in non-dimensional terms $z = 1 + \alpha\eta$. Repeating the process as above for the kinematic boundary condition (1.6), one can show after some simplifications that

$$\eta_t + \alpha \phi_x \eta_x - \frac{1}{\beta} \phi_z = 0, \tag{1.19}$$

on $z = 1 + \alpha\eta$. The same can also be done for the Bernoulli equation on the boundary, and gives

$$ga\phi_t + (\frac{ga}{c_0})^2\frac{\phi_x^2}{2} + (\frac{g\lambda a}{c_0 h_0})^2\frac{\phi_z^2}{2} + ga\eta = 0.$$

Resulting in

$$\phi_t + \frac{1}{2}\alpha\phi_x^2 + \frac{1}{2}\frac{\alpha}{\beta}\phi_z^2 + \eta = 0.$$

Now that we have every equation written in non-dimensional terms we would like to apply the expansion for ϕ. Its non-dimensional form reads

$$\phi = \sum_{n=0}^{\infty}(-1)^n\frac{z^{2n}}{(2n)!}\frac{\partial^{2n}f}{\partial x^{2n}}\beta^n.$$

Plug it into the kinematic boundary condition (1.6):

$$\eta_t + \alpha[\sum_{n=0}^{\infty}(-1)^n\frac{z^{2n}}{(2n)!}\frac{\partial^{2n+1}f}{\partial x^{2n+1}}\beta^n]\eta_x - \frac{1}{\beta}[\sum_{n=1}^{\infty}(-1)^n\frac{z^{2n-1}}{(2n-1)!}\frac{\partial^{2n}f}{\partial x^{2n}}\beta^n] = 0.$$

After some rearrangement and neglecting terms containing powers of β, the equation yields

$$\eta_t + \alpha f_x\eta_x + zf_{xx} - \{\frac{z^3}{6}f_{xxxx}\beta + \frac{z^2}{2}f_{xxx}\eta_x\beta\} + \mathcal{O}(\beta^2) = 0.$$

This is a boundary condition on the free surface, so we have that $z = 1 + \alpha\eta$. Thus,

$$\eta_t + \{(1+\alpha\eta)f_x\}_x - \{\frac{1}{6}(1+\alpha\eta)^3 f_{xxxx} + \frac{1}{2}(1+\alpha\eta)^2\eta_x f_{xxx}\}\beta + \mathcal{O}(\beta^2) = 0, \quad (1.20)$$

noting that we also factored one term due to the product rule. Finally, repeating the same procedure we obtain an equation for the equation of motion

$$\eta + f_t + \frac{1}{2}\alpha f_x^2 - \frac{1}{2}(1+\alpha\eta)^2\{f_{xxt} + \alpha f_x f_{xx} - \alpha f_{xx}^2\}\beta + \mathcal{O}(\beta^2) = 0. \quad (1.21)$$

Simplification can be made to both equations when considering the expansion of ϕ_x

$$\phi_x = f_x - \frac{z^2}{2}f_{xxx}\beta + \mathcal{O}(\beta^2). \quad (1.22)$$

Neglecting terms containing β we see that $\phi_x = f_x$, being the velocity in the $x-$component of u. Another observation, taking our two equations (1.20) and differentiate (1.21) with

respect to x and neglecting all terms containing β, one can easily verify that it simplifies to the shallow-water equations. Though, attaining the correct order leads to the Boussinesq equations:

$$\eta_t + \{(1+\alpha\eta)u\}_x - \frac{1}{6}\beta u_{xxx} + \mathcal{O}(\alpha\beta, \beta^2) = 0, \tag{1.23}$$

$$u_t + \alpha u u_x + \eta_x - \frac{1}{2}\beta u_{xxt} + \mathcal{O}(\alpha\beta, \beta^2) = 0. \tag{1.24}$$

We are interested in a simpler model, considering only unidirectional waves. Combining this assumption with the observation that the Boussinesq equations at lowest order is reduced to a system of transport equations

$$\eta_t + \eta_x = 0,$$
$$u_t + \eta_x = 0,$$

and must have the solution $\eta = u$. We deduce the solution at the correct order on the form

$$u = \eta + \alpha A + \beta B + \mathcal{O}(\alpha^2 + \beta^2).$$

Additionally, from the transport equation we must have $\eta_t = -\eta_x + \mathcal{O}(\alpha, \beta)$. Using equation (1.23) and (1.24) one can choose the functions A and B in terms of η and η_x such that both equations are consistent. Indeed,

$$\eta_t + \eta_x + \alpha(A_x + 2\eta\eta_x) + \beta(B_x - \frac{1}{6}\eta_{xxx}) + \mathcal{O}(\alpha^2 + \beta^2) = 0,$$
$$\eta_t + \eta_x + \alpha(A_t + \eta\eta_x) + \beta(B_t - \frac{1}{2}\eta_{xxt}) + \mathcal{O}(\alpha^2 + \beta^2) = 0,$$

arguing by consistency and the fact that the solution satisfies the transport equation to first-order gives

$$2A_x + \eta\eta_x = 0,$$
$$2B_x - \frac{2}{3}\eta_{xxx} = 0.$$

Clearly, $A = -\frac{1}{4}\eta^2$ and $B = \frac{1}{3}\eta_{xx}$, gives rise to the horizontal velocity

$$u = \eta - \frac{1}{4}\alpha\eta^2 + \frac{1}{3}\beta\eta_{xx} + \mathcal{O}(\alpha^2 + \beta^2), \tag{1.25}$$

and the famous Korteweg-de Vries equation

$$\eta_t + \eta_x + \frac{3}{2}\alpha\eta\eta_x + \frac{1}{6}\beta\eta_{xxx} + \mathcal{O}(\alpha^2 + \beta^2) = 0, \tag{1.26}$$

or in dimensional form

$$\eta_t + c_0(1 + \frac{3}{2}\frac{\eta}{h_0})\eta_x + \frac{h_0^2}{6}\eta_{xxx} = 0. \tag{1.27}$$

1.2.1 Some useful quantities in the KdV equation

Before proceeding with the solution of constant form in the KdV approximation, we find it useful to summarize some of the results. First, we simplify the notation by setting $\varepsilon = \alpha = \beta$ since $\mathcal{O}(\varepsilon^2) = \mathcal{O}(\alpha^2, \alpha\beta, \beta^2)$ are neglected terms. The non-dimensional form of the KdV equation is then given by

$$\eta_t + \eta_x + \frac{3}{2}\varepsilon\eta\eta_x + \frac{1}{6}\varepsilon\eta_{xxx} = 0.$$

It will later turn out that some useful quantities in this context are: ϕ_x and the dynamic pressure P, when deriving balance equations in the KdV equation in Section 2.2.1 and convergence proofs to the full Euler system in Chapter 3. The first quantity is given by

$$\phi_x = f_x - \frac{z^2}{2}\varepsilon f_{xxx} + \mathcal{O}(\varepsilon^2).$$

where f_x is the horizontal velocity u, given by equation (1.25):

$$u = \eta - \frac{1}{4}\varepsilon\eta^2 + \frac{1}{3}\varepsilon\eta_{xx} + \mathcal{O}(\varepsilon^2).$$

Substituting this expression and neglecting higher-order terms leads to

$$\phi_x = \eta - \frac{1}{4}\varepsilon\eta^2 + \varepsilon(\frac{1}{3} - \frac{z^2}{2})\eta_{xx} + \mathcal{O}(\varepsilon^2).$$

By a similar procedure we have that

$$\phi_z = -\varepsilon f_{xx} + \mathcal{O}(\varepsilon^2),$$

form the asymptotic expansion. From the relation $f_x = u = \eta + \mathcal{O}(\varepsilon)$, it follows that

$$\phi_z = -\varepsilon\eta_x + \mathcal{O}(\varepsilon^2).$$

Next, we would like to express the pressure in terms of the surface elevation η satisfying the KdV equation. This can be done by considering the dynamic pressure $P' = P - P_{atm} + gz$ and use the Bernoulli equation within the fluid domain [61] to find:

$$P' = -\phi_t - \frac{1}{2}|\nabla\phi|^2.$$

Applying the same dimensional arguments as before together with the expansion (1.17) leads to

$$P' = \eta - \frac{1}{2}\varepsilon(z^2-1)\eta_{xx} + \mathcal{O}(\varepsilon^2).$$

The same expression can also be found in [5, 6]. We will later use these expressions to form a system of the shoaling process, but we first need the traveling-wave solution of η satisfying the KdV equation.

1.2.2 Cnoidal wave solution

We will later present an explicit model describing the shoaling of long waves up a gently sloping beach. The idea is to use the well-known cnoidal wave solution for periodic waves in the KdV equation to approximate the deformation of η. The solution of the KdV equation for waves of constant form was first discovered by Korteweg and deVries in 1895 [36] and we will first offer some brief remarks. This will in turn help us better understand the system in the end. With that said, we proceed by assuming the traveling-wave solution of constant shape

$$\eta(x,t) = h_0 f(\xi(x,t)) = h_0 f(x-ct).$$

Consequently, one can be verify that the KdV equation (1.27) reduces to an ODE on the form

$$(1-\frac{c}{c_0})f' + \frac{3}{2}ff' + \frac{h_0^2}{6}f''' = 0.$$

First integrate the above equation,

$$(1-\frac{c}{c_0})f + \frac{3}{4}f^2 + \frac{h_0^2}{6}f'' + A = 0,$$

then multiply with f' and integrate once more to obtain

$$-\frac{h_0^2}{3}\left(\frac{df}{d\xi}\right)^2 = F(f) = f^3 + 2\left(1-\frac{c}{c_0}\right)f^2 + Af + B, \tag{1.28}$$

with $A, B \in \mathbb{R}$ being constants of integration. There are several solutions to this differential equation, but for practical application we only seek real bounded solutions of the wave-profile f [17].

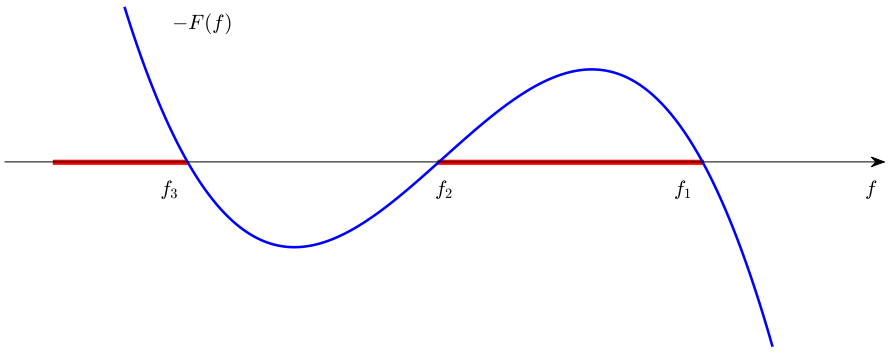

Fig. 1.2 The red lines denotes the values of f such that $-F \geq 0$ and f_1, f_2, f_3 are its roots.

First, we want the solution to be real, i.e. from (1.28) we see that $-F(f)$ must be positive. Also, assuming there are three distinct roots such that $f_3 < f_2 < f_1$ allows us to write

$$F(f) = (f-f_1)(f-f_2)(f-f_3). \tag{1.29}$$

In order to understand the behavior of the polynomial $F(f)$ for particular values of c, A and B one can simply plot the function. From Figure 1.2, there is a region between f_2 and f_1 such that f only omits real values. Furthermore, having solutions such that $f_2 \leq f \leq f_1$ will describe the free surface in between the trough and crest at f_2 and f_1, respectively. As a result, we denote the waveheight at any point by the difference $H = f_1 - f_2$. Returning to the ODE, we have

$$\frac{df}{d\xi} = \pm\frac{\sqrt{3}}{h_0^2}\sqrt{(f-f_1)(f-f_2)(f-f_3)}, \tag{1.30}$$

from which we deduce the implicit solution

$$\int_{\xi_1}^{\xi} d\xi' = \pm\frac{h_0^2}{\sqrt{3}}\int_{f_1}^{f(\xi)} \frac{dz}{\{(z-f_1)(z-f_2)(z-f_3)\}^{\frac{1}{2}}}. \tag{1.31}$$

Now substitute $z = f_1 + (f_2 - f_1)\sin^2\theta$ with the Jacobian $\frac{dz}{d\theta} = 2(f_2 - f_1)\sin\theta\cos\theta$. It follows after some simplification

$$\xi = \xi_1 \pm \frac{2h_0^2\sqrt{f_2 - f_1}}{\sqrt{3}} \int_0^{\varphi(\xi)} \frac{\cos\theta d\theta}{\{(f_1 + (f_2 - f_1)\sin^2\theta - f_2)(f_1 + (f_2 - f_1)\sin^2\theta - f_3)\}^{\frac{1}{2}}}.$$

Factoring common terms in the denominator and defining $m = \frac{f_1 - f_2}{f_1 - f_3}$ will simplify the expression, resulting in an elliptic integral with known solution:

$$\xi = \xi_1 \mp \frac{2h_0^2}{\sqrt{3(f_1 - f_3)}} \int_0^{\varphi(\xi)} \frac{d\theta}{\{1 - m\sin^2\theta\}^{\frac{1}{2}}},$$

satisfying the relation (see [39])

$$\cos\varphi = \mathrm{cn}\Big(\frac{\xi - \xi_1}{\sigma} \mid m\Big),$$

where $\sigma^2 = \frac{4}{3(f_1 - f_3)}$. Considering the transformation $z = f_1 + (f_2 - f_1)\sin^2\theta$, it is clear that the solution of f is given implicitly in terms of φ by

$$\begin{aligned} f &= f_1 + (f_2 - f_1)\sin^2\varphi \\ &= f_1 + (f_2 - f_1)(1 - \cos^2\varphi) \\ &= f_2 + (f_1 - f_2)\mathrm{cn}^2\Big(\frac{\xi - \xi_1}{\sigma} \mid m\Big). \end{aligned}$$

Furthermore, half a wavelength corresponds to integrating (1.31) from trough to crest, or setting the angle $\varphi = \frac{\pi}{2}$:

$$\lambda = 2\sigma \int_0^{\frac{\pi}{2}} \frac{d\theta}{\sqrt{1 - m\sin^2\theta}} = 2\sigma K(m). \tag{1.32}$$

The integral formulation is known as the complete elliptic integral of the first kind [17, 39]. Also, comparing (1.28) and (1.29), we may express the wavespeed as

$$c = c_0\Big(1 + \frac{f_1 + f_2 + f_3}{2h_0}\Big).$$

Returning the solution to its original variables and dropping the face shift and substituting $\lambda = cT$ in conjunction with (1.32), we get the following expression

$$\eta(x,t) = f_2 - H\mathrm{cn}^2\Big(2K(m)(\frac{t}{T} - \frac{x}{\lambda}), m\Big), \tag{1.33}$$

for traveling wave solutions of constant form in the KdV equation. The shape of the cnoidal wave solution is therefore uniquely determined by the three roots f_1, f_2 and f_3. For convenience, we would like to express these roots in terms of m, H and the mean surface level $\overline{\eta}$. We observe,

$$\begin{aligned}\overline{\eta} &= \frac{1}{T}\int_0^T \eta dt \\ &= f_2 - H\frac{1}{T}\int_0^T \mathrm{cn}^2\Big(2K\frac{t}{T}\Big)dt \\ &= f_2 - \frac{H}{2K}\int_0^{2K} \mathrm{cn}^2(u)du,\end{aligned}$$

where

$$\int_0^{2K} cn^2(u)du = \frac{2}{m}E(m) - \frac{1-m}{m}2K(m),$$

as given in Abramowitz and Stenguns book on special functions [3]. Hence, the mean surface level is expressed by

$$\overline{\eta} = f_2 + \frac{H}{mK(m)}\Big(E(m) - (1-m)K(m)\Big). \tag{1.34}$$

Using the definition of $m = \frac{f_1-f_2}{f_1-f_3}$ we may manipulate the expression (1.34) and solve for f_3. This result in the following implicit relation

$$f_3 = \overline{\eta} - (f_1 - f_3)\frac{E(m)}{K(m)}.$$

Now, recalling the expression for waveheight given by $H = f_1 - f_2$ allows us to write

$$\begin{cases} f_3 &= \overline{\eta} - \frac{HE(m)}{mK(m)}, \\ f_1 &= f_3 + \frac{H}{m}, \\ f_2 &= f_1 - H. \end{cases} \tag{1.35}$$

Clearly, having the waveheight H, the modulus m, and the mean surface level $\overline{\eta}$ is enough to determine the surface profile at a specific depth. This will be the subject of Chapter 2, where we use conservation principles to determine these three parameters.

Chapter 2

Applications to cnoidal shoaling

This Chapter is devoted to modeling the development of surface waves across a sloping bottom profile. Our main goal is the prediction of the waveheight of a periodic wave as it enters an area of shallow depth using conservation laws. The numerical modeling of the nearshore zone has all but replaced the traditional methods of finding the development of a shoaling wave. The traditional method is based on the observation that the energy flux of a wave is conserved as it shoals on a gentle beach, since the flow velocity at the bottom is tangent to the bottom. While the conservation of energy flux has been replaced with the conservation of wave action in spectral models, it can be used to obtain a quick estimate of the expected waveheight using linear wave theory. This classical approach can be found in textbooks on coastal engineering, such as [16, 65], and will be presented in Section 2.1. The proceeding sections contain new work based on these classical ideas, and is submitted for publication [51].

The linear relation works well for a wave of moderate amplitude. For large-amplitude waves, it can be replaced by the Dean-Dixon method, but this is more computationally demanding. A good compromise can be reached by using periodic waves described by the KdV equation. This works for waves of moderate amplitude. Of course large-amplitude waves are breaking, and it can also be presumed that large amplitude waves are changing so rapidly that the steady theory ceases to be applicable. Thus, it can be gathered that the KdV approach appears to be the best compromise. The approach was used by Svendsen Buhr Hansen (SBH), and found to be good compared to experimental data [66]. However, there was one problem. SBH used KdV in connection with the linear formulation of the energy flux. Unfortunately, this led to a discontinuity at the matching point between the linear shoaling equation given by (2.2) and the nonlinear theory based on the KdV. To remedy this issue, a fully nonlinear expression will be derived in Section 2.2. Here we will derive the energy balance and momentum balance in the context of the KdV as outlined in [6]. Building on that

work, we derive a new expression for radiation stress in Section 2.3, which will include the effects of set-down of mean surface level. Where set-down is a well-established phenomenon due to the breaking of waves and plays an important role to understand potential run-up on a beach [46, 47].

2.1 Conservation laws in linear theory and linear shoaling

In order to get a better understanding of the model we give a brief presentation of shoaling in linear theory. In a nutshell, the waveheight of a shoaling wave is obtained by imposing conservation of the energy flux Ec_g, where E is the energy density,

$$E = \frac{1}{\lambda}\int_0^{\lambda}\int_{-h}^{0}\Big\{\frac{\rho}{2}|\nabla\phi|^2 + \rho g z\Big\}dzdx,$$

and c_g is the group velocity defined by

$$c_g = \frac{d\omega}{dk}, \tag{2.1}$$

known as the velocity of for the overall envelope of a wave train. Now, using the solution of the velocity potential from Section 1.1.1 we can show that the total energy is given by

$$E = \frac{1}{8}\rho g H^2,$$

and

$$c_g = \frac{c}{2}\Big[1 + \frac{2kh}{\sinh(2kh)}\Big],$$

when computing the integrals and taking the derivative (see for example [37, 16]). As a result, assuming no reflection, energy conservation implies

$$H = H_0\sqrt{\frac{c_{g0}}{c_g}}. \tag{2.2}$$

Meaning, the waveheight H at current local depth is determined by the waveheight at previous depth (subscript '0'), the group velocity which is a function of the wavenumber and is given by the dispersion relation (1.14). Namely, imposing conservation of period T, we may insert it into the dispersion relation

$$\frac{2\pi}{T} - gk\tanh(kh) = 0,$$

solving the nonlinear equation for k, which in turn allows us to determine H by (2.2).

This simple procedure is presented in the code below using MATLAB syntax [48].

```
function [H, h] = LinearShoaling(L0, H0, h0)
% ------------------------------------------------------------------------
% This function computes the waveheight using the theory of linear
% wave shoaling.

% Input:  L0 - original wavelength at deep water
%         H0 - original waveheight at deep water
%         h0 - initial local depth

% Output: H - waveheight
%         h - depth
% ------------------------------------------------------------------------
    % Parameters
    g = 9.81;                                   %% gravity
    K0 = 2*pi/L0;                               %% wavenumber
    w = sqrt(g*K0*tanh(K0*h0));                 %% circ. frequency
    cg0 =(1+2*K0*h0/sinh(2*K0*h0))*w/(2*K0);    %% Initial group velocity

    % Run linear shoaling from current depth while H/L>0.1
    LocalDepth = linspace(h0,0,k)
    i=0;
    while h/L>0.1
        i = i+1;
        h = LocalDepth(i);

        % Use nonlinear solver to find the wavenumber K
        K = fsolve(@(K) w^2-g*K*tanh(K*h), K0, options);

        % New group velocity
        cg =(1+(2*K*h)/sinh(2*K*h))*w/(2*K);

        % Store waveheight
        H(i) = H0*sqrt(cg0/cg);

        % Update values for next step
        H0 = H(i); h0 = h; L0 = 2*pi/K;
        K0 = 2*pi/L0;
        w = sqrt(g*K0*tanh(K0*h0));
        cg0 =(1+2*K0*h0/sinh(2*K0*h0))*w/(2*K0);
    end
end
```

2.1.1 Numerical experiment

We will now consider a numerical experiment using the linear shoaling equation (2.2). The comparison is based on experimental data observed in a wave tank by Svendsen and Brink-Kjær [67]. These waves were produced by a wavemaker, where the waves propagated initially at a constant depth of 36 cm until it reached a gently slope with steepness 1 : 35. In turn, this leads to a deformation of the initial wave-profile. The idea is now to use the initial wave-profile as deep water data and apply the shoaling equation to approximate the deformation. A schematic of the process is shown below.

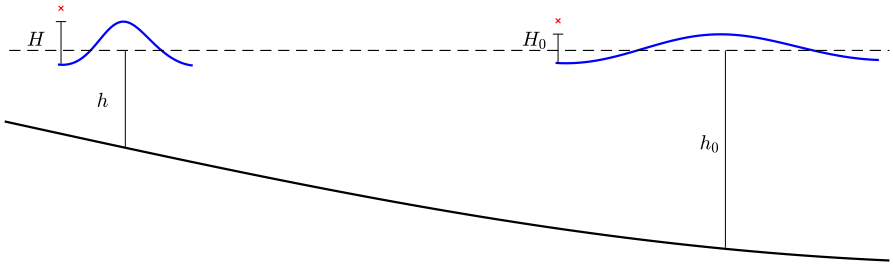

Fig. 2.1 Deep water waves propagating up a gently sloping beach with same frequency and carrying an equal amount of energy. The red crosses denotes the waveheight measured from the stippled line, representing the still water level.

In Figure 2.1, a deep water wave is propagating up a gently sloping beach with initial deep water parameters H_0, h_0 and at a certain period T, from which we find the deep water wavelength (see [37] for the deep water approximation of the wavelength):

$$\lambda_0 = \frac{g}{2\pi} T^2.$$

Now, imposing conservation of period and energy flux will allow us to use the scheme presented in the previous section and solve for the development of the wave-profile near the shore. We will run the code for a deep water wave characterized by the non-dimensional numbers

$$\frac{H_0}{\lambda_0} = 0.0099 \quad \text{and} \quad T\sqrt{\frac{g}{h}} = 8.70.$$

The result of this scenario is depicted in Figure 2.2, with depth on the $x-$axis decreasing from right to left and waveheight plotted on the $y-$axis in centimeters. The solid blue line is a result of the linear shoaling theory, while the stippled line is the result of higher-order theory discussed in the next section. Further, the red crosses are experimental data collected in [67].

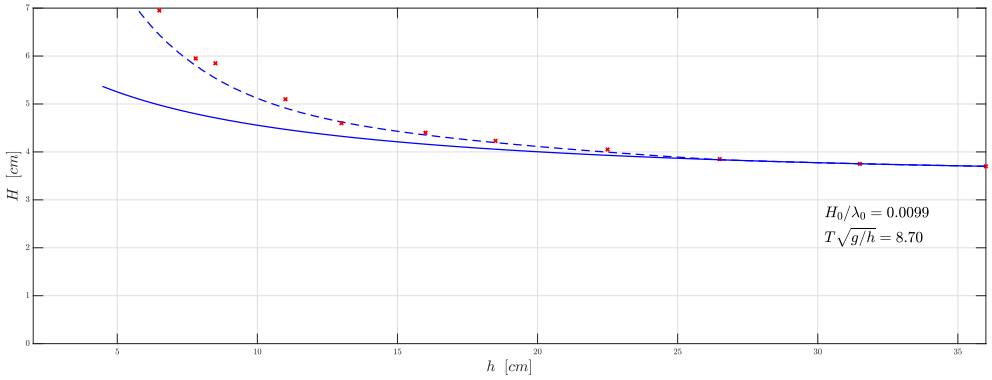

Fig. 2.2 Deep water wave characterized by $\frac{H_0}{\lambda_0} = 0.0099$ and $T\sqrt{\frac{g}{h}} = 8.70$. Solid blue line denotes waveheight in linear theory, stippled blue line is higher order theory in the context of the KdV equation and red crosses denotes measurements found in [67].

We observe that the result in Figure 2.2 that there is fairly good agreement in the deep water region. Though, as the wave reaches the shore the linear theory fails to predict the waveheight compared to the experimental data. This is natural if we recall the basic assumption of linear theory from Section 1.1 was imposing the criterion; amplitude over wavelength is small compared to unity. A measure of the validity of the linear theory in terms of wavenumber and amplitude is given by

$$k\frac{H}{2} << 1, \tag{2.3}$$

as $k = \frac{2\pi}{\lambda}$. Returning now to the case considered in Figure 2.2, the number specified by (2.3) ranges from a value of 0.04 in the start to 0.10 at $h = 5.0$ cm. A clear quantification for when the theory is valid is hard to give, but at least the example gives an indication on when it fails to work. In that regard, in order to get further into the shoaling region we need a higher-order approximation of the shoaling process. Analogous theory will now be developed in the KdV regime, using the cnoidal wave solution to approximate the deformation of the waveheight using conservation principles. Note also that the MATLAB code runs the linear shoaling algorithm while local depth and the wavelength in deep water satisfy $h/\lambda_0 > 0.1$. At this

point the cnoidal theory is found to be valid [60] and is the subject of the proceeding sections of this chapter.

2.2 Conservation laws in the KdV equation

Conservation laws in the context of the KdV equation will now be put forward to describe the shoaling process. The idea is the same as for the linear theory, namely use the traveling solution of constant form (1.33) to approximate the dynamic problem with varying depth. We also recall that fixing H, m and $\overline{\eta}$ is enough to determine any cnoidal wave. The relation between these parameters is given by the three roots (1.35), and we must therefore have three fundamental equations. We will consider two different systems.

First we will consider a system with zero set-down of mean surface level inside the shoaling region i.e. $\overline{\eta} = 0$. Further, we impose conservation of energy flux and conservation of period. This will be based on previous work where energy flux was derived in the context of the full KdV equation in [6]. Additionally, such a system has been implemented as a system of three equations in [35]. Our hope is to improve this system and write it as a single equation making more stable and allowing for computations further into the shoaling region.

Secondly, we improve on the system by dropping the assumption $\overline{\eta} = 0$. Including this additional phenomena will of course require another balance equation, and will here be written in terms of the radiation stress. Though, in order to do so we must find its representation in terms of the KdV equation. The derivation of radiation stress is given in Section 2.3 and related to momentum balance. Then again imposing conservation of energy flux and period will result in a system of three equations with three unknowns describing the shoaling process.

The structure of this chapter will first be on the derivations of conserved quantities and radiation stress in the KdV equation. Then a numerical solution strategy is given and comparisons are made with previous theory and real data retrieved from wave tank experiments.

2.2.1 Momentum and energy balance

In order to express the shoaling process in the context of the KdV equation we will need an expression of momentum and energy balance. Starting with the momentum balance law we will use the quantities derived in Section 1.2 to give an expression for momentum flux in the KdV equation. In the context of the full Euler equations with surface boundary conditions, the momentum balance is expressed by [16]:

$$\frac{\partial}{\partial t}\int_{-h_0}^{\eta}\phi_x dz+\frac{\partial}{\partial x}\int_{-h_0}^{\eta}\{\phi_x^2+P\}dz=0. \tag{2.4}$$

Written in its non-dimensional form gives

$$\frac{c_0}{l}\frac{\partial}{\partial\tilde{t}}\int_0^{1+\alpha\tilde{\eta}}\frac{ga}{c_0}\tilde{\phi}_{\tilde{x}}h_0 d\tilde{z}+\frac{1}{l}\frac{\partial}{\partial\tilde{x}}\int_0^{1+\alpha\tilde{\eta}}\{\frac{g^2a^2}{c_0^2}\tilde{\phi}_x^2+ag\tilde{P}'+gh_0(1-\tilde{z})\}h_0 d\tilde{z}=0, \tag{2.5}$$

or simply

$$\alpha\frac{\partial}{\partial\tilde{t}}\int_0^{1+\alpha\tilde{\eta}}\tilde{\phi}_{\tilde{x}}h_o d\tilde{z}+\frac{\partial}{\partial\tilde{x}}\int_0^{1+\alpha\tilde{\eta}}\{\alpha^2\tilde{\phi}_x^2+\alpha\tilde{P}'+(1-\tilde{z})\}h_0 d\tilde{z}=0, \tag{2.6}$$

using the limiting long-wave speed $c_0=\sqrt{gh_0}$. Substituting the two expressions $\tilde{\phi}_x$, $\tilde{P}'$ from Section 1.2.1 and evaluate the integral,

$$(\alpha\tilde{\eta}+\frac{3}{4}\alpha^2\tilde{\eta}^2+\frac{1}{6}\alpha\beta\,\tilde{\eta}_{\tilde{x}\tilde{x}})_{\tilde{t}}+(\frac{1}{2}+\alpha\tilde{\eta}+\frac{3}{2}\alpha\tilde{\eta}^2+\frac{1}{3}\beta\,\tilde{\eta}_{\tilde{x}\tilde{x}})_{\tilde{x}}=\mathcal{O}(\alpha^2,\alpha\beta,\beta^2).$$

From this relation, we identify the non-dimensional momentum density

$$\tilde{I}=\alpha\tilde{\eta}+\frac{3}{4}\alpha^2\tilde{\eta}^2+\frac{1}{6}\alpha\beta\,\tilde{\eta}_{\tilde{x}\tilde{x}},$$

and the non-dimensional momentum flux

$$\tilde{q}_I=\frac{1}{2}+\alpha\tilde{\eta}+\frac{3}{2}\alpha\tilde{\eta}^2+\frac{1}{3}\beta\,\tilde{\eta}_{\tilde{x}\tilde{x}}.$$

Returning the expression to its dimensional forms through the scaling $I=c_0h_0\tilde{I}$ and $q_I=c_0^2h_0\tilde{q}_I$ yields

$$I=c_0\Big(\eta+\frac{3}{4h_0}\eta^2+\frac{h_0^2}{6}\eta_{xx}\Big),$$

and

$$q_I=c_0^2\Big(\frac{h_0}{2}+\eta+\frac{3}{2h_0}\eta^2+\frac{h_0^2}{3}\eta_{xx}\Big). \tag{2.7}$$

Similarly, we can give the energy balance in the full Euler equations as

$$\frac{\partial}{\partial t}\int_{-h_0}^{\eta}\Big\{\frac{1}{2}|\nabla\phi|^2+g(z+h_0)\Big\}dz+\frac{\partial}{\partial x}\int_{-h_0}^{\eta}\Big\{\frac{1}{2}|\nabla\phi|^2+g(z+h_0)+P\Big\}\phi_x dz=0,$$

and following the same procedure as above will lead to the expressions

$$E = c_0^2\Big(\frac{1}{h_0}\eta^2 + \frac{1}{4h_o^2}\eta^3 + \frac{h_0}{6}\eta\eta_{xx} + \frac{h_0}{6}\eta_x^2\Big),$$

and

$$q_E = c_0^3\Big(\frac{1}{h_0}\eta^2 + \frac{5}{4h_0^2}\eta^3 + \frac{h_0}{2}\eta\eta_{xx}\Big), \tag{2.8}$$

denoting the energy density and energy flux respectively. Note that q_E is of second order, while the energy presented in [67] is given by

$$q_E = c_0 g\eta^2.$$

and is of first order. We will also use momentum flux q_I, to expand on the idea of radiation stress and write it in the context of the KdV equation. Adding to this, the conservation of energy flux will be included to form a well-defined system of the shoaling problem.

2.3 Radiation stress

Radiation stress plays an important role when trying to understand changes in the mean water level. With this in mind we try to expand our understanding of the concept in the context of the KdV equation using the momentum balance equation and then investigate some consequences of shoaling with respect to mean surface levels. A physical interpretation of the word radiation stress is given by Longuet-Higgins and Stewart [47] to mean "*the excess of momentum due to the presence of the waves*". Analyzing this definition in terms of gravity waves with a flat bottom one can simply think of radiation stress as the total momentum flux of a progressive wave averaged over one period minus the momentum flux for when the fluid is at rest. As previously discussed we consider a wave propagating in the $x-$direction neglecting all transverse effects, thus giving the principal component of the radiation stress in its classical presentation

$$\overline{S}_{xx} = \overline{\int_{-h_0}^{\eta}(\rho u^2 + P)dz} - \int_{-h_0}^{0}\rho g z dz.$$

The first term is expressing the total flux of momentum across a plane integrated from the bottom to the free surface and with unit width. This is given by equation (2.7) in the KdV equation when rescaled for a fluid with density ρ. Consequently, the $x-$component of the radiation stress is obtained in the context of the full KdV equation as

$$\begin{aligned}\overline{S}_{xx} &= \overline{q_I} - \int_{-h_0}^{0} \rho g z dz \\ &= \rho g h_0 \Big(\frac{h_0}{2} + \overline{\eta} + \frac{3}{2h_0}\overline{\eta^2} + \frac{h_0^2}{3}\overline{\eta}_{xx} \Big) - \frac{1}{2}\rho g h_0^2 \\ &= \rho g \Big(h_0 \overline{\eta} + \frac{3}{2}\overline{\eta^2} + \frac{h_0^3}{3}\overline{\eta}_{xx} \Big). \end{aligned} \tag{2.9}$$

There are several applications for the improved formulation (compared to [65]) of radiation stress. One area of particular interest is the study of shoaling. In this regard let us consider a deep-water wave encountering a sloping beach. Then the momentum flux is reduced in the onshore direction due to the horizontal force, which is generated by the bottom pressure acting in the direction opposing the wave.

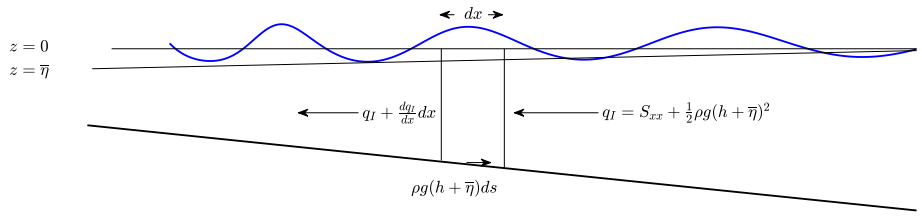

Fig. 2.3 Schematic of the forces acting on a fluid column.

As shown in [16, 46, 47] and indicated by Figure 2.3, the flux of momentum through a fluid column is given in terms of radiation stress by

$$q_I = S_{xx} + \int_{-h}^{\overline{\eta}} \rho g(\overline{\eta} - z) dz = S_{xx} + \frac{1}{2}\rho g(\overline{\eta} + h)^2,$$

when accounting for the set-down of mean surface level. Further, the flux of momentum is reduced due to the weight of the fluid $\rho g(h+\overline{\eta})ds$, with ds denoting the length element joining the planes in Figure 2.3. In other terms, one may write the pressure force exerted on the bottom as

$$\rho g(h+\overline{\eta})ds = \rho g(h+\overline{\eta})h_x dx. \tag{2.10}$$

Also, the flux of momentum across the other end of the fluid element will increase by

$$\frac{d}{dx}[S_{xx}+\frac{1}{2}\rho g(h+\overline{\eta})^2]dx. \tag{2.11}$$

Therefore, it can be seen that momentum balance requires (2.10) and (2.11) to be equal. Imposing the gently sloping criterion allows for a simplified equation and as a result the balance of momentum demands

$$\frac{dS_{xx}}{dx}+\rho g(\overline{\eta}+h)\frac{d\overline{\eta}}{dx}=0. \tag{2.12}$$

A thorough approach is given in [47], discussing the validity of the approximation. In order to develop the shoaling equation, we integrate over the control interval $[x,x+dx]$ to get

$$\int_x^{x+dx}\frac{dS_{xx}}{d\tau}d\tau+\int_x^{x+dx}\rho g\overline{\eta}\frac{d\overline{\eta}}{d\tau}d\tau+\int_x^{x+dx}\rho gh\frac{d\overline{\eta}}{d\tau}d\tau=0.$$

The first integrals are straight forward to compute, while the last integral is evaluated first by integration by parts and the trapezoidal rule. Evaluating the integrals and defining the difference of any quantity F as $\Delta F=F|_{x+dx}-F|_x$ we get,

$$\Delta S_{xx}=-\frac{\rho g}{2}\Delta\overline{\eta}^2-\frac{\rho g}{2}(h_0+h)\Delta\overline{\eta}. \tag{2.13}$$

Recall that we are interested in the averaged behavior of the waveheight for a wave-train approaching the beach. We find it useful to define the changes in radiation stress averaged over a period

$$\Delta\overline{S}_{xx}=-\frac{1}{T}\int_0^T\left\{\frac{\rho g}{2}\Delta\overline{\eta}^2+\frac{\rho g}{2}(h_0+h)\Delta\overline{\eta}\right\}dt, \tag{2.14}$$

where S_{xx} is defined by (2.9). Having this formulation, the idea is to use the solution for periodic waves of constant form in the KdV to approximate the shoaling problem. That is the subject of the next section.

2.4 Nonlinear shoaling in the KdV equation

In this section we give an explicit formulation of the shoaling phenomena to second order with respect to the Euler equations. The idea is to use the cnoidal wave solution that appears naturally as a traveling-wave solution to the KdV equation. We recall that the solution is given by the explicit form:

$$\eta(x,t)=f_2-(f_2-f_1)\mathrm{cn}^2\left(2K(m)(\frac{t}{T}-\frac{x}{\lambda}),m\right). \tag{2.15}$$

Here m is a parameter and gives periodic waves for $0 \leq m < 1$. For the special case $m = 0$, the solution coincides with linear theory [65]. On the other side of the spectrum, where the nonlinear terms are more dominant, the parameter m will increase and cause a deformation of the surface with sharper crests and flatter troughs [17] where the solution converges to the solitary wave solution for $m \to 1^-$ [17]. We also note that it is given in terms of the parameters,

$$m = \frac{f_1 - f_2}{f_1 - f_3}, \qquad c = c_0\Big(1 + \frac{f_1 + f_2 + f_3}{2h_0}\Big), \qquad \lambda = K(m)\sqrt{\frac{16h_0^3}{3(f_1 - f_3)}}. \tag{2.16}$$

Observe that both the cnoidal wave solution and the wavelength depends on the function $K(m)$ which is the complete elliptic integral of first kind [39]. With roots explicitly given by

$$\begin{cases} f_3 &= \overline{\eta} - \frac{HE(m)}{mK(m)}, \\ f_1 &= f_3 + \frac{H}{m}, \\ f_2 &= f_1 - H. \end{cases} \tag{2.17}$$

As previously stated $\overline{\eta}$ denotes the mean surface level, while $E(m)$ is the elliptic function of second kind [39]. At this point, it is clear that having three equations would be enough to determine the free surface η.

Consider the following system:

$$\begin{cases} \nu(f_1, f_2, f_3) = \frac{c}{\lambda}, & (2.18) \\ \overline{q}_E(f_1, f_2, f_3) = \frac{1}{T}\int_0^T (\frac{1}{h_0}\eta^2 + \frac{5}{4h_0^2}\eta^3 + \frac{h_0}{2}\eta\,\eta_{xx})\,dt, & (2.19) \\ \Delta\overline{S}_{xx}(f_1, f_2, f_3) = -\frac{1}{T}\int_0^T \Big\{\frac{\rho g}{2}\Delta\overline{\eta}^2 + \frac{\rho g}{2}(h_0 + h)\Delta\overline{\eta}\Big\}dt. & (2.20) \end{cases}$$

The first equation is conservation of frequency ν, while the second equation expresses conservation of energy flux integrated over a period T [6]. Finally, the third equation is (2.14) and is a formulation of momentum flux expressed in terms of radiation stress. Expressed in more explicit form, we redefine the system in terms of the parameters (2.16), (2.17). The frequency equation will then turn into a cubic equation for H:

$$\frac{-3g(\frac{3E(m)}{mK(m)} - \frac{2}{m} + 1)^2}{64K(m)^2h^4m}H^3 + \frac{3g(\frac{3\overline{\eta}}{2h} + 1)(\frac{3E(m)}{mK(m)} - \frac{2}{m} + 1)}{16K(m)^2h^3m}H^2 + -\frac{3g(\frac{3\overline{\eta}}{2h} + 1)^2}{16K(m)^2h^2m}H + \frac{1}{T^2} = 0. \tag{2.21}$$

Similarly we can manipulate the equation describing the changes in radiation stress to find an expression for the set-down. Indeed, (2.20) reduces to the quadratic equation

$$-\overline{\eta}^2 + \mathcal{A}\overline{\eta} + \mathcal{B} = 0, \tag{2.22}$$

with

$$\mathcal{A} = \Big(3H - \frac{3h}{2} + \frac{h_0}{2} - 3\overline{\mathrm{cn}^2}(m) - \frac{3H}{m} + \frac{3HE(m)}{mK(m)}\Big),$$

and

$$\begin{aligned}\mathcal{B} = \overline{S}_{xx,0}(m) - \frac{\overline{\eta^2}_0(m)}{2} - -\frac{3}{2}H^2\overline{\mathrm{cn}^4}(m) - \frac{(h)^3\overline{\eta_{xx}}(m)}{3} - \frac{1}{2}(h+h_0)\overline{\eta}_0(m) \\ -3\Big((H - \frac{H}{m} + \frac{HE(m)}{mK(m)})^2 + H\overline{\mathrm{cn}^2}(m)(H - \frac{H}{m} + \frac{HE(m}{mK(m)})\Big).\end{aligned}$$

Note that we had to integrate various powers and derivatives of $\mathrm{cn}^2(\xi;m)$. These formulas are based on calculations made by Lawden and Abramowitz et al. [39, 3] and are given in explicit form in the appendix. Having this representation we can in principle write (2.21) as $H = F(m,\overline{\eta})$ and take (2.22) to be $\overline{\eta} = G(m,H)$ in explicit terms as two coupled equations. To uncouple the two equations we may iterate between the two equations at current local depth h as follows; first initialize the procedure with $\overline{\eta}_0(m)$ and then find H by

$$H(m)^{i+1} = F(m,\overline{\eta}^i(m)),$$

solving the cubic equation. This can in turn be used to update the set-down by

$$\overline{\eta}(m)^{i+1} = G(m,H^{i+1}(m)).$$

Repeating this process, we continue to approximate the H and $\overline{\eta}$ until a stopping criteria has been reached. This means for each m we iterate between (2.21) and (2.22) such that $H = H(m)$ and $\overline{\eta} = \overline{\eta}(m)$. Using this reduction allows to use a nonlinear solver to determine m by conservation of energy flux. Let $\overline{q}_E$ denote the conserved energy at one point. Then energy conservation implies

$$F(m) = \frac{1}{h}\overline{\eta^2}(m) + \frac{5}{4h^2}\overline{\eta^3}(m) + \frac{h}{2}\overline{\eta\,\eta}_{xx}(m) - \overline{q}_E = 0, \tag{2.23}$$

with functions depending on m. We let the system defined by the equations (2.21), (2.22), (2.23) be known as the shoaling equations.

2.4.1 Implementation of the shoaling equation

This section will deal with the implementation of the nonlinear model and produce shoaling curves for various deep water data. The method developed here follows three steps, similar to what was proposed by [67, 66]. First, the linear shoaling equation is used up to the point $h/\lambda_0 > 0.1$. At this point the cnoidal theory is valid [60] and we use a matching technique to obtain the fundamental parameters of the nonlinear wave. Lastly, we use the nonlinear KdV theory to follow the shoaling curve until the highly nonlinear region.

Step 1. Linear theory in deep water: Following the derivation in Section 1.1 we find the dispersion relation

$$\omega^2 - gk\tanh(kh) = 0, \tag{2.24}$$

which in turn can be solved for the wavenumber k by a nonlinear solver to find the waveheight

$$H = H_0\sqrt{\frac{C_{g_0}}{C_g}}. \tag{2.25}$$

Here C_g is the group velocity depending on the wavenumber and depth (the subscript '0' denotes known values) as previously stated in Section 2.1 in details.

Step 2. Matching linear and non-linear theory: Before initializing the nonlinear solver we need to match the parameters $H, \lambda, c, \nu, \overline{q}_E$ from linear theory at last iteration step. We would like to choose one of these parameters and then vary $m \in (0,1)$ such that the nonlinear parameters match. In principle we can only match one parameter and hopefully the rest will follow, but which one is not clear. To investigate this further, define the root problems

$$\lambda^{lin} - \lambda^{nonlin}(m) = 0, \qquad c^{lin} - c^{nonlin}(m) = 0,$$

$$\nu^{lin} - \nu^{nonlin}(m) = 0, \qquad \overline{q}_E^{lin} - \overline{q}_E^{nonlin}(m) = 0.$$

By inspection we can see which one would be best suited. Here the linear parameter is a fixed constant while the nonlinear quantity is a function of m and given in the previous section. Plotting the root problems we observe that matching wavelength would be the best choice.

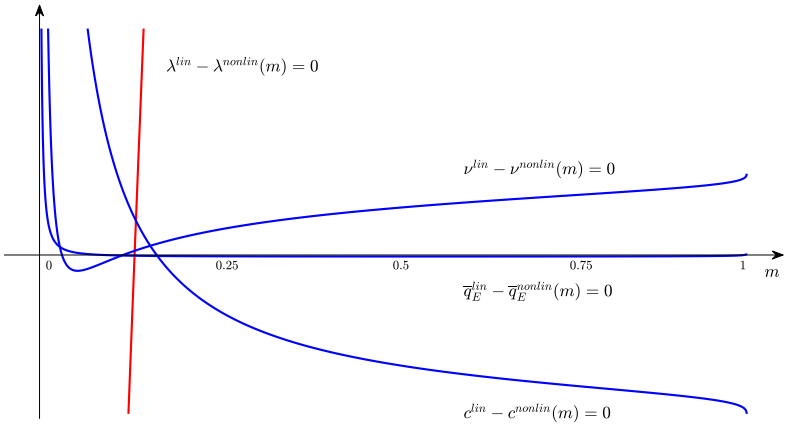

Fig. 2.4 Root problems defined by the parameters $\lambda, c, \nu, \overline{q}_E$ as a function of m.

Indeed, from Figure 3.2 we see for a particular example that most parameters have common root around $m = 0.15$, but the one defined by the wavelength (colored red) is the most distinct. Also note that $H^{nonlin} = H^{lin}$ due to using the roots defined by (2.17). A pseudo code of the matching technique is given below to offer some clarity.

Briefly put, the code will take as input values: the current wavelength, waveheight and local depth and try a range of values of m. Using a special function 'ellipke' [49] to compute the Jacobi functions, we may use the system 2.17 to define the roots and by extension the quantities in (2.16). Specifically, the wavelength in the context of the KdV equation and then compare it with the initial value.

```
function [f] = GetNonLinearWave(L, H, h)
% ------------------------------------------------------------------------
% This program will compute a range of values for m in (0,1) such that
% it satisfies the system defined below and matching wavelength from
% linear theory.

% Input:  L - wavelength
%         H - waveheight
%         h - local depth

% Output: f - vector with f_1, f_2, f_3
% ------------------------------------------------------------------------
    % Number of iterations
    N = 1000000;

    for i = 2:N
        % Range of different values of m
        m = (i-1)/N;

        % Jacobi functions
        [K,E] = ellipke(m);

        % System described by the roots f_1, f_2 and f_3
        f3 = etabar - (H0*E)/(m*K);
        f1 = f3 + H0./m;
        f2 = f1 - H0;

        % Wavelength in non-linear theory
        l = K .* sqrt (16 *h0^3 ./ (3.* (f1 - f3)));

        % Match wavelength
        if  abs(l - l0) < tol
            break
        end
    end
end
```

Step 3. Cnoidal shoaling The final step is solving for waveheight using the scheme defined in Section 6. First, define H and $\overline{\eta}$ as a function of m as given by formula (2.21) and (2.22). Then use a nonlinear solver to find m from equation (2.23). Having m one can determine the waveheight $H(m)$ at the current local depth. Repeating this procedure will then determine

changes of waveheight at each point by approximating the solution with a cnoidal wave. A pseudo-code of the entire procedure is given below.

```
function [H, h] = CnoidalShoaling(L0, H0, h0)
% ------------------------------------------------------------------------
% This function computes the waveheight using the theory of linear
% shoaling and then coupled by non-linear model from cnoidal wave
% theory based on the KdV equation and conservation laws. In particular,
% conservation of frequency, energy flux. Additionally, set-down is
% incorporated  using the radiation stress approach.

% Input:  L0 - original wavelength at deep water
%         H0 - original waveheight at deep water
%         h0 - initial local depth

% Output: H - waveheight
%         h - depth
% ------------------------------------------------------------------------
    % Run the linear model up to the point H/L = 0.1
    [L, H, h] =  LinearShoaling(L0, H0, h0);

    % Matching point between linear and non-linear model
    [f] = GetNonlinearWave(H, h, L);

    % Retrieve conserved quantities
    [Freq] = Frequency(f, h);
    [intqE] = EnergyFlux(f, h);

    % Run nonlinear shoaling from current depth to the shore
    LocalDepth = linspace(h,0,k)
    for i = 1:k-1
        h = LocalDepth(i+1);

        % Use nonlinearsolver to solve the root problem for f_1,f_2 and f_3
        fn  = fsolve(@(fNew) SystemOfEquations(fNew, f0, h, h0, Freq, qE), f);
        f = fn;

        % Store waveheight
        H(i + 1) = f(1) - f(2);
    end
end
```

2.4.2 The radiation stress approach

Having defined the scheme we may plot the development of the waveheight and set-down for given deep water values. We will compare the numerical results with the wave tank data collected by Saville [59] and the linear theory in Figure 2.5 below. The stippled blue lines are the result of linear theory as presented in Section 2.1, while the continuous line represents the shoaling model presented in Section 2.4. The wave under consideration has a deep water wavelength of $\lambda_0 = 202$ cm, waveheight $H_0 = 6.45$ cm at 400 cm distance from the still water line (S.W.L) on a beach with slope 1 : 12.

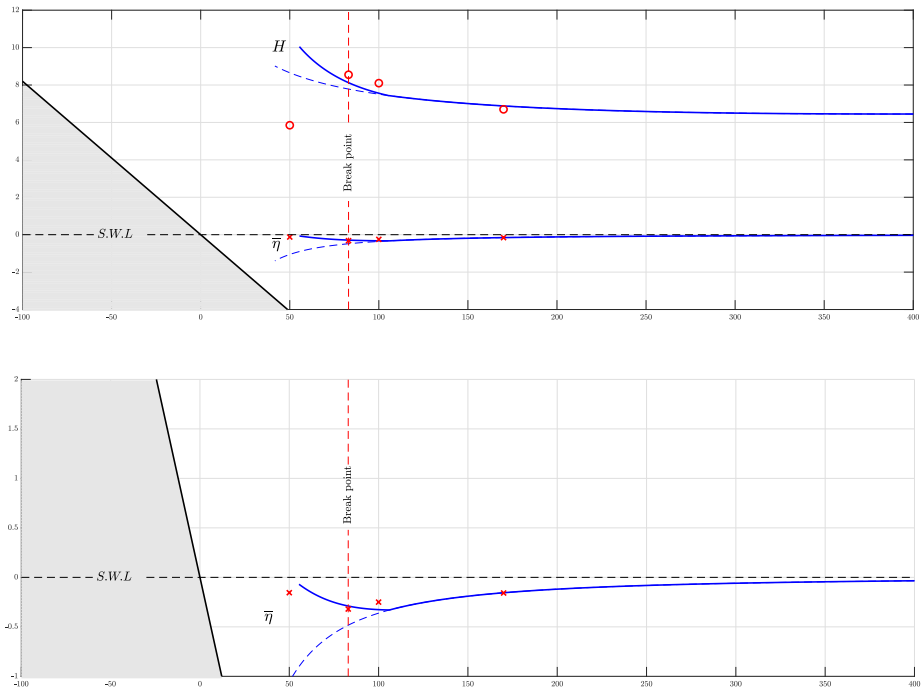

Fig. 2.5 Profile of the mean water level $\overline{\eta}$ and the waveheight H compared to data points presented in [11]. Wave period, 1.14 sec; $H_0 = 6.45$cm; breaking $H_b = 8.55$; slope 0.082. The bottom figure depicts the same scenario with zoom in around the still water line.

The linear model agrees well with the experimental data until it starts reaching the shore (for more details see [11]). On the other hand we see the benefit of the nonlinear formulation, seeming to better fit the data around the braking point of the wave.

This simulation will serve as a benchmark for future research and possible applications. For instance the radiation stress has been used to model currents [65] where our formulation can offer increased performance. Another possibility would be to use our model as a way to transport initial data in deep water through the shoaling region and then as initial data for the surf zone where breaking occurs. Though, on the other hand we may in many situations

neglect the level of set-down inside the surf zone which simplifies the system. We present this simplification in the next sections, having $\overline{\eta} = 0$ and run comparisons with wave tank experiments.

2.4.3 Zero mean surface level

In many cases, set-down of the mean surface level is assumed to be negligible [65]. We will in this section impose this assumption and update equation (2.22) to be $\overline{\eta} = 0$. Then use the same three steps in Section 2.4.1 to determine the development of the waveheight in the shoaling region. Svendsen did this with a first-order approximation of energy flux in the KdV equation with a discontinuity in waveheight between linear and their nonlinear theory [66]. Then Khorsand and Kalisch extended the theory in light of work done by [6] to hold for a second-order approximation, exploiting the full range of the KdV equation [35]. Though, they presented the scheme as a system of three equations giving rise to some numerical instabilities. Instead, we purpose the following:

First formulate $H = H(m)$ according to formula (2.21) given in Section 2.4. Then use the assumption of no set down of mean surface level to find the roots given by (2.17). Having the roots as a function of m we may use energy conservation to define a nonlinear equation as done in equation (2.23). Solving for m we are free to determine the waveheight at a specified depth h and reproduce the shoaling profiles for a range of deep water waves.

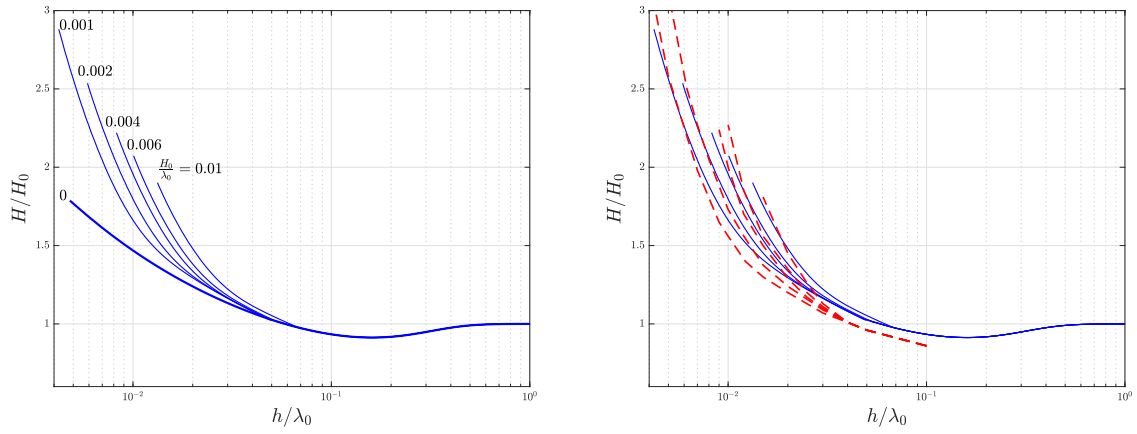

Fig. 2.6 Shoaling curves based on present theory in blue compared to the theory presented by Svendsen and Brink-Kjaer [67] in red. Deep water values $H_0/\lambda_0 = \{0.001, 0.002, 0.004, 0.006, 0.01\}$.

We note that the present implementation is able to determine the waveheight further into the shoaling region compared to the curves presented by [35]. This is due to the simplicity of the implementation, solving one nonlinear equation rather than three. Also we see in

Figure 2.6 that our theory is in fairly good agreement with the shoaling curves presented by Svendsen and Brink-Skjaer in [67]. Though, our model is of second-order and has a continuous transition between the linear and nonlinear theory. In order to further validate the model we will compare it to wave tank experiments.

2.4.4 Wave tank experiments

In this section, comparisons of shoaling curves based on wave tank experiments are presented. The data is collected from [66] where there was taken considerable precautions to stay within the framework we are considering. The waves was generated by a piston type wave generator traveling first over a flat bottom with constant form. Then a data analyzer retrieves the initial data at the bottom of the slope. At this point the waves will start to deform due to the presence of the bottom. We are considering six experiments with a still water depth of 36 cm with plane slope of 1 : 35.

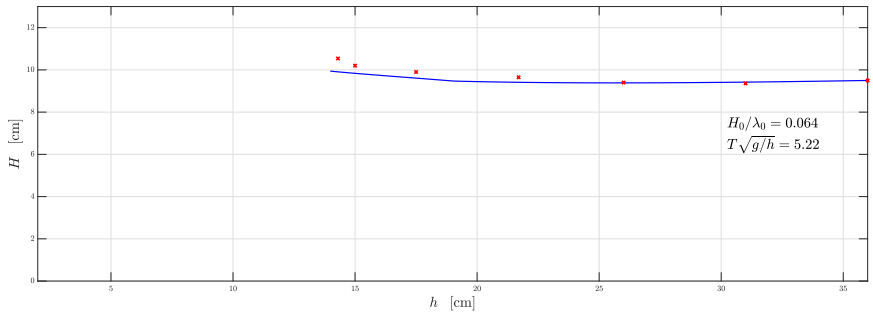

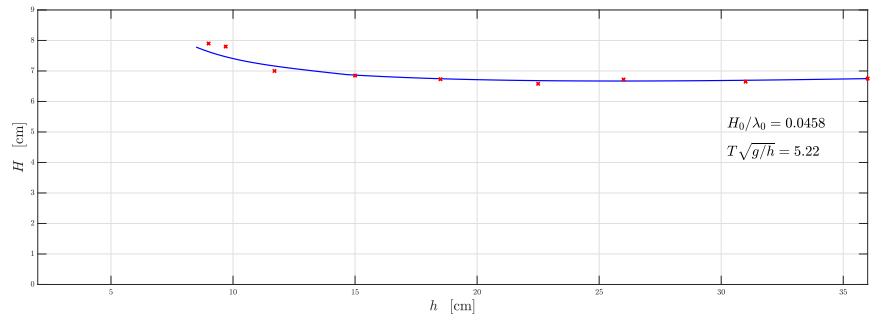

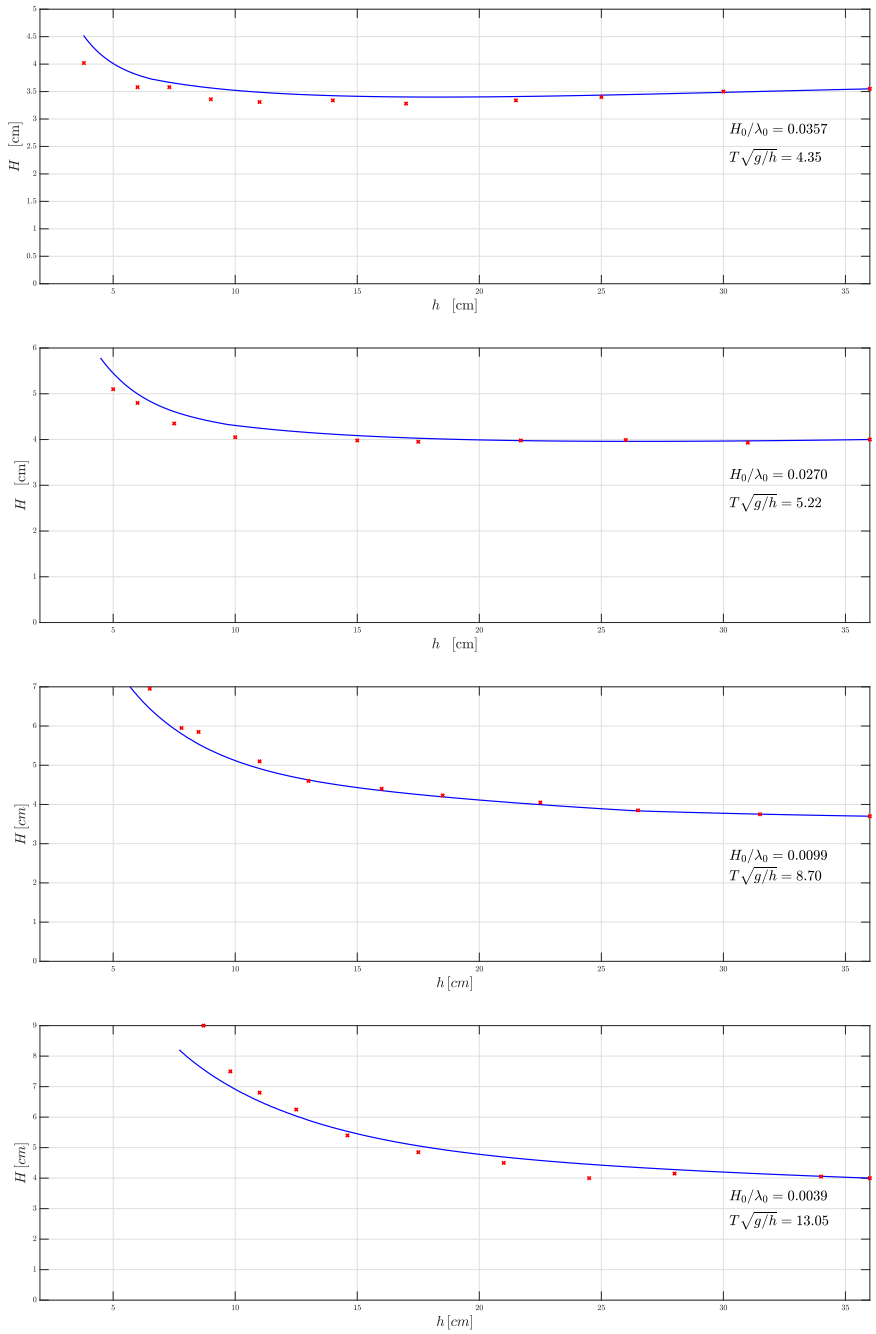

Fig. 2.7 Shoaling curves produced by the theory of this chapter compared with experimental data (red crosses) from [66].

We initialize the code by collecting the initial data at depth $h = 36$ cm. Then it computes H by the linear model up to $h/\lambda_0 > 0.1$ for which the cnoidal theory is valid [60]. Once in this region we keep running the linear model up to the point where the parameters are best matched providing a continuous transition to the non-linear model. We observe in

Figure 2.7 that there is quite good agreement between the numerical model (in blue) and the experimental data (red crosses). The only exception is the first one with deep water steepness $H_0/\lambda_0 = 0.064$. This is a rather steep wave and we observed that the parameters did not line up to well due to linear theory failed to transport the data in a reasonable manner. On the other hand, as the deep water steepness goes down we observe fairly good agreement with the plots and the matching of parameters aligned very well. Therefore, if the linear theory holds until the matching point starts we may expect better results when compared to experimental data.

We will also note that a higher order-theory by Cokelet was presented for the same data set in [58] and observed a tendency of waves shoaling to early. They remarked that exactness of a theory is not a guarantee for better performance when applied outside the given framework of assumptions from which it is derived. Further, the theory presented here takes care of the discontinuity that is appearing in [66].

2.5 Conclusions

The models derived in this section nicely joins the work presented in Chapter 1 together with conservation principles. We have presented how we implement linear shoaling and how to extend it to the nonlinear framework provided by the KdV equation. Implementing the shoaling equations gave good agreement with existing theory and took care of the discontinuity observed in [66].

For future work, it would be interesting to compare the actual wave-profile with a Boussinesq type model like [57]. As an example take case number five in Figure 2.7, we may plot η predicted by linear and nonlinear theory to predict the evolution up a sloping beach.

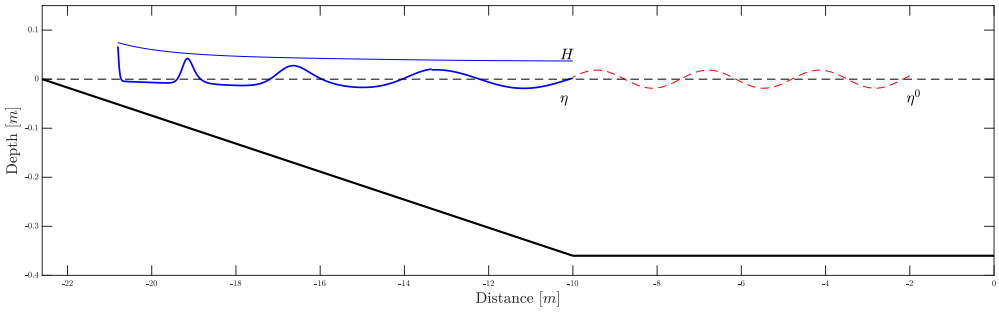

Fig. 2.8 The red stippled line denotes the initial wave η_0, while η is the change as the wave feels the presence of the sloping bottom and H is the difference between crest and trough.

Leaving this issue for the future we now turn to the validity of the new mechanical quantity: (2.9) derived in the KdV equation.

Chapter 3

A mathematical justification of radiation stress in the KdV equation

In this chapter, we turn to the question of whether the derivation of radiation stress makes sense with respect to the general system. Taking a rigorous approach, we will prove the convergence of radiation stress in the full Euler equations. Similar justifications are given for several mechanical balance laws formulated in the KdV approximation (see [26, 24, 25]), but we include some of their work with more details for the purpose of verification and sake of completeness. The main theorem to be proved:

Theorem 2. *Let* $(\eta^{Euler}, \phi^{Euler})$ *be a solution of the water wave problem defined by* $(1.4)-(1.7)$ *with given initial data* $(\eta_0, \phi_0) \in H^s(\mathbb{R}) \times H^s(\Omega)$*, for s large enough. Let* η^{KdV} *be a solution of the KdV equation* (1.27) *with corresponding initial data. Then there exist a constant* $C > 0$ *independent from* ε*, such that*

$$\sup_{t\in[0,\frac{T}{\varepsilon}]} ||(S_{xx}^{Euler} - S_{xx}^{KdV})(\cdot,t)||_{L^\infty} \leq C\varepsilon^2, \tag{3.1}$$

where the non-dimensional radiations stress in the full Euler equations is given by

$$S_{xx}^{Euler} = \int_0^{1+\varepsilon\eta^{Euler}} \{\varepsilon^2(\phi_x^{Euler})^2 + \varepsilon(P')^{Euler} - (z-1)\}dz - \int_0^1 (z-1)dz,$$

and the radiation stress in the context of the KdV:

$$S_{xx}^{KdV} = \varepsilon\eta + \varepsilon^2\frac{3}{2}\eta^2 + \frac{\varepsilon^2}{3}\eta_{xx}.$$

Notation 1. *Here we consider solutions in spaces of the form* $\mathscr{H}_T^s = C([0,T];H^s(\mathbb{R}))$*, which consists of functions* $u : \mathbb{R}\times[0,T] \to \mathbb{R}$ *with norm*

$$||u||_{\mathscr{H}^s_T} = \sup_{t\in[0,T]} ||u(\cdot,t)||_{H^s}.$$

This space enjoys many of the same properties as $H^s(\mathbb{R})$, and some notes are given in the next section. In particular, analogues of Theorem 4 *and* 5 *are valid and will be used later in this chapter. A nice summary of useful properties is given in [10]. We will also ease notation by setting*

$$\sup_{t\in[0,\frac{T}{\varepsilon}]} ||u(\cdot,t)||_{L^\infty} = ||u||_{L^\infty_{x,t}},$$

and taking the $L^\infty-$norm over both spacial coordinates when it is natural.

The proof of this theorem will rely on several classical results and we will now give a brief outline of what will be needed. First, we join the Euler equations with the KdV through the approximated velocity potential:

$$\phi^{\text{app}} = \sum_{j=0}^{N} \varepsilon^j \phi_j,$$

which will in turn allow us to estimate central quantities. In particular, we will provide estimates on the form (possibly of higher order in ε)

$$||\phi^{\text{app}} - \phi^{\text{Euler}}||_{L^\infty_{x,t}} \leq C\varepsilon,$$

following the proof outlined in [25]. Note that we have not specified in what sense we take ϕ, this will be made formal in the next sections. Though, building on this idea we may use a consistency result between the KdV and the Boussinesq equations to prove estimates of the type

$$||\phi^{\text{app}} - \phi^{\text{KdV}}||_{L^\infty_{x,t}} \leq C\varepsilon.$$

By extension we can estimate $\phi^{\text{KdV}}, \phi^{\text{KdV}}_x, (\phi^{\text{KdV}}_x)^2, \phi^{\text{KdV}}_z, (\phi^{\text{KdV}}_z)^2$ and $(P')^{\text{KdV}}$ in the full Euler equations to second order and the main theorem will follow.

As stated above we need to specify the space where we seek a solution to make sense of the estimates. This will be based on Zakharov-Craig-Sulem equations from which we can obtain a local well-posedness result of the water wave system. We therefore find it natural to start the analysis with the functional setting and then derive this system. The derivation is mainly based on the book "The Water Wave Problem" by David Lannes [38], where we seek to present the global idea and some results needed to prove the main theorem.

3.1 Function spaces

Before starting the derivation of the Zakharov-Craig-Sulem equations a word must be spent on the functional setting. We will mainly consider standard results on the L^2-based Sobolev spaces and then relate some special results needed to handle water wave problems. Assuming knowledge of the basic properties of the Fourier transform and L^p theory (see [42, 15, 20] for relevant properties), we start with the definition.

Definition 1. *Let $s \in \mathbb{R}$, we define H^s as the space of functions:*

$$H^s(\mathbb{R}^n) := \{f \in \mathcal{S}'(\mathbb{R}^n) \ : \ (1+|\xi|^2)^{\frac{s}{2}}\hat{f} \in L^2(\mathbb{R}^n)\}, \tag{3.2}$$

with norm

$$||f||_{H^s} := ||(1+|\xi|^2)^{\frac{s}{2}}\hat{f}||_{L^2} = \Big\{\int_{\mathbb{R}^n}(1+|\xi|^2)^s|\hat{f}(\xi)|^2 d\xi\Big\}^{\frac{1}{2}}, \tag{3.3}$$

induced by the standard scalar product.

Here $\mathcal{S}'(\mathbb{R})$ denotes the space of tempered distributions and the main importance for this thesis relies on the fact that the Fourier transform is well-defined and turns derivatives into multiplication [20]. Indeed, if $f \in \mathcal{S}'(\mathbb{R}^n)$, we have by the properties of the Fourier transform that $(-\Delta f)\hat{}\,(\xi) = |\xi|^2\hat{f}(\xi)$ in the distributional sense. Consequently, $\{(1+|\xi|^2)\hat{f}\}\check{} = f + (|\xi|^2\hat{f})\check{} = (1-\Delta)f$ motivating the following definition.

Definition 2. *We define the Bessel potential of order $-s \in \mathbb{R}$ by $\Lambda^s := (1-\Delta)^{\frac{s}{2}} : \mathcal{S}'(\mathbb{R}^n) \to \mathcal{S}'(\mathbb{R}^n)$ with the mapping*

$$f \mapsto \Big\{(1+|\xi|^2)^{\frac{s}{2}}\hat{f}\Big\}\check{}.$$

Typically, one introduces the Fourier transform on the Schwartz space $\mathcal{S}(\mathbb{R}^n)$, which is the space of functions whose derivative are rapidly decreasing. It can be shown that if $f \in \mathcal{S}(\mathbb{R}^n)$ we have that $\mathcal{F}f(\xi) = \hat{f}(\xi) := \int_{\mathbb{R}^n} f(x)e^{2\pi i x\cdot\xi}dx$ is also an element of $\mathcal{S}(\mathbb{R}^n)$. The same goes for the inverse, and it can be shown that both $\mathcal{F}$ and $\mathcal{F}^{-1}$ are one-to-one mappings of $\mathcal{S}(\mathbb{R}^n)$ onto itself (in other words an isomorphism [20]). Similarly, we obtain the same properties on $L^2(\mathbb{R}^n)$ through an extension process using density, i.e. $\overline{\mathcal{S}(\mathbb{R}^n)}^{L^2} = L^2(\mathbb{R}^n)$, combined with the preservation of the norm (isometry) under the Fourier transform by Plancherel [15].

Theorem 3. *(Plancherel's identity) Let $f, g \in \mathcal{S}(\mathbb{R}^n)$, then*

$$\langle f, g\rangle_{L^2} = \langle \hat{f}, \hat{g}\rangle_{L^2}.$$

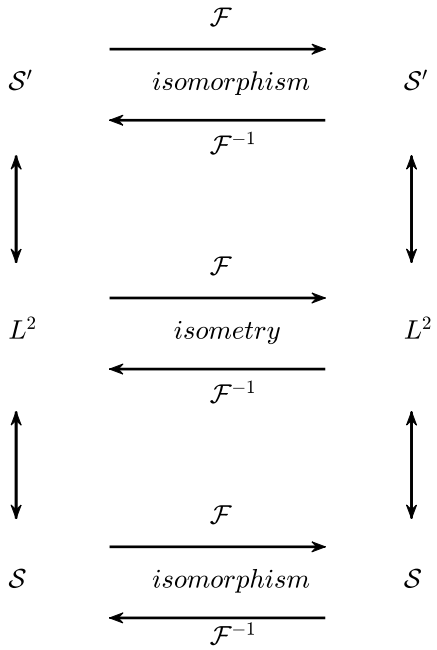

Fig. 3.1 The Fourier transform and its inverse is well-defined on the denoted spaces with an isometry (norm preserving) on $L^2(\mathbb{R}^n)$.

Building on these ideas we can define the Fourier transform in the distributional sense on $\mathcal{S}'(\mathbb{R}^n)$ and we summarize the connections in Figure 3.1.

Remark 2. *For any $f \in H^s(\mathbb{R}^n)$, we have by Plancherel's theorem [15]*

$$||f||_{H^s} = ||\{\Lambda^s f\}\hat{}\,||_{L^2} = ||(1-\Delta)^{\frac{s}{2}} f||_{L^2}.$$

We now give two important properties of the Sobolev spaces.

Theorem 4. *(Sobolev embedding) Let $s > \frac{n}{2} + k$, then $H^s(\mathbb{R}^n) \hookrightarrow C^k_\infty(\mathbb{R}^n)$, i.e. H^s is continuously embedded in the space of continuous functions of order k, vanishing at infinity and for $|\alpha| \leq k$ we have*

$$||\partial^\alpha f||_{L^\infty} \leq C_s ||f||_{H^s}.$$

for some positive constant depending on s.

Proof. For simplicity we give the proof for $k = 0$. By observation we note:

$$|\hat{f}\check{}\,(x)| = |\int_{\mathbb{R}^n} \hat{f}(\xi) e^{2\pi i x\cdot\xi} dx| \leq ||\hat{f}||_{L^1},$$

combined with Cauchy-Schwartz implies

$$||f||_{L^\infty} \leq ||\hat{f}||_{L^1} \leq \Big\{ \int_{\mathbb{R}^n} \frac{d\xi}{(1+|\xi|^2)^s} \Big\} \int_{\mathbb{R}^n} (1+|\xi|^2)^{\frac{s}{2}} |\hat{f}(\xi)| d\xi = C_s ||f||_{H^s},$$

with C_s finite for $s > \frac{n}{2}$ by the "$n-$dimensional $p-$test". Thus, having $f \in H^s(\mathbb{R}^n)$ implies $\hat{f} \in L^1(\mathbb{R}^n)$ and by extension $f = (\hat{f})^\vee \in C_\infty^0(\mathbb{R}^n)$ using the Riemann-Lebesgue lemma (see [20]). □

Another important result on H^s to be used later is the algebra property.

Theorem 5. *Let $f, g \in H^s(\mathbb{R}^n)$, if $s > \frac{n}{2}$, then $f \cdot g \in H^s(\mathbb{R}^n)$.*

The proof of Theorem 5 is a nice application of Young's inequality for convolution, Plancherel and the embedding and can be found in [42, 20] for details. Furthermore, the results also hold for semi-bounded domains and the theory can therefore be used for the water wave problem, where we apply the Fourier transform in the $x-$coordinate. Though, some special care needs to be given to the velocity potential, as it cannot be assumed to be zero at infinity. In particular, if we define the trace of the velocity potential at the surface to be $\phi = \psi|_\eta$, then it does not necessarily belong to a Sobolev space. To remedy this issue, we need to introduce the Beppo-Levi spaces:

Definition 3. *Let $s \in \mathbb{R}$, then we define $\dot{H}^s(\mathbb{R}^n)$ as the space of functions:*

$$\dot{H}^s(\mathbb{R}^n) := \{ f \in L^2_{loc}(\mathbb{R}^n) \ : \ \nabla f \in L^2(\mathbb{R}^n) \}, \tag{3.4}$$

equipped with the semi-norm

$$|f|_{\dot{H}^{s+1}} = ||\nabla f||_{H^s}.$$

There are several technical difficulties to be tackled here, and is of importance if one wants to fully understand the existence and uniqueness results on the general water wave system. The main properties are summed up in Proposition 2.3 in [38], but we make one important remark.

Remark 3. *Consider the fluid domain without the free surface: $\Omega_{bott} = \Omega \cup \{z = 0\}$. Let $u \in C_c^1(\Omega_{bott})$. We observe:*

$$\begin{aligned} |u(x,z)|^2 &= \Big| \int_z^{1+\varepsilon\eta} \partial_z u(x,z') dz' \Big|^2 \\ &\leq \Big(\int_0^{1+\varepsilon\eta} |\partial_z u(x,z')| dz' \Big)^2 \\ &\leq \sup_{x\in\mathbb{R}} (1+\varepsilon\eta(x)) \int_0^{1+\varepsilon\eta} |\partial_z u(x,z')|^2 dz', \end{aligned}$$

by the fundamental theorem of calculus and Cauchy-Schwartz inequality. As a result from integrating over x and z we obtain the Poincaré inequality:

$$||u||_{L^2} \leq C||\nabla u||_{L^2}. \tag{3.5}$$

Then in general if $u \in H^1(\Omega_{bott})$ and for a sufficiently regular boundary one can use a density argument to obtain the same result (see trace theorem [18] and density of differentiable functions with compact support in L^p [20]).

The Poincaré inequality is fundamental for obtaining well-posedness results in elliptic theory. For instance, one typically obtain existence and uniqueness results using the Lax-Milgram's theorem [18] and relies heavily on Poincaré inequality to obtain coercivity of an operator. It is therefore natural to seek a solution in the space:

Definition 4. *In accordance with the notation in [38] we define $H^1_{0,surf}(\Omega)$ to be the completion of $C_c^\infty(\Omega_{bott})$ in $H^1(\Omega)$.*

We also note that we are able to handle functions like $\psi \in \dot{H}^1(\Omega)$ by equivalence of norms using (3.5). This is also fundamental for the coming results to make sense and will be used without further mention.

3.2 The Zakharov-Craig-Sulem equations

To start, we will need the non-dimensional form of the general water wave problem, the asymptotic expansion, and results for the KdV equation. For simplicity let $\varepsilon = \alpha = \beta$ since we neglect the square and the product of α and β in the KdV approximation. Imposing the natural scaling (1.8), the general water wave problem or Euler system for irrotational flow is given by

$$\varepsilon\phi_{xx} + \phi_{zz} = 0 \quad \text{for } 0 < z < 1 + \varepsilon\eta, \tag{3.6}$$

with boundary conditions

$$\phi_z = 0 \quad \text{on } z = 0, \tag{3.7}$$

$$\eta_t + \varepsilon\phi_x\eta_x - \frac{1}{\varepsilon}\phi_z = 0 \quad \text{on } z = 1 + \varepsilon\eta, \tag{3.8}$$

$$\phi_t + \frac{1}{2}(\varepsilon\phi_x^2 + \phi_z^2) + \eta = 0 \quad \text{on } z = 1 + \varepsilon\eta. \tag{3.9}$$

The main observation is that (3.6) and (3.7) defines a Laplace problem with Neumann boundary condition on the bottom, and with a domain depending on the unknown η. While

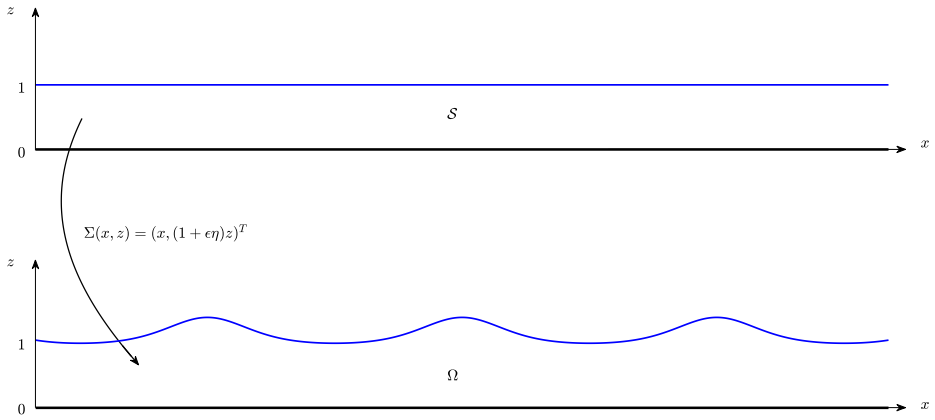

Fig. 3.2 Transforming the Laplace problem on Ω satisfied by ϕ into a boundary value problem on $\mathcal{S} = \mathbb{R} \times (0,1)$ satisfied by $\varphi = \phi \circ \Sigma$ [38].

(3.8) and (3.9) are highly nonlinear equations that is the cause of the great difficulty with this system. The idea is to decouple the part of the equation that is well-known and see whether we can handle the nonlinear equations that follow. The trick (first posed in [71]), is to define the trace of the velocity potential at the surface by:

$$\psi = \phi|_{z=1+\varepsilon\eta}. \tag{3.10}$$

Subsequently, we have Laplace problem with Neumann and Dirichlet boundary conditions given by (3.6), (3.7) and (3.10), but with a domain depending on η. Moreover, we would like to have estimates in some Sobolev space relying on tools from harmonic analysis. The main tool is the Fourier transform, and for it to make sense we need to consider the transformed Laplace problem defined on a strip $\mathcal{S} = \mathbb{R} \times (0,1)$. Taking $(x,z) \in \mathcal{S}$ on a fixed domain, and map it onto the fluid domain $\Omega = \{(x,z) \ : \ 0 < z < 1 + \varepsilon\eta\}$ with

$$\Sigma(x,z) = \begin{pmatrix} x \\ (1+\varepsilon\eta)z \end{pmatrix}.$$

We consider the function $\varphi = \phi \circ \Sigma$, in order to obtain estimates on ϕ.

The main goal of the section is to prove Theorem 2, so we will simply reference the results from Lannes book [38] and explain how they apply to our situation. In particular, the gradient transforms according to the rule: $\nabla\phi = |\det J| J^{-1}(J^{-1})^T \nabla\varphi =: P\nabla\varphi$, with J denoting the Jacobian. For the simple transformation Σ we have

$$J = \begin{pmatrix} 1 & 0 \\ \varepsilon z \eta_x & 1+\varepsilon\eta \end{pmatrix}.$$

With the determinant given by

$$\det J = 1 + \varepsilon\eta =: h.$$

Thus, the change of coordinates is admissible if we bound the waveheight from below by imposing that $h > h_{\min} > 0$ for all $x \in \mathbb{R}$. Moreover, the matrix P given with the correct scaling is

$$P = \begin{pmatrix} h & -\varepsilon^{\frac{3}{2}} z\eta_x \\ -\varepsilon^{\frac{3}{2}} z\eta_x & \frac{1+\varepsilon^3(z\eta_x)^2}{h} \end{pmatrix}.$$

Having the transformation will in turn reveal the transformed Laplace operator:

$$\begin{aligned} \nabla^\varepsilon \cdot P\nabla^\varepsilon \varphi &= \begin{pmatrix} \sqrt{x}\partial_x & \partial_z \end{pmatrix} \begin{pmatrix} h & -\varepsilon^{\frac{3}{2}} z\eta_x \\ -\varepsilon^{\frac{3}{2}} z\eta_x & \frac{1+\varepsilon^3(z\eta_x)^2}{h} \end{pmatrix} \begin{pmatrix} \sqrt{\varepsilon}\partial_x\varphi \\ \partial_z\varphi \end{pmatrix} \\ &= \varepsilon\partial_x\Big(h\partial_x\varphi\Big) - \varepsilon\sqrt{\varepsilon}z\partial_x\Big(\eta_x\partial_x\varphi\Big) - \varepsilon\sqrt{\varepsilon}\partial_z\Big(z\eta_x\partial_x\varphi\Big) + \frac{1}{h}\partial_z^2\varphi + \varepsilon^3\partial_z\Big(\frac{(z\eta_x)^2}{h}\partial_z\varphi\Big) \\ &=: \frac{1}{h}\partial_z^2\varphi + \varepsilon A(\partial_x, \partial_z)\varphi. \end{aligned} \tag{3.11}$$

Similarly, one can verify that $\partial_z\phi \circ \Sigma = \frac{1}{h}\partial_z\varphi$. Then φ satisfies the system:

$$\begin{cases} \nabla^\varepsilon \cdot P\nabla^\varepsilon \varphi = 0 & \text{in} \quad \mathcal{S}, \\ \frac{1}{h}\partial_z\varphi = 0 & \text{on} \quad z = 0, \\ \varphi = \psi & \text{on} \quad z = 1. \end{cases} \tag{3.12}$$

Additionally, it can be shown that this system admits a unique solution for $\varphi \in H^1_{0,\text{surf}}(\mathcal{S})$ in the variational sense if $(\eta, \psi) \in H^s(\mathbb{R}) \times \dot{H}^1(\mathbb{R})$ with $s > \frac{3}{2}$ by Proposition 2.25 in [38]. The result is a direct consequence of Lax-Milgram's theorem, where the functional setting of $H^1_{0,\text{surf}}(\mathcal{S})$ allows us to use the Poincaré inequality (see Remark 3).

We now turn to the boundary conditions of the water wave system and again try to define the problem on a fixed domain. This will be achieved through the Dirichlet-Neumann operator:

Definition 5. *We relate the trace ψ and the normal derivative of the velocity potential by defining the Dirichlet-Neumann operator:*

$$G(\eta) : \psi \mapsto \sqrt{1+(\eta_x)^2}\ \phi_n, \tag{3.13}$$

where $\phi_n = \nabla\phi \cdot \mathbf{n}_s$ *with the normal vector on the surface given by*

$$\mathbf{n}_s = \Big(1+(\eta_x)^2\Big)^{-\frac{1}{2}} \begin{pmatrix} -\eta_x \\ 1 \end{pmatrix}.$$

One quick remark, we may write (3.13) as

$$G(\eta)\psi = -\phi_x\eta_x + \phi_z$$

and can be directly related to the kinematic boundary condition (3.8) through

$$\eta_t + G(\eta)\psi = 0.$$

Moreover, the operator can be related to the Bernoulli equation (3.9) using the relations

$$\psi_t = \phi_t + \phi_z\eta_t$$

and

$$\psi_x = \phi_x + \phi_z\eta_x$$

found by the chain rule. In turn, these relations implies

$$\begin{aligned} G(\eta)\psi + \psi_x\eta_x &= \phi_x\eta_x + \phi_z(\eta_x)^2 + G(\eta)\psi \\ &= \phi_z\Big((\eta_x)^2+1\Big), \end{aligned}$$

allowing us to express

$$\phi_z = \frac{G(\eta)\psi + \phi_x\eta_x}{1+(\eta_x)^2}.$$

Combining the relations above leads to the Zakharov-Craig-Sulem equations:

$$\begin{cases} \eta_t + G(\eta)\psi = 0, \\ \psi_t + \eta + \frac{1}{2}(\psi_x)^2 - \dfrac{\Big(G(\eta)\psi+\eta_x\psi_x\Big)^2}{2\Big(1+(\eta_x)^2\Big)} = 0, \end{cases} \tag{3.14}$$

effectively reducing the dimension of the problem by one and is given on a fixed domain: $(x,t) \in \mathbb{R} \times \mathbb{R}^+$. The main question to be answered is on the solution of this system and of course in which sense. This question was first answered by Shinbrot [63] and Kano and Nishida [27] for analytic initial data. These results have been a source of constant improvements and we give the result stated in [38], adopted to our case in the following theorem:

Theorem 6. *Let the initial data be given* $(\eta^0, \psi^0) \in H^3(\mathbb{R}) \times \dot{H}^2(\mathbb{R})$. *Then there exists a unique solution* $(\eta, \psi) \in C([0, \frac{T}{\varepsilon}]; H^3(\mathbb{R}) \times \dot{H}^2(\mathbb{R}))$ *with* $T > 0$ *satisfying the system* (3.14).

Remark 4. *For simplicity, we will consider the initial data sufficiently smooth such that* (η, ψ) *returns a velocity potential with sufficient regularity. For us the main importance of the theorem is that it provides a candidate for the solution of* φ*, allowing us to compare it with quantities in the KdV equation. In that regard, we do not seek the optimal regularity on the solution, but rather sufficient/reasonable regularity such that a consistency argument can be made.*

The more general statement is found in [38] on page 102 with a detailed proof. We will omit the proof, but having this very consequential result will allow us to claim the existence and uniqueness of the velocity potential φ given in (3.12) by the Lax-Milgram lemma [38]. Consequently, we are able to reconstruct $\mathbf{u}$ by taking the gradient, and determine the pressure by the momentum equation (3), solving the water wave problem on a finite time scale.

3.2.1 Approximated quantities

We will now use the transformed Laplace problem to retrieve approximated solutions of the velocity potential on the form

$$\varphi^{\text{app}} = \sum_{j=0}^{N} \varepsilon^j \varphi_j. \tag{3.15}$$

First, we note that applying $\nabla^\varepsilon \cdot P \nabla^\varepsilon$ gives the relation

$$\begin{aligned} \frac{1}{h}\partial_z^2 \varphi_j &= -\varepsilon A(\partial_x, \partial_z)\varphi_j \\ &= -A(\partial_x, \partial_z)\varphi_{j-1}. \end{aligned}$$

with the convention $\phi_{-1} = 0$. Combining this with the general problem (3.12), we have for $j = 0$:

$$\begin{cases} \frac{1}{h}\partial_z^2\varphi_0 = 0 & \text{in} \quad \mathcal{S}, \\ \frac{1}{h}\partial_z\varphi_0 = 0 & \text{on} \quad z=0, \\ \varphi_0 = \psi & \text{on} \quad z=1, \end{cases}$$

and is a simple ODE with solution $\phi_0 = \psi$ in the fluid domain. Continuing for $j=1$ we obtain the system:

$$\begin{cases} \frac{1}{h}\partial_z^2\varphi_1 = -A(\partial_x,\partial_z)\psi & \text{in} \quad \mathcal{S}, \\ \frac{1}{h}\partial_z\phi_1 = 0 & \text{on} \quad z=0, \\ \phi_1 = 0 & \text{on} \quad z=1. \end{cases}$$

Integrating the first equation with respect to z gives

$$\frac{1}{h}\phi_1 = -\frac{z^2}{2}(h\psi_x)_x + \sqrt{\varepsilon}\frac{z^3}{6}(\eta_x\psi_x)_x + \sqrt{\varepsilon}(\eta_x\psi_x) + zB + C,$$

with $B = B(x,t)$ and $C = C(x,t)$ being constants of integration. Next, imposing no flow through the bottom implies $B=0$, and the Dirichlet condition implies $C = \frac{1}{2}(h\psi_x)_x - \frac{\sqrt{\varepsilon}}{6}(\eta_x\psi_x)_x - \frac{\sqrt{\varepsilon}}{2}(\eta_x\psi_x)$. It yields

$$\frac{1}{h}\varphi_1 = \frac{1}{2}(1-z^2)(h\psi_x)_x + \sqrt{\varepsilon}\frac{1}{6}(z^3-1)(\eta_x\psi_x)_x + \sqrt{\varepsilon}\frac{1}{2}(2-1)(\eta_x\psi_x). \tag{3.16}$$

Similarly, we can obtain an expression for φ_2 in terms of some combination of $\varepsilon, h, \psi, \eta$ and its derivatives to some power. Having the three first terms of the approximated velocity potential will be sufficient to estimate φ in the Euler equations to second-order. This will be made evident in the next proposition, and turn out to be crucial when approximating the quantities in the KdV formulation. With this mind, we simplify the notation by redefining φ^{app} to mean

$$\varphi^{\text{app}} := \varphi_0 + \varepsilon\varphi_1 + \varepsilon\varphi_2. \tag{3.17}$$

By construction we have that

$$\begin{aligned} \nabla^\varepsilon \cdot P\nabla(\varphi_0 + \varepsilon\varphi_1 +^2 \varphi_2) &= \frac{1}{h}\partial_z^2(\varphi_0 + \varepsilon\varphi_1 + \varepsilon^2\varphi_2) + \varepsilon A(\partial_x,\partial_z)(\varphi_0 + \varepsilon\varphi_1 + \varepsilon^2\varphi_2) \\ &= \varepsilon^3 A(\partial_x,\partial_z)\varphi_2 \\ &=: \varepsilon^3 R_\varepsilon. \end{aligned}$$

Remark 5. *We note that having $f \in H^s(\mathbb{R})$ then $f, f', ..., f^{(s-1)}$ are bounded and uniformly continuous functions converging to* 0 *at* $\pm\infty$ *[10]. This is a result of Theorem* 4*, so having $s > 7$ would ensure the boundedness of terms like $\partial_x^6 \psi$. Also, by Theorem* 5 *we have that $f, g \in H^s(\mathbb{R})$ implies $f \cdot g \in H^s(\mathbb{R})$ and takes care of terms like $\eta_x \psi_{xx}$. Similarly, these results can be generalized to hold in $\mathscr{H}_T^s$ [10]. Consequently, there exist $C > 0$ such that*

$$\sup_{t \in [0, \frac{T}{\varepsilon}]} ||R_\varepsilon(\cdot, t)||_{L^\infty} \leq C,$$

when working in a similar framework as the one provided by Theorem 6 for sufficiently smooth initial data.

In fact, this result is just a special case of Lemma 3.42 in [38] and moreover it follows:

Proposition 1. *Let $(\eta, \psi) \in H^s(\mathbb{R}) \times \dot{H}^s(\mathbb{R})$ for $s > 7$, then $u := \varphi - \varphi^{app}$ satisfies the boundary value problem*

$$\begin{cases} \nabla^\varepsilon \cdot P^\varepsilon u = \varepsilon^3 R_\varepsilon & in \quad \mathcal{S}, \\ \partial_z u = 0 & on \quad z = 0, \\ u = 0 & on \quad z = 1, \end{cases}$$

with the estimate

$$||\Lambda^s \nabla^\varepsilon u||_{L^2} \leq C\varepsilon^3. \tag{3.18}$$

The proof of this result is found on page 83 in [38] and relies on several results from harmonic analysis. We will omit the proof and use the adaptation to make the following remark.

Remark 6. *Observe,*

$$\varepsilon \int_{\mathcal{S}} (\partial_x u)^2 \leq \int_{\mathcal{S}} \varepsilon (\partial_x u)^2 + (\partial_z u)^2.$$

By (3.18) *we have $||\partial_x u||_{H^s} \leq C\varepsilon^{\frac{5}{2}}$ for all $t \in [0, \frac{T}{\varepsilon}]$. Additionally, it follows that $||\partial_z u||_{H^s} \leq C\varepsilon^3$. Since we only need the bound to hold up to second order to prove the main theorem, we simplify the notation by setting $||\partial_{x_i} u||_{H^s} \leq C\varepsilon^2$ (consistent with the notation in [25]).*

A similar result can be found for the $t-$derivative on page 124 in [38]. Thus, using the Sobolev embedding in Theorem 4 and returning to the original function ϕ, we summarize the results needed for later:

Corollary 1. *Making the same assumptions as in Proposition 1, we have the following estimates*

$$||\phi_x^{app} - \phi_x^{Euler}||_{L^\infty_{x,t}} \leq C\varepsilon^2, \tag{3.19}$$

$$||\phi_z^{app} - \phi_z^{Euler}||_{L^\infty_{x,t}} \leq C\varepsilon^2, \tag{3.20}$$

$$||\phi_t^{app} - \phi_t^{Euler}||_{L^\infty_{x,t}} \leq C\varepsilon^2. \tag{3.21}$$

Remark 7. *Working with ϕ on Ω, we have that*

$$\phi^{app} = \psi - \varepsilon\Big\{\frac{1}{2}(z^2-1)\psi_{xx} + \varepsilon\eta\psi_{xx}\Big\} + \varepsilon^2\Big\{\frac{1}{24}z^4\psi_{xxxx} - \frac{1}{4}z^2\psi_{xxxx} + \frac{5}{24}\psi_{xxxx}\Big\} + \mathcal{O}(\varepsilon^3), \tag{3.22}$$

and can be derived the same way as we did for φ^{app} by letting P equal to the identity mapping (for details see [33]).

The natural next step is to extend the estimates from the approximated velocity field to the KdV equation (as shown in [25]). To that end, we define

$$f := \psi + \frac{1}{2}\varepsilon\psi_{xx}, \tag{3.23}$$

and is of second order since $f = \phi^{\text{app}}|_{z=0}$. Also note that the kinematic boundary condition can be used to relate f and η^{Euler} by substituting the approximated velocity potential given above (3.22) into (3.8):

$$\eta_t^{\text{Euler}} + f_{xx} + \varepsilon\eta^{\text{Euler}}f_{xx} + \varepsilon\eta_x^{\text{Euler}}f_x - \frac{1}{6}\varepsilon f_{xxxx} = \mathcal{O}(\varepsilon^2).$$

Similarly, by the bottom condition (3.7) gives

$$\eta^{\text{Euler}} + f_t - \frac{\varepsilon}{2}f_{xxt} + \frac{\varepsilon}{2} = \mathcal{O}(\varepsilon^2). \tag{3.24}$$

Further, we denote $u = f_x$, representing the horizontal velocity at the boundary. We differentiate (3.24) and identify $\eta_x = -u_t + \mathcal{O}(\varepsilon)$. These relations will be useful when proving the convergence of important quantities formulated in the KdV to the Euler system. In fact, we note that $u^{\text{KdV}} = u^{\text{Euler}} + \mathcal{O}(\varepsilon)$ due to Corollary 1, and recall from Section 1.2.1 that we have horizontal velocity

$$\phi_x^{\text{KdV}} = \eta^{\text{KdV}} - \frac{1}{4}\varepsilon(\eta^2)^{\text{KdV}} + \varepsilon(\frac{1}{3} - \frac{z^2}{2})\eta_{xx}^{\text{KdV}} + \mathcal{O}(\varepsilon^2), \tag{3.25}$$

the vertical velocity

$$\phi_z^{\mathrm{KdV}} = -\varepsilon z \eta_x^{KdV}, \tag{3.26}$$

and the pressure

$$(P')^{\mathrm{KdV}} = \eta^{\mathrm{KdV}} - \frac{1}{2}\varepsilon(z^2-1)\eta_{xx}^{\mathrm{KdV}} + \mathcal{O}(\varepsilon^2), \tag{3.27}$$

in the KdV. It have been proved in [25] that quantities of interest satisfy the estimates

$$||\eta^{\mathrm{KdV}} - \eta^{\mathrm{Euler}}||_{L^\infty_{x,t}} \leq C\varepsilon, \tag{3.28}$$

$$||\phi_x^{\mathrm{KdV}} - \phi_x^{\mathrm{Euler}}||_{L^\infty_{x,t}} \leq C\varepsilon, \tag{3.29}$$

$$||\phi_z^{\mathrm{KdV}} - \phi_z^{\mathrm{Euler}}||_{L^\infty_{x,t}} \leq C\varepsilon. \tag{3.30}$$

In order to prove the first two estimates we must go through the Boussinesq system and use a consistency result found in [38]. Then use ϕ^{app} to approximate ϕ^{KdV}, where the results follow by the Minkowski inequality. We will leave this out for the sake of brevity. Though, using the same type of ideas we can prove the convergence of $(P')^{\mathrm{KdV}}$ in the Euler system, going through the calculations in [25].

To make sense of the solution of the KdV equation we need a classical result [10]:

Theorem 7. *Let $\eta_0^{KdV} \in H^s(\mathbb{R})$ be the initial data of the KdV equation (1.27) with $s \geq 2$. Then there exists a unique solution $\eta^{KdV} \in \mathscr{H}^s_\infty$.*

We may now combine the previous results to obtain:

Proposition 2. *Under the same provisions as in Proposition 1 and Theorem 7, we have the following estimate:*

$$||(P')^{KdV} - (P')^{Euler}||_{L^\infty_{x,t}} \leq C\varepsilon, \tag{3.31}$$

for $C > 0$ independent of ε.

Proof. The pressure formulated in the full Euler equations is given by $(1.2.1)$

$$(P')^{\mathrm{Euler}} := -\phi_t^{\mathrm{Euler}} - \frac{1}{2}\Big(\varepsilon(\phi_x^{\mathrm{Euler}})^2 + (\phi_z^{\mathrm{Euler}})^2\Big).$$

We may rewrite this equation by adding and subtracting convenient terms,

$$(P')^{\text{Euler}} = -(\phi_t^{\text{Euler}} - \phi_t^{\text{app}}) - \phi_t^{\text{app}} - \frac{1}{2}\varepsilon\Big((\phi_x^{\text{Euler}})^2 - (\phi_x^{\text{KdV}})^2\Big) - \frac{1}{2}\varepsilon(\phi_x^{\text{KdV}}) \\ -\frac{1}{2}\Big((\phi_z^{\text{Euler}})^2 - (\phi_z^{\text{KdV}})^2\Big) - \frac{1}{2}(\phi_z^{\text{KdV}})^2.$$

We then find that each term within the brackets are bounded as a result of Corollary 1 and the inequalities given by (3.29) and (3.30). Indeed, for each time $t \in [0, \frac{T}{\varepsilon}]$ we have $(\phi^{\text{Euler}}, \phi^{\text{KdV}}) \in (H^s(\Omega))^2$ leading to

$$||(\phi_x^{\text{Euler}})^2 - (\phi_x^{\text{KdV}})^2||_{H^s} \leq ||(\phi_x^{\text{Euler}} - \phi_x^{\text{KdV}})||_{H^s}\, ||(\phi_x^{\text{Euler}} + \phi_x^{\text{KdV}})||_{H^s} \leq C\varepsilon,$$

by the properties of H^s. Now, $||\phi(\cdot,t)||_{H^s}$ is bounded for $t \in [0, \frac{T}{\varepsilon}]$ in both systems, and thus have combined with the embedding that,

$$||(\phi_x^{\text{Euler}})^2 - (\phi_x^{\text{KdV}})^2||_{L^\infty_{x,t}} \leq C\varepsilon.$$

Further, the square of ϕ_z is of order $\mathcal{O}(\varepsilon^2)$ by definition (3.26). We must therefore understand the relation:

$$-\phi_t^{\text{app}} - \frac{1}{2}\varepsilon(\phi_x^{\text{KdV}})^2. \tag{3.32}$$

Using (3.22) and (3.23), we obtain

$$\begin{aligned}\phi_t^{\text{app}} &= \psi_t - \frac{1}{2}\varepsilon(z^2-1)\psi_{xxt} + \mathcal{O}(\varepsilon^2) \\ &= f_t - \frac{1}{2}\varepsilon z^2 f_{xxt} + \mathcal{O}(\varepsilon^2).\end{aligned}$$

Recognising the formulation of η^{Euler} by (3.24) and using the usual trick $\eta_x = -(f_x)_t + \mathcal{O}(\varepsilon)$ (3.24), gives

$$\begin{aligned}\phi_t^{\text{app}} &= -\eta^{\text{Euler}} + \frac{\varepsilon}{2}(z^2-1)f_{xxt} - \frac{1}{2}\varepsilon f_x^2 + \mathcal{O}(\varepsilon^2) \\ &= -\eta^{\text{Euler}} + \frac{\varepsilon}{2}(z^2-1)\eta_{xx}^{\text{Euler}} - \frac{1}{2}\varepsilon f_x^2 + \mathcal{O}(\varepsilon^2).\end{aligned}$$

Again, adding and subtracting convenient terms and noting that $f_x = u$ implies

$$\phi_t^{\text{app}} = -(\eta^{\text{Euler}} - \eta^{\text{KdV}}) - \eta^{\text{KdV}} + \frac{\varepsilon}{2}(z^2-1)(\eta_{xx}^{\text{Euler}} - \eta_{xx}^{\text{KdV}}) + \frac{\varepsilon}{2}(z^2-1)\eta_{xx}^{\text{KdV}} - \frac{1}{2}\varepsilon((u^{\text{Euler}})^2 - (u^{\text{KdV}})^2) - \frac{1}{2}\varepsilon(u^{\text{KdV}})^2 + \mathcal{O}(\varepsilon^2).$$

Noting that mist terms can be neglected we return to the relation (3.32) and write

$$-\phi_t^{\text{app}} - \frac{1}{2}\varepsilon(\phi_x^{\text{KdV}})^2 = \eta^{\text{KdV}} - \frac{1}{2}\varepsilon(z^2-1)\eta_{xx}^{\text{KdV}} + \mathcal{O}(\varepsilon),$$

due to (3.28) and Corollary 1. By definition of the dynamic pressure in the KdV (3.27) we have

$$(P')^{\text{Euler}} = (P')^{\text{KdV}} + \mathcal{O}(\varepsilon),$$

and completes the proof of the proposition.

□

3.2.2 Proof of the main theorem

Proof of Theorem 2. We have that

$$S_{xx}^{\text{Euler}} = \int_0^{1+\varepsilon\eta^{\text{Euler}}} \Big\{\varepsilon^2(\phi_x^{\text{Euler}})^2 + \varepsilon(P')^{\text{Euler}} - (z-1)\Big\}dz - \int_0^1 (z-1)dz,$$

and

$$S_{xx}^{\text{KdV}} = \varepsilon\eta + \varepsilon^2\frac{3}{2}\eta^2 + \frac{\varepsilon^2}{3}\eta_{xx}.$$

From the derivation in Section 2.3, we know it is equivalent to the integral formulation

$$S_{xx}^{\text{KdV}} = \int_0^{1+\varepsilon\eta^{\text{KdV}}} \Big\{\varepsilon^2(\phi_x^{\text{KdV}})^2 + \varepsilon(P')^{\text{KdV}} - (z-1)\Big\}dz - \int_0^1 (z-1)dz,$$

in non-dimensional form. For simplicity let E and K denote the integrand of S_{xx}^{Euler} and S_{xx}^{KdV}, respectively. Then,

$$\begin{aligned} S_{xx}^{Euler} - S_{xx}^{KdV} &= \int_0^{1+\eta^{\text{Euler}}} E dz - \int_0^{1+\eta^{\text{KdV}}} K dz \\ &= \int_0^{1+\eta^{\text{KdV}}} (E-K)dz - \int_{1+\varepsilon\eta^{\text{Euler}}}^{1+\varepsilon\eta^{\text{KdV}}} E dz \\ &=: I + II. \end{aligned}$$

We may bound the first term using (3.29) and Proposition 2:

$$||I||_{L^\infty_{x,t}} \leq C||E-K||_{L^\infty_{x,t}} \leq C\Big(\varepsilon^2||(\phi_x^{\text{Euler}})^2-(\phi_x^{KdV})^2||_{L^\infty_{x,t}}+\varepsilon||(P')^{\text{Euler}}-(P')^{\text{KdV}}||_{L^\infty_{x,t}}\Big),$$

and is of order $\mathcal{O}(\varepsilon^2)$. Similarly for the second term, using that E is bounded for $t \in [0, \frac{T}{\varepsilon}]$, with s sufficiently large (see Remark 4) and by (3.28) we deduce that

$$||II||_{L^\infty_{x,t}} \leq \varepsilon C||\eta^{\text{Euler}}-\eta^{\text{KdV}}||_{L^\infty_{x,t}},$$

and is of order $\mathcal{O}(\varepsilon^2)$. Combining these results proves the theorem.

□

3.3 Conclusions

Summarizing the results; we proved in Theorem 2 the consistency of radiations stress formulated in the KdV with the general water wave system. This was not an easy exercise that relied heavily on the article by Israwi and Kalisch [25] together with the techniques and results provided in [38]. Moreover, in order to make sense of the statement in the Theorem 2 we needed the existence and uniqueness result of both systems, which was provided in Theorem 6 and 7. These are both classical results, but it is interesting to see how they could be joined with intermediate steps using the approximated velocity potential and consistency results on the Boussinesq equations. We also included some basic results on Sobolev spaces in Section 3.1, but as a goal for future academic research it would be interesting to better understand the tools of harmonic analysis and how it is linked to water wave theory. For instance, in the proof of Proposition 1, one needs to understand commutator estimates for functions on a strip [38]. In general, learning similar tools can then be used to tackle other interesting problems in this field.

Chapter 4

The Riemann problem for the shallow-water equations

The goal of this chapter is to better understand some of the technicalities that occurs in the shallow-water region. To exemplify potential issues, consideration is given to the theory of 'system of conservation laws', where we derive necessary conditions on the solution and apply the theory for piecewise constant initial data known as the Riemann problem. Having an understanding of the general theory we will use it to describe the propagation of long waves at the surface of an incompressible inviscible fluid of constant depth by the shallow-water equations. In particular, we will investigate shock interactions featured in the shallow-water theory with Riemann initial data. This is a new result and is excepted for publication in Zeitschrift für Naturforschung A, entitled "Admissibility conditions for Riemann data in shallow-water theory" [50].

In general, we have that any conservation laws are first-order quasilinear partial differential equations, and for one-dimensional problems they can be written in the general form

$$\begin{cases} \mathbf{u}_t + \mathbf{F}(\mathbf{u})_x = \mathbf{0} & \text{in} \quad \mathbb{R} \times \mathbb{R}^+, \\ \mathbf{u}(x,0) = \mathbf{g}(x) & \text{on} \quad \mathbb{R} \times \{t = 0\} \end{cases} \tag{4.1}$$

where $\mathbf{u}$ is a bounded vector of unknowns, x is the one-dimensional spatial coordinate, and t is the time. The flux function $\mathbf{F}$ is a nonlinear vector function often satisfying certain mild assumptions, such as that the function is twice continuously differentiable, the flux Jacobian $\nabla\mathbf{F}$ have a full set of distinct eigenvalues and the wave families be either genuinely nonlinear or linearly degenerate [21, 40, 55]. Due to the special nonlinear structure of such systems,

solutions naturally develop discontinuities in time, even if the original state of the system is given by a smooth function of x. Once a discontinuity has developed, the solutions of the system need to be interpreted in a weak sense. Namely,

$$\int_0^\infty \int_{-\infty}^\infty \mathbf{u}\cdot\mathbf{v}_t + \mathbf{F}(\mathbf{u})\cdot\mathbf{v}_x dxdt + \int_{-\infty}^\infty \mathbf{g}\cdot\mathbf{v}|_{t=0} dx = 0. \tag{4.2}$$

This is a standard formulation derived by integrating over the domain, applying Fubini's theorem and integration by parts with $\mathbf{v} \in C_c^\infty(\mathbb{R}\times\mathbb{R}^+)$ and assuming sufficient regularity on $\mathbf{u}$ [18]. Having this notion of weak solutions we may define a class of bounded solutions in this sense.

Definition 6. *We say that* $\mathbf{u} \in L^\infty(\mathbb{R}\times\mathbb{R}^+)$ *is a weak solution of* (4.1) *if* (4.2) *holds for all smooth test functions* $\mathbf{v}$ *with compact support.*

Seeking such solutions one can derive conditions that are necessary in the hope to obtain a unique solution. This will be the subject of Section 4.1 where we derive two conditions; Rankine-Hugoniot and the entropy conditions. With these conditions at hand, we will continue our discussion of water waves using the shallow-water system. The idea will be to discuss solution of this system with initial data

$$\mathbf{u}(x,0) = \begin{cases} \mathbf{u}_L & \text{for} \quad x<0, \\ \mathbf{u}_R & \text{for} \quad x>0, \end{cases} \tag{4.3}$$

for some constant vector functions $\mathbf{u}_L$ and $\mathbf{u}_R$. This is a well-known system where the initial value problem (4.1) with initial data (4.3) is known as the Riemann problem. We will later use this problem to retrieve admissibility conditions for the shallow-water equations, which appears in the general form (4.1) when defining the principal unknown vector $\mathbf{u}$ and the flux function $\mathbf{F}$, respectively by

$$\mathbf{u} = \begin{bmatrix} h \\ hu \end{bmatrix}, \qquad \mathbf{F}(\mathbf{u}) = \begin{bmatrix} hu \\ hu^2 + \frac{1}{2}gh^2 \end{bmatrix}.$$

In physical terms, the unknown $h(x,t)$ represents the local flow depth at a point x in space and at a time t. The unknown $u(x,t)$ represents the horizontal fluid velocity at x and t, averaged over the fluid column.

The solution of the Riemann problem for the shallow-water equations is classical, and can be found in many texts on conservation laws (cf. [2, 21]). One way to normalize the problem is to consider the left state $\mathbf{u}_L$ given, and look at all possible right states. Since h represents the total flow depth of the fluid, an additional admissibility condition is usually

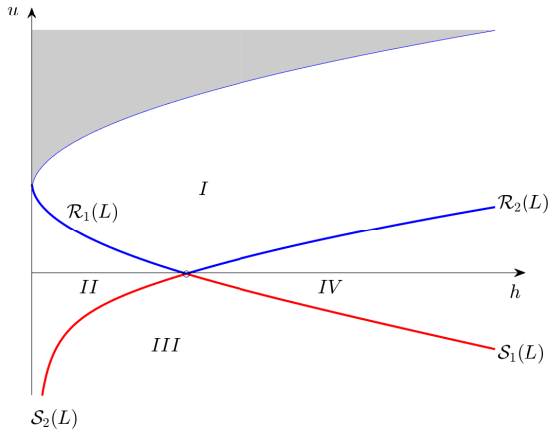

Fig. 4.1 Phase space for a particular left state (h_L, u_L). The red curves denoted by $\mathcal{S}_1$ and $\mathcal{S}_2$ indicate possible right states which can be reached through a single discontinuity. The blue curves denoted by $\mathcal{R}_1$ and $\mathcal{R}_2$ show right states which can be reached through a continuous solution.

imposed, requiring both $\mathbf{u}_L$ and $\mathbf{u}_R$ to feature non-negative flow depth. Indeed, if imposing the requirement that $h_L \geq 0$ and $h_R \geq 0$, then it can be shown that the Riemann problem can be solved for all right states, and given $\mathbf{u}_L$, satisfying this admissibility condition.

As can be gleaned from Figure 4.1, the condition that h be non-negative restricts the analysis to the right half-plane in the (h,u) phase space. However, if we looks closely at the solution of the Riemann problem, it appears that the solution features dry states for many possible right states (see Figure 4.1). In particular, in order to resolve the Riemann problem with a right state in the shaded region in Figure 4.1, one needs to incorporate a dry region ($h = 0$) into the solution. Even though the solution is well-defined mathematically, from a physical point of view, it does not seem reasonable for a dry region to develop from initial conditions which otherwise seem perfectly normal (just as it does not seem reasonable to include states with $h < 0$).

A clear goal will be stated in Section 4.2 but in short; we wish to show that the appearance of such dry states can be avoided when imposing mild assumptions on the initial data. Though, we must first we must develop the necessary tools in order to handle discontinuities in the solution of a nonlinear problem on the form (4.1).

4.1 Selection of admissible shock solutions

In order to consider the initial value problem (4.1) with discontinuous initial conditions like (4.3) then shocks may be a dominant feature in the solution. To handle this issue, we must go through the weak formulation and find conditions that are necessary in order to hope for

a unique solution for a given initial data. In general, under the conditions on **F** mentioned in the introduction, the Riemann problem can always be solved as long as the left and right states are close enough (see [21, 40, 43, 44]). However, if the left and right state are not close, then there is no general theory guaranteeing the existence of a solution to the Riemann problem (see [12]). Indeed, it can be shown explicitly, that there is no solution using the standard theory in some cases because the solution becomes unbounded [68]. On the other hand, for a large number of systems, solutions of the Riemann problem can be shown to exist by elementary methods.

In this section we will derive the necessary tools in order to find weak solutions of (4.1) following the outline in [18] and adding some details to the proofs. Having the conditions, we can apply them to the shallow-water system where we give the derivation of the properties of basic admissible waves for the shallow-water system. Moreover the standard solution of the Riemann problem is explained later using the techniques developed in this section. Even though this is standard fare, we find it useful as various formulas are needed in order to set up the problem to be attacked in Section 4.2.

4.1.1 Rankine-Hugoniot condition

We will now consider the occurrence of discontinuities forming from smooth initial data or initial data of the form (4.3). For a moment consider the situation of having a smooth integral solution **u**, on either side of a curve ξ, for which the solution has simple jump discontinuities.

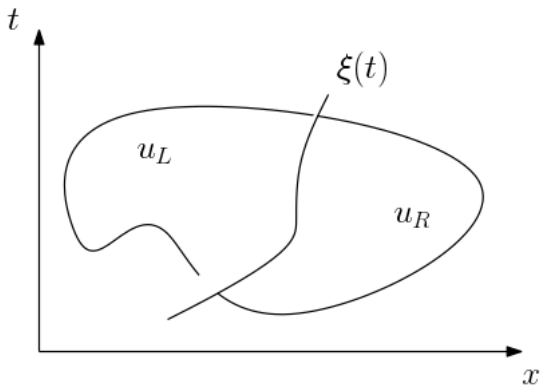

Fig. 4.2 Simple jump discontinuities across a smooth shock curve ξ.

First define the limit on either side of the discontinuity by

$$\mathbf{u}_L = \mathbf{u}(\xi(t)^-, t), \qquad \mathbf{u}_R = \mathbf{u}(\xi(t)^+, t), \tag{4.4}$$

and from [18] we give the first condition:

Theorem 8 (Rankine-Hugoniot condition)**.** *Let $\Omega \subset \mathbb{R} \times (0,\infty)$ be a region separated by a smooth curve $\xi(t)$ and $\mathbf{u}$ be a smooth solution on either side of the curve. If $\mathbf{u}$ omits simple jump discontinuities along $\xi(t)$, then the weak solution in the sense* 4.2 *must satisfy the relation*

$$\mathbf{F}(\mathbf{u}_L) - \mathbf{F}(\mathbf{u}_R) = \sigma(\mathbf{u}_L - \mathbf{u}_R), \tag{4.5}$$

with σ being the speed of the curve.

Proof. Consider $\Omega = \Omega^- \cup \Omega^+ \subset \mathbb{R} \times (0,\infty)$ denoting the domain on either side of the discontinuity and let $\mathbf{v} \in C_c^\infty(\Omega)$. Then split (4.2) into two separate integrals representing the solution on each side of the shock as shown below.

$$0 = \int_{\Omega^-} \mathbf{u} \cdot \mathbf{v}_t + \mathbf{F}(\mathbf{u}) \cdot \mathbf{v}_x dA + \int_{\Omega^+} \mathbf{u} \cdot \mathbf{v}_t + \mathbf{F}(\mathbf{u}) \cdot \mathbf{v}_x dA. \tag{4.6}$$

Now consider the weak solution on the left-hand side of the discontinuity and apply the Gauss-Green theorem:

$$\int_{\Omega^-} \mathbf{u} \cdot \mathbf{v}_t + \mathbf{F}(\mathbf{u}) \cdot \mathbf{v}_x dA = -\int_{\Omega^-} \{\mathbf{u}_t + \mathbf{F}(\mathbf{u})_x\} \cdot \mathbf{v} dA + \int_{\partial\Omega} \{\mathbf{u} n_2 + \mathbf{F}(\mathbf{u}) n_1\} \cdot \mathbf{v} ds.$$

The first term is away from the discontinuity and therefore satisfies the solution (4.1) in a classical sense. Further, since $\mathbf{v}$ has compact support in Ω^-, we are only left with the boundary term along the curve $\xi(t)$. Together with definition (4.4) and (4.6) we have

$$\int_{\Omega^-} \mathbf{u} \cdot \mathbf{v}_t + \mathbf{F}(\mathbf{u}) \cdot \mathbf{v}_x dA = \int_{\partial\Omega} \{\mathbf{u} n_2 + \mathbf{F}(\mathbf{u}) n_1\} \cdot \mathbf{v} ds.$$

Similar computations can be made for the weak solution on Ω^+. Thus, combing the two with (4.6) gives the following relation

$$0 = \int_{\partial\Omega} \Big[(F(\mathbf{u}_L) - F(\mathbf{u}_R)) n_1 + (\mathbf{u}_L - \mathbf{u}_R) n_2 \Big] \cdot \mathbf{v} dA, \tag{4.7}$$

for all test functions $\mathbf{v}$. We may therefore conclude (as done in [18] omitting the measure result) that whenever there is a shock, the solution must satisfy

$$\mathbf{F}(\mathbf{u}_L) - \mathbf{F}(\mathbf{u}_R) = \sigma(\mathbf{u}_L - \mathbf{u}_R) \tag{4.8}$$

along the curve ξ with

$$\sigma = -\frac{n_1}{n_2} = \frac{dt}{dx} = \frac{1}{\xi'(t)},$$

denoting the speed of the discontinuity.

□

This is a necessary condition for the solution whenever there is a discontinuity and is known as the Rankine-Hugoniot condition, but it is not sufficient. We also need the criteria for admissible shock waves, namely the entropy conditions.

4.1.2 Entropy conditions

We will now derive another condition, using the method of vanishing viscosity [18]. The idea is to consider the parabolic system

$$\begin{cases} \mathbf{u}^\varepsilon_t + \mathbf{F}(\mathbf{u}^\varepsilon)_x = \varepsilon \mathbf{u}^\varepsilon_{xx}, & \text{in} \quad \mathbb{R}\times\mathbb{R}^+ \\ \mathbf{u}^\varepsilon = \mathbf{g} & \text{in} \quad \mathbb{R}\times\{t=0\} \end{cases} \tag{4.9}$$

exploiting its diffusive character trying to find a condition for which the solution $\mathbf{u}$ must satisfy as ε tends to zero. We will assume $\mathbf{u}^\varepsilon$ is a smooth solution of (4.9), rapidly decreasing and $\{\mathbf{u}\}_{0<\varepsilon\leq 1}$ uniformly bounded in $L^\infty(\mathbb{R}\times\mathbb{R}^+)$. We make the definition [18]:

Definition 7. *Two smooth functions $\Phi, \Psi : \mathbb{R}^n \to \mathbb{R}$ is said to be an entropy- flux pair for the conservation law* (4.1) *if Φ is convex and satisfies the relation*

$$\nabla\Phi(\mathbf{w})\nabla\mathbf{F}(\mathbf{w}) = \nabla\Psi(\mathbf{w}), \tag{4.10}$$

for some $\mathbf{w} \in \mathbb{R}^n$.

In particular we will impose the condition

$$\Phi(\mathbf{u})_t + \Psi(\mathbf{u})_x \leq 0, \tag{4.11}$$

for weak solutions $\mathbf{u}$ satisfying the system (4.1). These are called entropy solutions and are needed to resolve the issue of shocks forming. Since we are dealing with discontinuities in our solution we find it convenient to multiply with a test function $\mathbf{v} \in C_c^\infty(\mathbb{R}\times\mathbb{R}^+)$, apply Gauss-Green's theorem and the compactness

$$\int_0^\infty \int_{-\infty}^\infty \Psi(\mathbf{u})v_t + \Phi(\mathbf{u})v_x dx dt \geq 0, \tag{4.12}$$

as an alternative to (4.11). We will later give a more physical interpretation of this relation when we deal with the shallow-water equations and see how it relates to the energy. Though, for now we are ready to prove the following statement (see Evans [18] p. 649).

Theorem 9 (Entropy condition)**.** *If the function* $\mathbf{u}$ *is an integral solution in the sense* (4.2) *and satisfies* (4.12) *for any entropy-flux pair, then* $\mathbf{u}$ *is a solution of* (4.1).

Proof. As said previously, we will add a viscosity term to the system as described in (4.9) and exploit the diffusive character. Then evaluate the limit

$$\mathbf{u}^\varepsilon \to \mathbf{u},$$

almost everywhere as $\varepsilon \to 0$ for $\{\mathbf{u}^\varepsilon\}_{0<\varepsilon<1}$ uniformly bounded. First, observe by the chain rule

$$\Phi(\mathbf{u}^\varepsilon)_t + \Psi(\mathbf{u}^\varepsilon)_x = \nabla\Phi(\mathbf{u}^\varepsilon)\cdot\mathbf{u}^\varepsilon_t + \nabla\Psi(\mathbf{u}^\varepsilon)\cdot\mathbf{u}^\varepsilon_x, \tag{4.13}$$

Further, by definition (4.10) one can write

$$\nabla\Psi(\mathbf{u}^\varepsilon)\cdot\mathbf{u}^\varepsilon_x = \nabla\Phi(\mathbf{u}^\varepsilon)\nabla\mathbf{F}(\mathbf{u}^\varepsilon)\cdot\mathbf{u}^\varepsilon_x = \nabla\Phi(\mathbf{u}^\varepsilon)\mathbf{F}(\mathbf{u}^\varepsilon)_x,$$

and in combination with (4.9) and (4.13) implies

$$\begin{aligned}\Phi(\mathbf{u}^\varepsilon)_t + \Psi(\mathbf{u}^\varepsilon)_x &= \nabla\Phi(\mathbf{u}^\varepsilon)\{\mathbf{u}^\varepsilon_t + \mathbf{F}(\mathbf{u}^\varepsilon)_x\}\\ &= \varepsilon\nabla\Phi(\mathbf{u}^\varepsilon)\mathbf{u}^\varepsilon_{xx}\\ &= \varepsilon\Phi(\mathbf{u}^\varepsilon)_{xx} - \varepsilon(\nabla^2\Phi(\mathbf{u}^\varepsilon)\mathbf{u}^\varepsilon_x)\cdot\mathbf{u}^\varepsilon_x.\end{aligned} \tag{4.14}$$

In this context, ∇^2 is the Hessian matrix of Φ. By the convexity, we have that

$$\nabla^2\Phi(\mathbf{u}^\varepsilon)\mathbf{u}^\varepsilon_x\cdot\mathbf{u}^\varepsilon_x \geq 0 \tag{4.15}$$

Now multiplying (4.14) with a positive test function with compact support and integrate by parts to get

$$\begin{aligned}\int_0^\infty\int_{-\infty}^\infty \Phi(\mathbf{u}^\varepsilon)v_t + \Psi(\mathbf{u}^\varepsilon)v_x dxdt &= \int_0^\infty\int_{-\infty}^\infty \varepsilon(\nabla^2\Phi(\mathbf{u}^\varepsilon)\mathbf{u}^\varepsilon_x)\cdot\mathbf{u}^\varepsilon_x - \varepsilon\Phi(\mathbf{u}^\varepsilon)v_{xx}dxdt\\ &\geq -\int_0^\infty\int_{-\infty}^\infty \varepsilon\Phi(\mathbf{u}^\varepsilon)v_{xx}dxdt,\end{aligned} \tag{4.16}$$

using (4.15) and $v \geq 0$ to obtain the inequality. In order to establish (4.12) we need to evaluate the limit and show that the left hand-side is bounded by below by zero.

By definition 7 we have that both Φ and Ψ are smooth. We will use this to first prove the convergence of the right-hand side of (4.16) by the dominated convergence theorem, allowing us to pass the limit inside the integral [20]. To verify the assumptions of the theorem we must show that the limit of the integrand is converging and moreover is bounded by an integrable function. Starting with the first point, we note that $\mathbf{u}^\varepsilon$ is uniformly bounded with respect to time and space and it follows that Φ is given on a compact set K independent from ε and therefore by being smooth we get the bound $|\Phi(\mathbf{u}^\varepsilon)| \leq \sup_{\mathbf{x}\in K} |\Phi(\mathbf{x})| \leq C$, for all $0 < \varepsilon < 1$. Being bounded allows us to take the limit of the integrand

$$\lim_{\varepsilon\to 0} \varepsilon\Phi(\mathbf{u}^\varepsilon)v_{xx} = 0.$$

Furthermore, the integrand is bounded by a integrable function independent of ε:

$$|\varepsilon\Phi(\mathbf{u}^\varepsilon)v_{xx}| \leq C|v_{xx}|$$

due to $v_{xx} \in C_c^\infty(\mathbb{R}\times\mathbb{R}^+)$. By a similar argument we deduce that the left-hand side will converge and is bounded by an integrable function independent of ε. Therefore, we may conclude by the dominated convergence theorem that

$$\int_0^\infty \int_{-\infty}^\infty \Phi(\mathbf{u})v_t + \Psi(\mathbf{u})v_x dxdt \geq 0.$$

Lastly, we must show that $\mathbf{u}$ is an integral solution. Simply take a test function $\mathbf{v}$ and integrate (4.9) by parts to obtain

$$\int_0^\infty \int_{-\infty}^\infty \mathbf{u}^\varepsilon \cdot \mathbf{v}_t + \mathbf{F}(\mathbf{u}^\varepsilon)\cdot \mathbf{v}_x + \varepsilon\mathbf{u}^\varepsilon \cdot \mathbf{v}_{xx} dxdt + \int_{-\infty}^\infty \mathbf{g}\cdot\mathbf{v}|_{t=0} dx = 0. \tag{4.17}$$

The convergence is obtained with the same argument as above for a sufficiently regular flux function $\mathbf{F}$. Thus, $\mathbf{u}$ is an integral solution in the sense (4.2) and completes the proof.

□

These types of solutions are called entropy solutions and we must impose this criterion for any weak solution of the system of conservation laws. Additionally, a useful consequence is considering solutions separated by shock like we did for the Rankine-Hugoniot condition.

Corollary 2. *Let* $\mathbf{u}$ *be a en entropy solution of* (4.1)*, then it must satisfy the relation*

$$\Psi(\mathbf{u}_L) - \Psi(\mathbf{u}_R) \leq \sigma(\Phi(\mathbf{u}_L) - \Phi(\mathbf{u}_R)). \tag{4.18}$$

The proof follows by the same procedure as for the Rankin-Huiginuot condition, namely splitting the expression (4.12) into two terms and integrate by parts.

4.2 Admissibility conditions for Riemann data in shallow-water theory

In the remainder of the chapter, we aim to identify conditions on the right state $\mathbf{u}_R$ which will guarantee that the solution of the Riemann problem does not include a dry state. Recall that the shallow-water assumption applies to surface waves that are slowly varying, and a shock represents a bore, i.e. a traveling hydraulic jump, where the shock structure may feature oscillations or turbulent structures) has been neglected [69]. If this physical interpretation is taken as a point of departure, then it appears that a Riemann problem may develop from the collision of two bores, and a natural admissibility condition would be to consider only such Riemann problems. Thus, we will study the history of the Riemann problem, or more succinctly the backwards problem for $t < 0$. Examining possible solutions to the backwards problem will lead to clear conditions on whether or not a Riemann problem can develop. As it turns out, these conditions will exclude Riemann problems whose solution involves a dry state.

Note that a Riemann problem could also develop from certain initial data which are arranged in such a way that the solution lines up at some time so as to give a perfect Riemann problem. While this is possible, it would clearly be unstable to even the smallest perturbations. On the other hand, one might also consider the collision of three or more traveling hydraulic jumps, or the collision between rarefaction waves and shocks, but these situations are so unlikely to happen that they would constitute a set of measure zero in the configuration space. In the current work, we focus on the origin of the Riemann problem which can be represented by a set of non-zero measure in the configuration space given by the phase plane.

The outline of this section is as follows: In Section 4.2.1 and 4.2.2, a short discussion of the properties of basic admissible waves for the shallow-water system is given, using the conditions derived for a general system of conservation laws developed in Section 4.1. As a result, the standard solution of the Riemann problem is explained in Section 4.2.3. In Section 4.2.4, 4.2.5 and 4.2.6, Riemann problems originating from various configurations are investigated. Some ramifications of our results are discussed in the conclusion at the end.

4.2.1 Shock waves and bore properties

As already mentioned above, the shallow-water system can be written in terms of mass and momentum conservation in the form

$$h_t + (hu)_x = 0, \tag{4.19}$$

$$(hu)_t + \left(hu^2 + \frac{1}{2}gh^2\right)_x = 0. \tag{4.20}$$

A derivation of this system from first principles can be found in [61], where it is also shown that the conservation of energy is formulated as

$$\left(\frac{1}{2}hu^2 + \frac{1}{2}gh^2\right)_t + \left(\frac{1}{2}hu^3 + gh^2u\right)_x = 0. \tag{4.21}$$

Discontinuous solutions develop naturally in this system even in the case of flat bathymetry which is under study here. In the case when the solution features jumps, the imposition of mass and momentum conservation leads to an energy loss (see [54]) which has been the subject of a number of studies [4, 8, 28, 62]. In the context of the conservation laws, the energy loss means that (4.21) becomes an inequality, which is then taken as the mathematical entropy in order to pick out physically reasonable discontinuous solutions.

In the context of the shallow-water equations (4.19) and (4.20) the Rankine-Hugoniot condition (4.5) yields the following relations:

$$\begin{aligned}
&(h_R - h_L)\sigma = h_R u_R - h_L u_L,\\
&(h_R u_R - h_L u_L)\sigma = \left(h_R u_R^2 + \frac{1}{2}gh_R^2\right) - \left(h_L u_L^2 + \frac{1}{2}gh_L^2\right).
\end{aligned}$$

Combining these two equations enables us to find an expression for u_R in terms of h, h_L and u_L as shown in [2, 21]. Indeed, one may define the Hugoniot locus of all possible right states (h,u) for a given left state (h_L,u_L) in terms of the shock curves $\mathcal{S}_1$ and $\mathcal{S}_2$ as follows.

$$\mathcal{S}_1(L): \quad u(h) = u_L - (h-h_L)\sqrt{\frac{g}{2}(\frac{1}{h}+\frac{1}{h_L})}, \tag{4.22}$$

$$\mathcal{S}_2(L): \quad u(h) = u_L + (h-h_L)\sqrt{\frac{g}{2}(\frac{1}{h}+\frac{1}{h_L})}. \tag{4.23}$$

A useful observation to be used later is that the fluid velocity of u on $\mathcal{S}_1$ is strictly decreasing, while the velocity on $\mathcal{S}_2$ is strictly decreasing. In fact, taking the derivative yields

the expression

$$u'(h) = \mp \frac{\sqrt{\frac{g}{2}}(2h^2 + hh_L + h_L^2)}{2h^2 h_L \sqrt{\frac{1}{h} + \frac{1}{h_L}}},$$

where the minus sign refers to the $\mathcal{S}_1$ curve and the plus sign to the $\mathcal{S}_2$ curve. Inspecting the term on the right in the above relation confirms that the sign of the derivative $u'(h)$ depends only on whether the derivative is taken on $\mathcal{S}_1$ or on $\mathcal{S}_2$.

The Hugoniot loci may also be described in terms of the momentum $q = hu$. Indeed, for a given left (h_L, q_L), the possible right states must satisfy one of the following relations

$$\mathcal{S}_1(L): \quad q(h) = \frac{q_L}{h_L} h - h(h - h_L)\sqrt{\frac{g}{2}(\frac{1}{h} + \frac{1}{h_L})}, \tag{4.24}$$

$$\mathcal{S}_2(L): \quad q(h) = \frac{q_L}{h_L} h + h(h - h_L)\sqrt{\frac{g}{2}(\frac{1}{h} + \frac{1}{h_L})}. \tag{4.25}$$

Taking the second derivative of these expressions shows that these curves are strictly concave and convex, respectively:

$$q''(h) = \mp \frac{\sqrt{\frac{g}{2}}(8h^3 + 12h^3 h_L + 3hh_L^2 + h_L^3)}{4h^3 h_L^2 (\frac{1}{h} + \frac{1}{h_L})^{\frac{3}{2}}}.$$

Finally, the speed of the discontinuity may be found from the Rankine-Hugoniot condition as

$$\sigma = u_L \mp h_R \sqrt{\frac{g}{2}(\frac{1}{h_R} + \frac{1}{h_L})} = u_R \pm h_L \sqrt{\frac{g}{2}(\frac{1}{h_R} + \frac{1}{h_L})}. \tag{4.26}$$

Next, let us discuss the entropy condition for shock waves. It is well-known [21, 55] that it is necessary to impose both the Rankine-Hugoniot and the entropy condition to ensure the uniqueness of a solution. In the context of the shallow-water theory, the mechanical energy serves as a mathematical entropy. In fact, it is well-known that energy is lost in a shock either due to turbulence or the continuous creation of surface oscillations [4, 8, 61]. Similar

Fig. 4.3 Left panel: bore with flow depth $h_L < h_R$ which corresponds to the right state being on the shock curve $\mathcal{S}_1$. Right panel: bore with flow depth $h_R < h_L$ corresponding to the right state being on the shock curve $\mathcal{S}_2$. In both cases the bore front may feature positive (right-moving), zero, or negative (left-moving) propagation velocity.

Hugoniot locus	Fluid velocity $u(h)$		Momentum $q(h)$
$\mathcal{S}_1$	$u'(h) < 0$	$u''(h) > 0$	$q''(h) < 0$
$\mathcal{S}_2$	$u'(h) > 0$	$u''(h) < 0$	$q''(h) > 0$

Table 4.1 Properties of shock curves $\mathcal{S}_1$ and $\mathcal{S}_2$.

Hugoniot locus	$\mathcal{S}_1$	$\mathcal{S}_2$
Increase/decrease in flow depth	$h_L < h_R$	$h_L > h_R$
Front speed	$\sigma < 0$ or $\sigma > 0$	$\sigma < 0$ or $\sigma > 0$
Relative mass flux	$m > 0$	$m < 0$
Velocity relation	$u_R < u_L$	$u_R < u_L$
Velocity relation	$u_R > \sigma$	$u_R < \sigma$
Velocity relation	$u_L > \sigma$	$u_L < \sigma$

Table 4.2 Jump properties on $\mathcal{S}_1$ and $\mathcal{S}_2$.

considerations can be used in various other applications, such as for example in the context of porous media [1].

In the present case, the expected loss of mechanical energy is enforced by imposing the inequality

$$\Delta E = \underbrace{(\frac{1}{2}hu^2 + \frac{1}{2}gh^2)_t}_{\Phi(\mathbf{u})_t} + \underbrace{(\frac{1}{2}hu^3 + gh^2u)_x}_{\psi(\mathbf{u})_x} < 0, \tag{4.27}$$

for discontinuous solutions. It is also convenient to introduce the relative mass flux m by

$$m = h_R(u_R - \sigma) = h_L(u_L - \sigma) = \pm h_R h_L \sqrt{\frac{g}{2}(\frac{1}{h_R} + \frac{1}{h_L})}. \tag{4.28}$$

Using m, we can express the rate at which energy is lost at the shock by the entropy condition (4.18):

$$\begin{aligned} \Delta E &= \psi(\mathbf{u}_R) - \psi(\mathbf{u}_L) - \sigma(\Phi(\mathbf{u}_R) - \Phi(\mathbf{u}_L)), \\ &= -\frac{mg}{4}\frac{(h_R - h_L)^3}{h_R h_L}. \end{aligned}$$

Note that since we always require $\Delta E < 0$ for discontinuous solutions, if $h_L < h_R$, then we must have $m > 0$ from the previous relation. Invoking (4.28) then shows that $u_R > \sigma$ and $u_L > \sigma$. On the other hand, similar considerations show that if $h_L > h_R$, then (4.27) requires that $u_R < \sigma$ and $u_L < \sigma$. These relations show that fluid particles always move across the

shock from the region of lower depth to the region of higher depth, a fact already noted in [61]. Moreover, combining equation (4.22), (4.23) and (4.28) and using the condition (4.27) shows that we must have $u_R < u_L$ for all discontinuous solutions. The most important properties of the shock curves are summarized in Table 4.1 and 4.2.

One should also remark that both $\mathcal{S}_1$ and $\mathcal{S}_2$ shocks satisfy the Lax entropy condition (cf. [21]). This condition states that the speed σ_i of an $\mathcal{S}_i$ shock must satisfy the relation

$$\lambda_i(R) \leq \sigma_i \leq \lambda_i(L), \qquad i = 1,2, \tag{4.29}$$

where λ_i are the eigenvalues of the flux Jacobian matrix $\nabla\mathbf{F}$. For the shallow-water equations, these eigenvalues are given by

$$\lambda_1 = u - \sqrt{gh}, \qquad \lambda_2 = u + \sqrt{gh}. \tag{4.30}$$

A geometrical representation of the Lax entropy condition in the $(x,t)-$plane is shown in Figure 4.4 and 4.5.

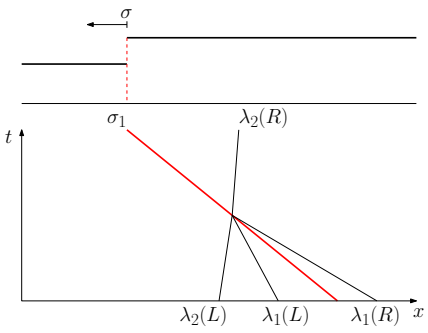

Fig. 4.4 Left moving bore with speed σ_1, $\lambda_i(L)$ and $\lambda_i(R)$ for a $\mathcal{S}_1$ shock.

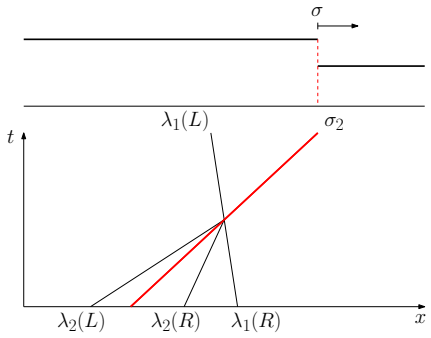

Fig. 4.5 Right moving bore with speed σ_2, $\lambda_i(L)$ and $\lambda_i(R)$ for a $\mathcal{S}_2$ shock.

4.2.2 Rarefaction waves

Following the classical theory (presented for example in [18, 69, 21]) we seek traveling wave solutions of the form $\mathbf{u}(x,t) = \mathbf{v}(\xi)$ with $\xi = \frac{x}{t}$. Substituting this term the into the conservation law one can easily verify that the system reduces to a system of ODEs of the form

$$\dot{\mathbf{v}} = \mathbf{r}(\mathbf{v}). \tag{4.31}$$

The solution is then given by the integral of (4.31). We may now exploit this insight using the theory of Riemann invariants $w : \mathbb{R}^2 \to \mathbb{R}$, which is a smooth function that is constant

along the integral curves [18]. For the shallow-water equations, the Riemann invariants are given by

$$w_1 = u - 2\sqrt{gh}, \qquad w_2 = u + 2\sqrt{gh}. \tag{4.32}$$

Going along a Riemann invariant, we find that the solution must satisfy

$$u_L \pm 2\sqrt{gh_L} = u_R \pm 2\sqrt{gh_R}. \tag{4.33}$$

Hence, for a given left state we may write the rarefaction wave solution as follows

$$\mathcal{R}_1(L): \quad u(h) = u_L - 2\sqrt{gh} + 2\sqrt{gh_L}, \tag{4.34}$$

$$\mathcal{R}_2(L): \quad u(h) = u_L + 2\sqrt{gh} - 2\sqrt{gh_L}. \tag{4.35}$$

By comparison, one can also show that $\dot{\mathbf{v}}$ is the right eigenvector $\mathbf{r}(\mathbf{v})$, and ξ is the corresponding eigenvalue $\lambda(\mathbf{v})$ belonging to the Jacobi matrix of the flux function. Having $\lambda = \xi$ would mean that the eigenvalues must be increasing from left to right. This implies $\lambda_i(L) < \lambda_i(R)$ and by equation (4.30) that $u_L < u_R$ whenever there is a rarefaction wave. Figure 4.6 and 4.7 depicts two rarefaction waves propagating left and right in the $(x,t)-$plane. Following the characteristics one can see how the waves moves forward in time.

In fluid mechanics, some refer to these waves as negative surges resulting from a decrease in flow depth [13]. Interestingly, Peregrine was able to show that a negative surge together with a bore advancing in positive direction originates from the collision of two fast shocks [53]. Therefore, we will discuss the development of the Riemann problem from a collision of two $\mathcal{S}_2$ shocks in Section 4.2.5.

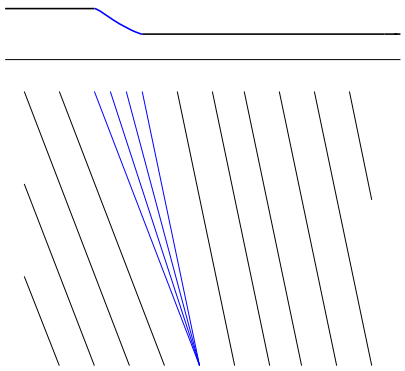

Fig. 4.6 Left moving rarefaction wave smoothly varying between $\lambda_1(L)$ and $\lambda_1(R)$.

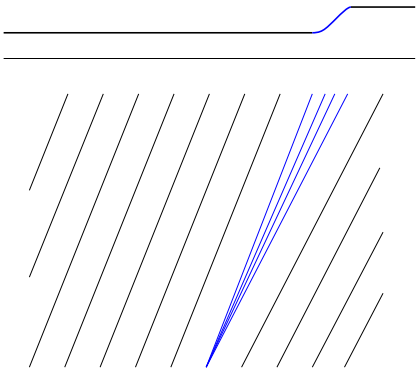

Fig. 4.7 Right moving rarefaction wave providing a smooth transition between $\lambda_2(L)$ and $\lambda_2(R)$.

4.2.3 General solution of the Riemann problem

Using the results from sections previous two sections, the general solution of the Riemann problem can be found using the rarefaction curves defined by (4.34) and (4.35)

$$\bullet\ \mathcal{R}_1(L): \quad u(h) = u_L - 2\sqrt{gh} + 2\sqrt{gh_L}, \qquad u > u_L,$$

$$\bullet\ \mathcal{R}_2(L): \quad u(h) = u_L + 2\sqrt{gh} - 2\sqrt{gh_L}, \qquad u > u_L,$$

and the shock curves (4.22) and (4.23)

$$\bullet\ \mathcal{S}_1(L): \quad u(h) = u_L - (h-h_L)\sqrt{\tfrac{g}{2}(\tfrac{1}{h}+\tfrac{1}{h_L})}, \qquad u < u_L,$$

$$\bullet\ \mathcal{S}_2(L): \quad u(h) = u_L + (h-h_L)\sqrt{\tfrac{g}{2}(\tfrac{1}{h}+\tfrac{1}{h_L})}, \qquad u < u_L.$$

In the following, it will be convenient to plot the integral curves and shock curves for a particular left state (h_L, u_L) plotted in two different coordinate systems. Figure 4.8 shows the integral curves in $(h,q)-$coordinates, where $q = hu$ is the momentum, while Figure 4.9 shows the integral curves in $(h,u)-$coordinates, The benefit of the former representation lies in the fact that the shock speed between q_1 and q_2 is given by

$$\sigma = \frac{q_1 - q_2}{h_1 - h_2},$$

which is simply the secant line joining the two states. For example, any right state given on the $\mathcal{S}_2(L)$ curve in Figure 4.9 would give rise to a right- moving bore since the slope of the secant line joining left and right states would be positive, i.e. $\sigma_R > 0$. Of course, if the right state is not given on any of the integral or shock curves, $\mathcal{S}_1, \mathcal{S}_2, \mathcal{R}_1$ and $\mathcal{R}_2$ need to be combined to give a solution of the Riemann problem. Indeed as explained in [21, 41], given a left state we may consider all possible right states and then find the solution depending on whether the right state is in region I, II, III or IV. For instance, let us say we have a right state somewhere in region four. Then in order to find an entropy solution we must define a middle state at some point (h_M, u_M) on the shock curve $\mathcal{S}_1(L)$ such that it is connected to a rarefaction curve $\mathcal{R}_2(M)$. Similarly, the entropy solution for each region is found by two elementary waves going through some middle state. For region I, we follow $\mathcal{R}_1(L)$ connecting the right state with $\mathcal{R}_2(M)$ for a middle state. In region II, we first go along $\mathcal{R}_1(L)$ then $\mathcal{S}_2(M)$. Finally, in region III we connect $\mathcal{S}_1(L)$ with $\mathcal{S}_2(M)$ for some middle state (see example in Figure 4.10 and 4.11). Concluding this section we remark that the solution is in fact unique since all of these solutions satisfy the admissibility conditions, and it has been shown that there is only one middle state M for each region.

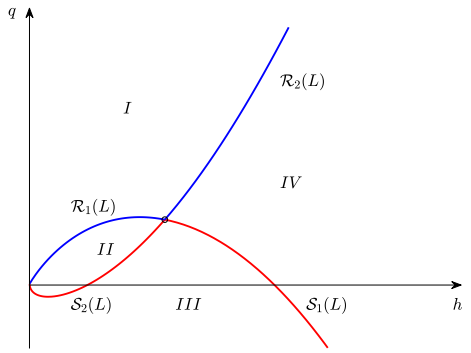

Fig. 4.8 Phase-space in $(h,q)-$coordinates.

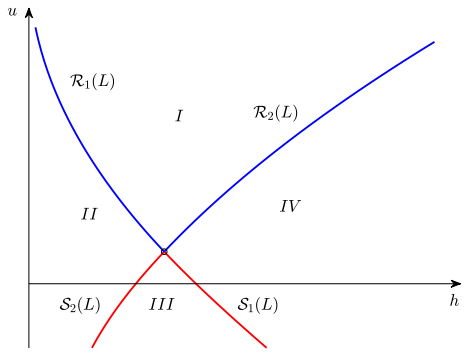

Fig. 4.9 Phase-space in $(h,u)-$coordinates.

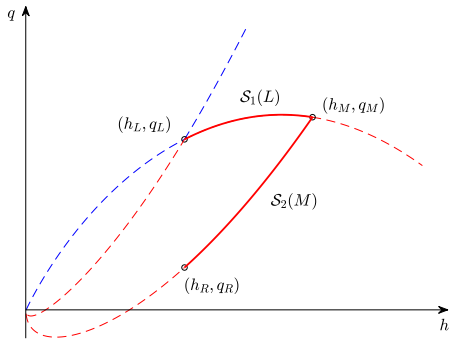

Fig. 4.10 Solution in region *III* using $(h,q)-$coordinates.

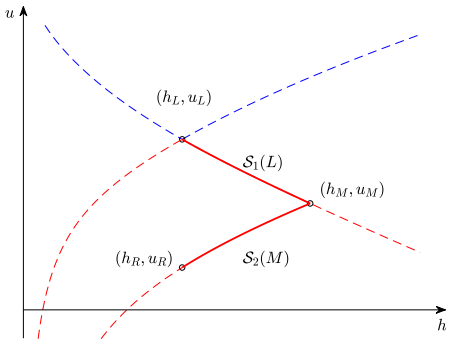

Fig. 4.11 Solution in region *III* using $(h,u)-$coordinates.

4.2.4 Development of the Riemann problem from a collision of $\mathcal{S}_2$ and $\mathcal{S}_1$ shocks

In this section, we will discuss the origin of the Riemann problem from a collision of two bores. It is most convenient to focus the discussion by assuming that a left state is given. With this proviso, we will prove that the Riemann problem associated to certain right states in region *III* arises from the head-on collision of two counter-propagating bores, while other right states are connected to an overtaking collision of co-propagating bores. Indeed, we will show that these two scenarios cover all possible right states in region *III*. Finally, we show that Riemann problems with right states in regions I, II and IV cannot develop from either head-on or overtaking collisions of an $\mathcal{S}_1$ and an $\mathcal{S}_2$ shock.

In order to understand how a given Riemann problem develops, we consider the backwards problem for $t < 0$. In order to solve the backwards problem, the usual disposition of a slow shock on the left and a fast shock on the right has to be reversed. Indeed, to solve

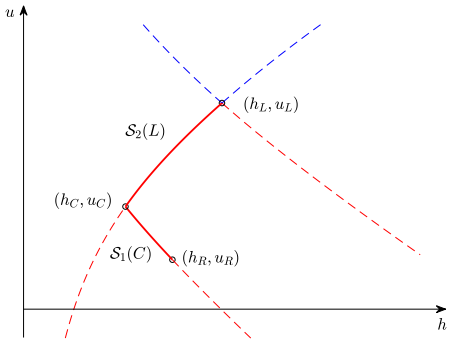

Fig. 4.12 Backwards problem in $(h,u)-$coordinates.

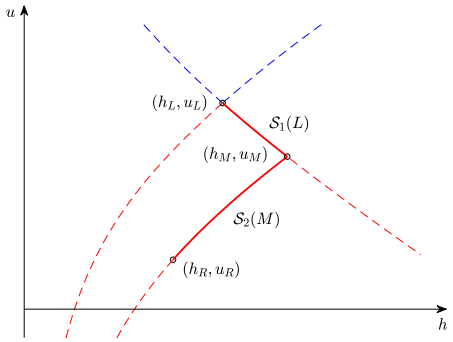

Fig. 4.13 Forward problem in $(h,u)-$coordinates.

the backwards problem, the left state is connected to a center state lying on the locus $\mathcal{S}_2(L)$. The center state is then connected to the right state by ensuring that the right state lies on the locus $\mathcal{S}_1(C)$. This configuration then leads to the collision of the two shocks at time $t = 0$. Note that we have chosen to use the term *center state* for the backwards problem versus *middle state* for the forward problem.

As indicated in Figure 4.13, the solution of the Riemann problem for a right state in region *III* consists of a $1-$shock and a $2-$shock connected by a middle state on $\mathcal{S}_1(L)$. Note that the flow depth of the middle state will always be higher than for both the left and the right state. Specifically we always have $h_M > h_L$ and $h_M > h_R$ in region *III*. In fact, it can be observed that fluid particles from both sides will move back towards the middle, thus contributing to the raised flow depth of the middle state. In that respect, it seems natural that the Riemann problem should result from two colliding bores. Figure 4.14 depicts the case of a head-on collision of a left-moving shock and a right-moving shock. Note that the backwards solution has the two shocks connected by a center state (h_C, u_C), then moving towards each other resulting in a Riemann problem at time $t = 0$.

Theorem 10. *Suppose that a left state $L = (h_L, u_L)$ for the Riemann problem is given. For any right state $R = (h_R, u_R)$ in region III, there exists a center state $C = (h_C, u_C)$ such that for $t < 0$, there is an $\mathcal{S}_2 - \mathcal{S}_1$ connection between L and R via C. The two shocks collide at $t = 0$, giving rise to a Riemann problem. On the other hand, it is not possible for a Riemann problem to develop from a $\mathcal{S}_2 - \mathcal{S}_1$ connection if the right state is in region I, II or IV.*

Proof. **Step 1. Existence of a center state:** We need to prove there is a center state connecting two colliding shock waves satisfying the bore conditions. Guided by the discussion above, and using an argument similar to one used in [32], we seek a point (h_C, u_C) on $\mathcal{S}_2(L)$

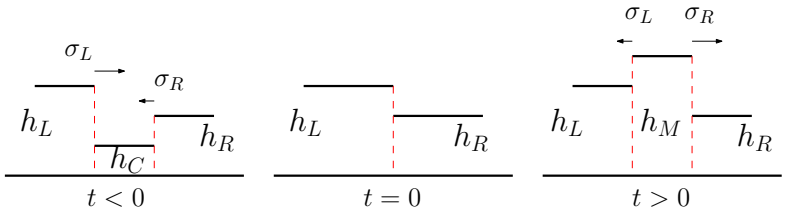

Fig. 4.14 The Riemann problem at $t = 0$ originates from two counter-propagating shocks ($t < 0$). The solution is given for $t > 0$.

giving rise to a $1-$shock, $\mathcal{S}_1(C)$ through (h_R, u_R). The equation defining the locus $\mathcal{S}_2(L)$ is given by

$$\mathcal{S}_2(L): \quad u = u_L + (h - h_L)\sqrt{\frac{g}{2}(\frac{1}{h} + \frac{1}{h_L})}. \tag{4.36}$$

As already indicated in Table 4.1, taking the derivative $u'(h)$ shows that u is strictly increasing on $\mathcal{S}_2(L)$ for $h \in (0, h_L]$ and with range $(-\infty, u_L)$. On the other hand, any right state $(h_R, u_R) \in$ *III* in the locus $\mathcal{S}_1(C)$ will satisfy the relation

$$\mathcal{S}_1(C): \quad u_R = u_C - (h_R - h_C)\sqrt{\frac{g}{2}(\frac{1}{h_R} + \frac{1}{h_C})}. \tag{4.37}$$

Keeping the right state fixed, and varying h_C shows that u_C is is strictly decreasing as a function of h_C with $h_C \in (0, h_L]$, and $u_C \in [u_R, \infty)$. Since $u_R < u_L$, the two loci defined above must necessarily intersect, thus defining the center state (h_C, u_C).

Step 2. Head-on collision and overtaking bores: We now analyze whether the center state found in *Step 1* actually leads to a collision of shocks. As will be shown presently, the center state will always give rise to a Riemann problem originating from either a head-on collision or an overtaking collision of two shocks. In order to prove this statement, we first note that having $(h_C, u_C) \in \mathcal{S}_2(L)$ implies that $h_C < h_L$ and $u_C < u_L$. From the bore properties in Section 4.2.1 we see that the left shock is described by

$$\sigma_L = \frac{h_L u_L - h_C u_C}{h_L - h_C} = u_C + h_L\sqrt{\frac{g}{2}(\frac{1}{h_C} + \frac{1}{h_L})}, \tag{4.38}$$

when substituting u_L from equation (4.36). Keeping this in mind, we now consider σ_R. Since the right state (h_R, u_R) is in the locus $\mathcal{S}_1(C)$, we must have $h_C < h_R$ and we may now use an argument reminiscent of the derivation of the Lax entropy condition (see [21], for example). The idea is to show that $\sigma_L > \sigma_R$ by considering the difference of these two quantities, and then using the mean-value theorem. Since q is continuous on $[h_C, h_R]$ and

differentiable on the open interval (h_C, h_R), it follows from the mean-value theorem that there exists $h_* \in (h_C, h_R)$ such that

$$\sigma_R = \frac{q_R - q_C}{h_R - h_C} = \left.\frac{dq}{dh}\right|_{h_*}.$$

In addition, differentiating $q(h)$ twice shows that the momentum q is a strictly concave function of h on the locus $\mathcal{S}_1(C)$ (see Table 4.1). Therefore, an upper bound on the derivative may be obtained by evaluating it at the leftmost point, h_C. Combining this observation with equation (4.38) yields the estimate

$$\begin{aligned}\sigma_L - \sigma_R &> \sigma_L - \frac{dq}{dh}|_{h_C} \\ &= h_L\sqrt{\frac{g}{2}(\frac{1}{h_C} + \frac{1}{h_L})} + \sqrt{gh_C} \\ &> 0.\end{aligned}$$

Hence we conclude that $\sigma_L > \sigma_R$ whenever the right state is in region *III*. This relation ensures that the center state chosen above gives rise to a Riemann problem. If σ_L and σ_R have the same sign, then the Riemann problem develops from an overtaking shock collision. If σ_L and σ_R have opposite signs, the Riemann problem develops from a head-on collision.

Step 3. Inadmissible connections: Regarding the last statement of the theorem, we will now argue that for a right state in region *I*, *II* or *IV* there is no admissible connection. If we first consider region *I*, we must choose u_C such that $u_C < u_L$ in order to satisfy the entropy condition in Section 4.2.1. Furthermore, in region *I* we have $u_R > u_L$, which means that $u_C < u_R$. This violates the entropy condition as a result of the center state being to the left, relative to the right state. In fact, the entropy condition ensures that the only admissible connection using one $1-$shock and one $2-$shock is a center state satisfying $u_L > u_C > u_R$, and this can obviously only be true for a right state in region *III*. □

Before proceeding, we will offer some clarifying remarks. For the shallow-water equation, given a left state we can always connect any right state with a middle state as mentioned earlier. Once you know the right state it is then possible to go back through a center state. We find it instructive to describe the solution for two particular states in both phase-space and in $(x,t)-$coordinates. Figure 4.16 depicts the special case from earlier in $(x,t)-$plane with two counter-propagating bores colliding at $t = 0$. Also observe that for $t < 0$, we need to consider the admissible connection from the perspective of the right state. Then of course,

a $\mathcal{S}_1(C) - \mathcal{S}_2(L)$ connection is entropy-satisfying, and is shown in Figure 4.15. On the other hand, for the forward problem, we connect $\mathcal{S}_1(L) - \mathcal{S}_2(M)$ as discussed in Section 4.2.3.

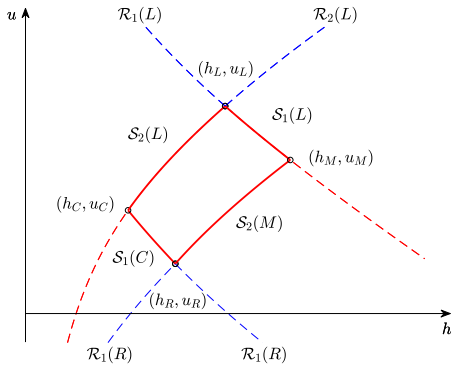

Fig. 4.15 Development of the Riemann problem in phase space.

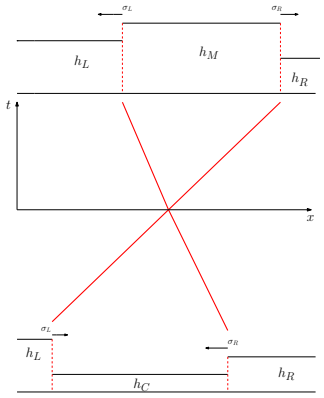

Fig. 4.16 Development of the Riemann problem in $(x,t)-$coordinates.

4.2.5 Development of the Riemann problem from a collision of two $\mathcal{S}_2$ shocks

Consideration will now be given to the Riemann problem arising from a $\mathcal{S}_2 - \mathcal{S}_2$ connection. As it will turn out, the resulting Riemann problem will have a right state in region *II*. As before, we consider the left state given. It is then straightforward to see that the center state in the backwards problem must lie in the Rankine-Hugoniot locus $\mathcal{S}_2(L)$. Thus the center state is given by the formula

$$u_C = u_L + (h_C - h_L)\sqrt{\frac{g}{2}\left(\frac{1}{h_C} + \frac{1}{h_L}\right)}. \tag{4.39}$$

On the other hand, if the center state is to be connected to the right state by an $\mathcal{S}_2$ -shock, then the right state must lie on the $\mathcal{S}_2(C)$ shock curve and therefore satisfy the relation

$$u_R = u_C + (h_R - h_C)\sqrt{\frac{g}{2}\left(\frac{1}{h_R} + \frac{1}{h_C}\right)}. \tag{4.40}$$

Putting these two formulas together defines the region of all possible right states as

$$\Omega_2 = \bigcup_{h_C \in (0,h_L)} \left\{ (h_R, u_R) \middle| u_R = u_L + (h_C - h_L)\sqrt{\tfrac{g}{2}(\tfrac{1}{h_C} + \tfrac{1}{h_L})} + (h_R - h_C)\sqrt{\tfrac{g}{2}(\tfrac{1}{h_R} + \tfrac{1}{h_C})}, 0 < h_R < h_C \right\}.$$

We have the following theorem.

Theorem 11. *Suppose that a left state $L = (h_L, u_L)$ for the Riemann problem is given. The set of all possible right states $R = (h_R, u_R)$ such that the Riemann problem originates from the collision of two $\mathcal{S}_2$ shocks is given by Ω_2. This set lies in region II, and the shock speeds of the backwards problem line up such that the two shocks meet at $t = 0$.*

On the other hand, it is not possible for a Riemann problem to develop from a $\mathcal{S}_2 - \mathcal{S}_2$ connection if the right state is in the complement of the set Ω_2.

Proof. First of all, the definition of the set Ω_2 is straightforward from the relations for the Hugoniot loci $\mathcal{S}_2(L)$ and $\mathcal{S}_2(C)$. Any state which does not lie in Ω_2 can therefore not be reached via a $\mathcal{S}_2 - \mathcal{S}_2$ connection.

To see that the state $R = (h_R, u_R)$ lies in region II, consider the difference between u_R given by (4.40) and (4.39) and u in the locus $\mathcal{S}_2(L)$ as defined by (4.23). Denoting this difference by $F(h) = u - u_R$, we obtain the formula

$$F(h) = u_L + (h - h_L)\sqrt{\frac{g}{2}(\frac{1}{h} + \frac{1}{h_L})} - u_L - (h_C - h_L)\sqrt{\frac{g}{2}(\frac{1}{h_C} + \frac{1}{h_L})} - (h - h_C)\sqrt{\frac{g}{2}(\frac{1}{h} + \frac{1}{h_C})}.$$

It needs to be shown that $F(h) < 0$ for $h < h_C$. Note first the $F(h_C) = 0$. If it can be shown that $F'(h) > 0$ for $h < h_C$ then we can conclude that $F(h)$ is strictly monotone increasing, and can therefore only cross the abscissa one time, so that $F(h)$ will have to be negative in the interval in question.

Evaluating the first and second derivative of $F(h)$ yields

$$F'(h) = \sqrt{\frac{g}{2}(\frac{1}{h} + \frac{1}{h_L})} - \frac{\sqrt{\frac{g}{2}}(h - h_L)}{2h^2\sqrt{\frac{1}{h} + \frac{1}{h_L}}} - \sqrt{\frac{g}{2}(\frac{1}{h} + \frac{1}{h_C})} + \frac{\sqrt{\frac{g}{2}}(h - h_C)}{2h^2\sqrt{\frac{1}{h} + \frac{1}{h_C}}},$$

and

$$F''(h) = -\frac{\sqrt{\frac{g}{2}}(5h_L + 3h)}{4h^4(\frac{1}{h} + \frac{1}{h_L})^{3/2}} + \frac{\sqrt{\frac{g}{2}}(5h_C + 3h)}{4h^4(\frac{1}{h} + \frac{1}{h_C})^{3/2}}.$$

By inspection, we see that $F''(h) < 0$ so that the derivative is strictly monotone decreasing. Therefore, we have $F'(h) > F'(h_C)$ for all $h < h_C$, and if it can be shown that $F'(h_C) > 0$, then we are done.

Lemma 1. *Given $F(h) = u - u_R$, we have $F'(h_C) > 0$.*

Proof. Evaluating the derivative $F'(h)$ given above at $h = h_C$ and multiplying with $\sqrt{\frac{2}{g}}$ for the sake of clarity yields

$$\begin{aligned}\sqrt{\frac{2}{g}}F'(h_C) &= \sqrt{\frac{1}{h_C}+\frac{1}{h_L}} - \frac{(h_C-h_L)}{2h_C^2\sqrt{\frac{1}{h_C}+\frac{1}{h_L}}} - \sqrt{\frac{1}{h_C}+\frac{1}{h_C}} \\ &= \sqrt{\frac{1}{h_C}+\frac{1}{h_L}} - \sqrt{\frac{2}{h_C}} - \frac{h_C}{2h_C^2\sqrt{\frac{1}{h_C}+\frac{1}{h_L}}} + \frac{h_L}{2h_C^2\sqrt{\frac{1}{h_C}+\frac{1}{h_L}}}.\end{aligned}$$

Next multiply with the positive number $\sqrt{\frac{1}{h_C}+\frac{1}{h_L}}$ to obtain

$$\begin{aligned}\sqrt{\frac{2}{g}}\sqrt{\frac{1}{h_C}+\frac{1}{h_L}}F'(h_C) &= \frac{1}{h_C}+\frac{1}{h_L} - \sqrt{\frac{2}{h_C}}\sqrt{\frac{1}{h_C}+\frac{1}{h_L}} - \frac{h_C}{2h_C^2} + \frac{h_L}{2h_C^2} \\ &= \frac{1}{2h_C}+\frac{1}{h_L} - \sqrt{\frac{2}{h_C}}\sqrt{\frac{1}{h_C}+\frac{1}{h_L}} + \frac{h_L}{2h_C^2}.\end{aligned}$$

Letting $h_C = \varepsilon h_L$ for $\varepsilon \in (0,1)$, we find

$$\sqrt{\frac{2}{g}}\sqrt{\frac{1}{h_C}+\frac{1}{h_L}}F'(h_C) = \frac{1}{2\varepsilon h_L}+\frac{1}{h_L} - \sqrt{\frac{2}{\varepsilon h_L}}\sqrt{\frac{1}{\varepsilon h_L}+\frac{1}{h_L}} + \frac{h_L}{2\varepsilon^2 h_L^2}.$$

Evidently, the proof will be achieved if it can be shown that the function

$$f(\varepsilon) = \varepsilon + 1 + 2\varepsilon^2 - 2\sqrt{2}\varepsilon\sqrt{\varepsilon+1},$$

is positive for all $\varepsilon \in (0,1)$. To this end, we take the first and second derivatives:

$$f'(\varepsilon) = 4\varepsilon - 2\sqrt{2}\sqrt{\varepsilon+1} - \frac{\sqrt{2}\varepsilon}{\sqrt{\varepsilon+1}} + 1,$$

$$f''(\varepsilon) = \frac{\sqrt{2}\varepsilon}{2(\varepsilon+1)^{3/2}} - \frac{2\sqrt{2}}{\sqrt{\varepsilon+1}} + 4.$$

Note that $f''(\varepsilon) > 0$ by inspection, and f is therefore strictly convex on $(0,1)$. Thus by convexity we know that $f'(\varepsilon)$ is strictly increasing, so that $f'(\varepsilon) < f'(1)$ for all $\varepsilon \in (0,1)$.

But evaluating $f'(\varepsilon)$ at 1 yields $f'(1) = 0$. Hence, $f'(\varepsilon) < f'(1) = 0$. So the function f is strictly decreasing on $(0,1)$ meaning $f(\varepsilon) > f(1) = 0$. □

Finally, denote the shock speeds of the backwards problem by

$$\sigma_R = \frac{q_R - q_C}{h_R - h_C},$$

and

$$\sigma_L = \frac{q_L - q_C}{h_L - h_C}.$$

Now recall that it was proved in Section 4.2.1 that the function $q(h)$ is convex, and note that the convexity on the Hugoniot locus $\mathcal{S}_2(C)$, including the admissible and the entropy-violating part guarantees that $\sigma_R > \sigma_L$, as is required for the two shocks to meet at $t = 0$. □

A particular example of the backwards problem is represented in phase space for (h,u) and (h,q) coordinates.

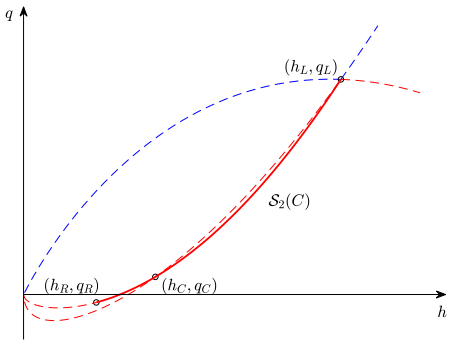

Fig. 4.17 Backwards problem in $(h,q)-$coordinates.

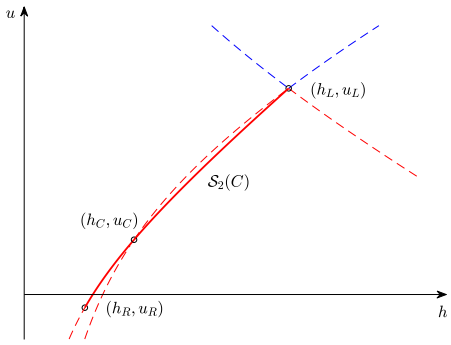

Fig. 4.18 Backwards problem in $(h,u)-$coordinates.

In Figure 4.18, we observe that $h_R < h_C < h_L$ and $u_R < u_C < u_L$. Also note that in Figure 4.17 the line joining each state has a positive slope, which implies that both states moves in the positive direction. From this we may hope to create a Riemann problem if the left sate is moving faster than the right state, causing an overtaking. Though, this is clear due to the fact that $\mathcal{S}_2$ is convex, i.e. the rate of change given by the shock speed σ is increasing from left to right. We state the general formulation in the next theorem.

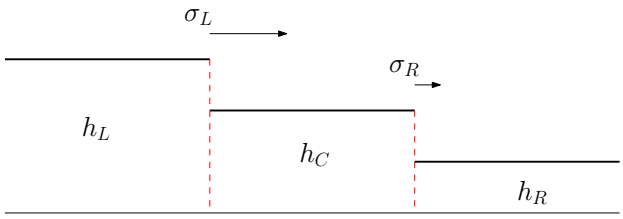

Fig. 4.19 Two colliding bores forming the Riemann Problem.

4.2.6 Development of the Riemann problem from a collision of two $\mathcal{S}_1$ shocks

The final case to be considered is when a Riemann problem develops from the collision between two $\mathcal{S}_1$ shocks. The situation is similar, and the arguments in the proofs are virtually the same as in the previous section. Finding a center state turns out to only be possible for some right states in region *IV*.

As before, we consider the left state given. It is then straightforward to see that the center state in the backwards problem must lie in the Rankine-Hugoniot locus $\mathcal{S}_2(L)$. Thus the center state is given by the formula

$$u_C = u_L - (h_C - h_L)\sqrt{\frac{g}{2}\Big(\frac{1}{h_C} + \frac{1}{h_L}\Big)}. \tag{4.41}$$

On the other hand, if the center state is to be connected to the right state by an $\mathcal{S}_1$ -shock, then the right state must lie on the $\mathcal{S}_1(C)$ shock curve and therefore satisfy the relation

$$u_R = u_C - (h_R - h_C)\sqrt{\frac{g}{2}\Big(\frac{1}{h_R} + \frac{1}{h_C}\Big)}. \tag{4.42}$$

Putting these two formulas together defines the region of all possible right states as

$$\Omega_4 = \bigcup_{h_C \in (0,h_L)} \Big\{(h_R,u_R)\Big| u_R = u_L - (h_C - h_L)\sqrt{\tfrac{g}{2}(\tfrac{1}{h_C}+\tfrac{1}{h_L})} - (h_R - h_C)\sqrt{\tfrac{g}{2}(\tfrac{1}{h_R}+\tfrac{1}{h_C})}, 0 < h_R < h_C\Big\}.$$

We have the following theorem.

Theorem 12. *Suppose that a left state $L = (h_L, u_L)$ for the Riemann problem is given. The set of all possible right states $R = (h_R, u_R)$ such that the Riemann problem originates from the collision of two $\mathcal{S}_1$ shocks is given by Ω_4. This set lies in region IV, and the shock speeds of the backwards problem line up such that the two shocks meet at $t = 0$.*

On the other hand, it is not possible for a Riemann problem to develop from a $\mathcal{S}_1 - \mathcal{S}_1$ connection if the right state is in the complement of the set Ω_4.

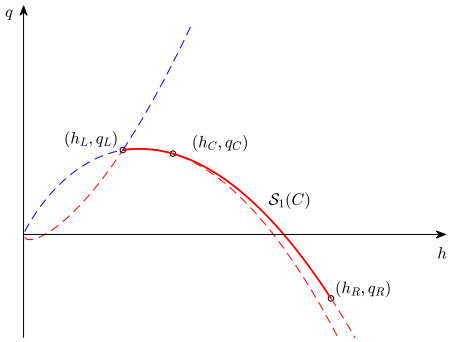

Fig. 4.20 Backwards problem in $(h,q)-$coordinates.

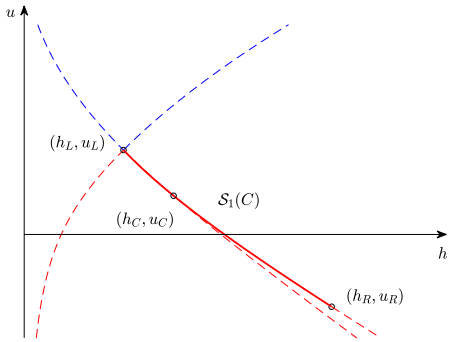

Fig. 4.21 Backwards problem in $(h,u)-$coordinates.

The proof of Theorem 12 is virtually the same as that of Theorem 11, except for changing signs in the right places. From Figure 4.20, we observe that both bores are moving to the left due to a negative slope. However, the right state moves faster than the left. This is also true in general since $\mathcal{S}_1$ is strictly concave in momentum coordinates. Again, we must also choose an admissible connection. Similar to the case in Section 4.2.5, we follow $\mathcal{S}_1(L)$ from left state to center state, continuing along the $\mathcal{S}_1(C)$ curve from the center state to the right state.

4.3 Conclusions

In this chapter, we have considered the Riemann problem associated to the shallow-water equations. The study of the Riemann problem is important when trying to understand the behavior of solutions of a system of conservation laws. For example the Riemann problem can be used as a tool in the front-tracking method where general initial data are decomposed into piecewise constant functions which gives rise to a series of Riemann problems [21]. This approach is used in existence proofs and numerical schemes, but one may face difficulties interpreting solutions of the Riemann problem for the shallow-water equations in the case when the solution includes a dry region ($h = 0$). In gas dynamics, this situation is known as cavitation and is a well-defined concept, but the creation of a dry zone between two propagating waves does not seem reasonable from a physical point of view in the case of shallow-water theory.

In the present work, we have imposed the condition that the Riemann problem should arise from the collision of two bores. With this condition in place, we were able to show that solutions of the Riemann problem do not feature cavitation. In summary, for a given left state, the collision of an $\mathcal{S}_1(L)$ and an $\mathcal{S}_2(L)$ shock gives rise to a Riemann problem in Region *III* (Theorem 10). The collision of two $\mathcal{S}_2(L)$ shocks gives rise to a Riemann problem in Region

II (Theorem 11), and the collision of two $\mathcal{S}_1(L)$ shocks gives rise to a Riemann problem in Region *IV* (Theorem 12). It is clear that a right state in region *I* is not permitted if these admissibility conditions are used. In particular, we avoid a right state in the shaded region of Figure 4.1 which is the region where the resolution of the Riemann problem features a dry state.

References

[1] I. Aavatsmark, *Kapillarenergie als Entropiefunktion*, Z. Angew. Math. Mech. **69** (1989), 319–327.

[2] I. Aavatsmark, *Bevarelsesmetoder for hyperbolske differensialligninger*, Lecture Notes, University of Bergen, (2003).

[3] M. Abramowitz and I. A. Stegun, *Handbook of mathematical functions with formulas, graphs, and mathematical table*, National Bureau of Standards Applied Mathematics series 55, (1965).

[4] A. Ali and H. Kalisch, *Energy balance for undular bores*, Compt. Rend. Mecanique, **338** (2010), 67-70.

[5] A. Ali and H. Kalisch, *Mechanical balance laws for Boussinesq models of surface water waves*, J. Nonlinear Sci. **22** (2012), 371–398.

[6] A. Ali and H. Kalisch, *On the formulation of mass, momentum and energy conservation in the KdV equation*, Acta Applicandae Mathematicae, **2** (2014), 113-131.

[7] A. Ali and H. Kalisch, *A dispersive model for undular bores*, Anal. Math. Phys. **2** (2012), 347–366.

[8] T. Benjamin and J. Lighthill, *On cnoidal waves and bores*, Proc. R. Soc. A **224** (1954), 448–460.

[9] M. Bjørkavåg and H. Kalisch, *Wave breaking in Boussinesq models for undular bores*, Phys. Lett. A **375** (2011), 1570–1578.

[10] J. Bona and R. Smith, *The initial-value problem for the Korteweg-de Vries equation*, Philosophical Transactions of the Royal Society of London. Series A, Mathematical and Physical Sciences, **278** (1975), 555-601.

[11] A. J. Bowen, D. L. Inman and V. P. Simmons, *Wave 'set-down'and set-up*Journal of Geophysical Research, Wiley Online Library **73** (1968), 2569-2577.

[12] S. Bianchini, A. Bressan, *Vanishing viscosity solutions of nonlinear hyperbolic systems*, Ann. of Math. **161** (2005), 223–352.

[13] H. Chanson, Hydraulics of open channel flow, (Arnold,1999).

[14] W. Cheney, *Analysis for applied mathematics*, Springer Science, **208** (2013).

[15] J. Duoandikoetxea, *Fourier analysis*, American Mathematical Soc. **29** (2001).

[16] R. G. Dean, *Advanced series on ocean engineering*, **2** (1984).

[17] P.G. Drazin and J. S. Robin, Solitons: an introduction, Cambridge university press, **2** (1989).

[18] L.C. Evans, *Partial differential equations*, Graduate Studies in Mathematics, American Mathematical Society, Providence, RI, **19** (1998).

[19] H. Favre, *Ondes de Translation*, (Dunod, Paris, 1935).

[20] G. Folland, *Real analysis: modern techniques and their applications*, John Wiley & Sons, (2013).

[21] H. Holden and N. H. Risebro, Front tracking for hyperbolic conservation laws, (Springer, New York, 2015).

[22] F.M. Henderson, Open channel flow (Prentice Hall, 1996).

[23] H.G. Hornung, C. Willert and S. Turner, *The flow field downstream of a hydraulic jump*, J. Fluid Mech. **287** (1995), 299–316.

[24] S. Israwi and H. Kalisch, *Approximate conservation laws in the KdV equation*, Physics Letters A,Elsevier, **383** (2019).

[25] S. Israwi and H. Kalisch *A Rigorous derivation of mechanical balance laws in the KdV equation*, To be submitted.

[26] S. Israwi and H. Kalisch *A mathematical justification of the momentum density function associated to the KdV equation*, (arXiv preprint arXiv:1808.06386, 2018).

[27] T. Kano and T. Nishida *Sur les ondes de surface de l'eau avec une justification mathématique des équations des ondes en eau peu profonde*, Journal of Mathematics of Kyoto University, **19** (1979), 335-370.

[28] H. Kalisch, Z. Khorsand and D. Mitsotakis, *Mechanical balance laws for fully nonlinear and weakly dispersive water waves*, Physica D **333** (2016), 243–253.

[29] H. Kalisch and D. Mitrović, *Singular solutions of a fully nonlinear* 2*x*2 *system of conservation laws*, Proc. Edinb. Math. Soc. **55** (2012), 711–729.

[30] H. Kalisch and D. Mitrović, *Singular solutions for the shallow-water equations*, IMA J. Appl. Math. **77** (2012), 340–350.

[31] H. Kalisch, D. Mitrovic and V. Teyekpiti, *Delta shock waves in shallow water flow*, Phys. Lett. A **381** (2017), 1138–1144.

[32] H. Kalisch, D. Mitrovic and V. Teyekpiti, *Existence and uniqueness of singular solutions for a conservation law arising in magnetohydrodynamics*, Nonlinearity **31**, (2018).

[33] B. Khorbatly, I. Zaiter and S. Isrwai, *Derivation and well-posedness of the extended Green-Naghdi equations for flat bottoms with surface tension*, Journal of Mathematical Physics, AIP

Publishing LLC, **59** (2018).

[34] Z. Khorsand, *Flow Properties of Fully Nonlinear Model Equations for Surface Waves*, The University of Bergen, (2017).

[35] Z. Khorsand and H. Kalisch, *On the shoaling of solitary waves in the KdV equation*, Coastal Engineering Proceedings, **34**, (2014).

[36] D. J. Korteweg and G. De Vries, *XLI. On the change of form of long waves advancing in a rectangular canal, and on a new type of long stationary waves*, The London, Edinburgh, and Dublin Philosophical Magazine and Journal of Science, Taylor & Francis, **39** (1895).

[37] Kundu, Cohen and Dowling, *Fluid Mechanics 4th*, Elsiver, **4**, (2008).

[38] D. Lannes, *The water waves problem: mathematical analysis and asymptotics*, American Mathematical Soc., **188**, (2013).

[39] D. F. Lawden, *Elliptic functions and applications*, Springer Science & Business Media **80** (2013).

[40] P.D. Lax, *Hyperbolic systems of conservation laws II*, Comm. Pure Appl. Math. **10** (1957), 537–566.

[41] R.J. LeVeque, *Finite volume methods for hyperbolic problems*, (Cambridge University Press, Cambridge, 2002).

[42] F. Linares and G. Ponce *Introduction to nonlinear dispersive equations*,Springer, (2014).

[43] T.P. Liu, *Existence and uniqueness theorems for Riemann problems*, Trans. Amer. Math. Soc. **212** (1975), 375–382.

[44] T.P. Liu, *The Riemann problem for general systems of conservation laws*, J. Differential Equations **18** (1975), 218–234.

[45] J Lighthill, *Waves in Fluids*Cambridge University Press (1978).

[46] M. S. Longuet-Higgins and R. W. Stewart, *Radiation stress and mass transport in gravity waves, with application to 'surf beats'* Journal of Fluid Mechanics, Cambridge University Press, **13** (1962), 481-504.

[47] M. S. Longuet-Higgins and R. W. Stewart, *Radiation stresses in water waves; a physical discussion, with applications,*Elsiver, **11** (1964), 529-562.

[48] MATLAB, *Version R2019a*, The MathWorks Inc, Natick, Massachusetts (2019).

[49] L. Shure and M. Igor, *Special functions: ellipke*, The MathWorks Inc, Natick, Massachusetts, downloaded 20. Jan 2019, <https://www.mathworks.com/help/matlab/ref/ellipke.html>.

[50] M. O. Paulsen and H. Kalisch, *Admissibility conditions for Riemann data in shallow-water theory*, Zeitschrift für Naturforschung A, To appear.

[51] M. O. Paulsen and H. Kalisch, *A Nonlinear Formulation of Radiation Stress and Applications to Cnoidal Shoaling*, Submitted.

[52] D.H. Peregrine, *Water-wave interaction in the surf zone*, Coastal Engineering Proceedings 1974, (1975), pp. 500–517.

[53] P.G. Peregrine, *Calculations of the development of an undular bore*, J. Fluid Mech. **25** (1966).

[54] L. Rayleigh, *Note on Tidal Bores*, Proc. Roy. Soc. London Ser. A **81** (1908), 448–449.

[55] M. Renardy and R.C. Rogers. An introduction to partial differential equations. Texts in Applied Mathematics **13** (Springer-Verlag, New York, 1993).

[56] G. Richard and S. Gavrilyuk, *The classical hydraulic jump in a model of shear shallow-water flows*, J. Fluid Mech. **725** (2013), 492–521.

[57] V. Roeber, K. F., Cheung, and M. H. Kobayashi, *Shock-capturing Boussinesq-type model for nearshore wave processes*, Coastal Engineering, **54**(4) (2010), 407-423.

[58] T. Sakai and J. A. Batthjes, *Wave shoaling calculated from Cokelet's theory*, Coastal Engineering, Elsevier, **4** (1980), 65-84.

[59] T. Saville, *Experimental determination of wave set-up*, Proc. 2nd Tech. Conf. on Hurricanes, Miami Beach, FL, (1961).

[60] O. Skovgaard, *Sinusoidal and cnoidal gravity waves formulae and tables*, Institute of Hydrodynamics and Hydraulic Engineering, Technical University of Denmark, (1974).

[61] J.J. Stoker, Water Waves: The Mathematical Theory with Applications, (Interscience Publishers, New York, 1957).

[62] B. Sturtevant, *Implications of experiments on the weak undular bore*, Phys. Fluids **8** (1965), 1052–1055.

[63] M. Shinbrot initial value problem for surface waves under gravity, I: the simplest case, Indiana University Mathematics Journal, **25** (1976), 291-300.

[64] R.E. Showalter, *Monotone operators in Banach space and nonlinear partial differential equations*,American Mathematical Soc., **49** (2013).

[65] I. A. Svendsen, *Introduction to nearshore hydrodynamics*,World Scientific, **24** (2006).

[66] I. A. Svendesen and J. Buhr Hansen, *The wave height variation for regular waves in shoaling water*, Coastal Engineering, Elsevier, **1** (1977), 261-284.

[67] I. A. Svendsen and Brink-Kjær, *Shoaling of cnoidal waves*, Proc. 13th Intern. Conf. Coastal Engrg., Vancouver 1 (1972), 365-383.

[68] C. Tsikkou, *Hyperbolic conservation laws with large initial data. Is the Cauchy problem well-posed?*, Quart. Appl. Math. **68** (2010), 765–781.

[69] G. B. Whitham, *Linear and Nonlinear Waves*, Wiley, New York, (1974).

[70] V. Zakharov, *Stability of periodic waves of finite amplitude on the surface of a deep fluid*, Journal of Applied Mechanics and Technical Physics, Springer, **9** (1968), 190–194.

[71] V. Zakharov, *Stability of periodic waves of finite amplitude on the surface of a deep fluid*, Journal of Applied Mechanics and Technical Physics, Springer, **9** (1968), 190–194.

Appendix A

Integration of cnoidal functions

In order to define the two shoaling models we need to handle integrals including different variations of η. In particular we need to determine $\overline{\eta}, \overline{\eta^2}, \overline{\eta^3}, \overline{\eta}_{xx}, \overline{\eta\eta}_{xx}$ to evaluate (2.22) and (2.23) in terms of m and current depth. First note that we can write the time averaged η given by (1.33) on the more convenient form

$$\overline{\eta} = \frac{1}{T}\int_0^T \eta\Big(2K(m)(\frac{t}{T} - \frac{x}{\lambda})\Big)dt = f_2 + H\int_0^1 \mathrm{cn}^2(2K(m)\xi;m)d\xi,$$

(for more details see [65]). Similarly we can find the average of the powers of η. We note that they will involve integrals of the form

$$\int_0^1 \mathrm{cn}^2(2K\xi;m)d\xi = \frac{1}{4mK}\Big(E-(1-m)K\Big),$$

$$\int_0^1 \mathrm{cn}^4(2K\xi;m)d\xi = \frac{1}{3m^2}\Big(3m^2-5m+2(4m-2)\frac{E}{K}\Big),$$

$$\int_0^1 \mathrm{cn}^6(2K\xi;m)d\xi = \frac{1}{5m^2}\Big(4(2m^2-1)\int_0^1 \mathrm{cn}^4(2K\xi;m)d\xi + 3(1-m^2)\int_0^1 \mathrm{cn}^2(2K\xi;m)d\xi\Big).$$

These expressions can be found in [39]. Also note that $\overline{\eta}_{xx}, \overline{\eta\eta}_{xx}$ will also include such terms. This is due to

$$\eta_{xx}(2K\xi;m) = 4K^2H(2-2m+(8m-4)\mathrm{cn}^2(2K\xi;m) - 6m\mathrm{cn}^4(2K\xi;m)),$$

and can be calculated from relations found in [3]. Combining the results above we deduce,

$$\overline{\eta} = f_2 + H\int_0^1 \mathrm{cn}^2(2K\xi;m)d\xi,$$

$$\overline{\eta^2} = f_2^2 + 2Hf_2\int_0^1 \mathrm{cn}^2(2K\xi;m)d\xi + H^2\int_0^1 \mathrm{cn}^4(2K\xi;m)d\xi,$$

$$\overline{\eta^3} = H^3\int_0^1 \mathrm{cn}^6(2K\xi;m)d\xi + 3H^2f_2\int_0^1 \mathrm{cn}^4(2K\xi;m)d\xi + 3Hf_2^2\int_0^1 \mathrm{cn}^2(2K\xi;m)d\xi + f_2^3,$$

$$\overline{\eta}_{xx} = \frac{3H^2}{2m}(-3m^2\int_0^1 \mathrm{cn}^4(2K\xi;m)d\xi + 4m^2\int_0^1 \mathrm{cn}^2(2K\xi;m)d\xi - 2\int_0^1 \mathrm{cn}^2(2K\xi;m)d\xi - m^2 + 1),$$

$$\begin{aligned}
\overline{\eta\eta}_{xx} = {} & 3H^2f_3\int_0^1 \mathrm{cn}^4(2K\xi;m)d\xi - 3H^2f_1\int_0^1 \mathrm{cn}^4(2K\xi;m)d\xi + \frac{3}{2}Hf_1f_2 - \frac{3}{2}Hf_2f_3 \\
& + \frac{3}{2}H^2f_1\int_0^1 \mathrm{cn}^2(2K\xi;m)d\xi - \frac{3}{2}H^2f_3\int_0^1 \mathrm{cn}^2(2K\xi;m)d\xi + 6H^2f_1m^2\int_0^1 \mathrm{cn}^4(2K\xi;m)d\xi \\
& - 6H^2f_3m^2\int_0^1 \mathrm{cn}^4(2K\xi;m)d\xi - \frac{3}{2}Hf_1f_2m^2 + \frac{3}{2}3Hf_2f_3m^2 - \frac{3}{2}H^2f_1m^2\int_0^1 \mathrm{cn}^2(2K\xi;m)d\xi \\
& + \frac{3}{2}H^2f_3m^2\int_0^1 \mathrm{cn}^2(2K\xi;m)d\xi - 3Hf_1f_2\int_0^1 \mathrm{cn}^2(2K\xi;m)d\xi + 3Hf_2f_3\int_0^1 \mathrm{cn}^2(2K\xi;m)d\xi \\
& - \frac{9}{2}H^2f_1m^2\int_0^1 \mathrm{cn}^6(2K\xi;m)d\xi + \frac{9}{2}H^2f_3m^2\int_0^1 \mathrm{cn}^6(2K\xi;m)d\xi \\
& + 6Hf_1f_2m^2\int_0^1 \mathrm{cn}^2(2K\xi;m)d\xi - 6Hf_2f_3m^2\int_0^1 \mathrm{cn}^2(2K\xi;m)d\xi \\
& - \frac{9}{2}Hf_1f_2m^2\int_0^1 \mathrm{cn}^4(2K\xi;m)d\xi + \frac{9}{2}Hf_2f_3m^2\int_0^1 \mathrm{cn}^4(2K\xi;m)d\xi.
\end{aligned}$$